

Antonia-Maria Charalampidi

# Evaluation of thermodynamic models for pure hydrogen and hydrogen-containing binary mixtures

Graduate thesis in Thermodynamics, Energy and Process Engineering

Supervisor: Professor Even Solbraa

Co-supervisor: Eleni Panteli

June 2022



Antonia-Maria Charalampidi

# **Evaluation of thermodynamic models for pure hydrogen and hydrogen- containing binary mixtures**

Graduate thesis in Thermodynamics, Energy and Process Engineering  
Supervisor: Professor Even Solbraa  
Co-supervisor: Eleni Panteli  
June 2022

Norwegian University of Science and Technology  
Faculty of Engineering  
Department of Energy and Process Engineering



## Acknowledgements

The present diploma thesis is a result of the collaboration of the Laboratory of Thermodynamics and Transfer Phenomena of the School of Chemical Engineering of the National Technical University of Athens and the department of Energy and Process Engineering of the Norwegian University of Science and Technology. During the past months I had the opportunity to meet and collaborate with several individuals who contributed significantly to the completion of this work.

Therefore, I would like to thank and express my appreciation to Professor Epaminondas Voutsas for his trust, his guidance and his knowledge-sharing the past months. I am grateful for having the opportunity to work with him and the Laboratory of Thermodynamics and Transfer Phenomena. I would like to express my sincere appreciation to the members of the Lab and especially Postdoctoral Researcher Vassilis Koulocheris and PhD candidate Akis Tassios for their help and guidance in several theoretical and technical matters.

Furthermore, I would like to thank my supervisor at NTNU Professor Even Solbraa as well as my co-supervisor Eleni Panteli for their advice and support during the months that I was completing my work in Norway.

Finally, I would like to thank my family and friends who have been by my side throughout the preparation of my diploma thesis.

## Abstract

Since the world is moving towards a new era which is based on zero greenhouse gas emissions in the atmosphere and renewable resources, emphasis should be placed on a substitute solution for the fossil fuels; hydrogen. Pure hydrogen, which is mainly produced by methane steam reforming and secondarily by water electrolysis in significantly fewer quantities, can be the “green weapon” against today’s environmental crisis. Nevertheless, in order to achieve the transition from fossil fuels to hydrogen, it is important to test if the existing pipeline and storage system that is used for natural gas streams can be applicable to hydrogen-containing streams as well.

In this work the main focus is paid to the properties related to pipeline design and storing-conditions determination for the cases of pure hydrogen and of binary mixtures between hydrogen and basic natural-gas components. More specifically, several thermodynamic models have been evaluated in terms of prediction-accuracy comparing to the available online experimental datasets of the desired examined properties.

The properties of major importance as it comes to transporting and storage are; vapor pressures, as it comes to pure components, or vapor-liquid equilibrium information, as it comes to mixtures, which can be used to properly determine the operating conditions of the production chain for the desired mixture-phases, the system’s density, which is important for calculating the frictional pressure loss inside a pipe, the residual parts of the energetic properties of molar heat capacity and enthalpy and also JT coefficient, which are important for determining temperature changes of a fluid, and lastly the speed of sound, which is important for defining the critical mass flux of pipeline flows.

Additionally, the components that were considered as components of interest and were examined when mixed with hydrogen in terms of binary mixture were the main components of natural gas stream that can be found in hydrogen’s production via steam reforming and these are: methane, which is the most important one, ethane, propane, carbon monoxide, carbon dioxide and nitrogen.

Lastly, the thermodynamic models that have been tested for the abovementioned calculations are; GERG-2008 EoS which is the reference equation for natural gas streams and similar gases’ streams and it is important to see if it can be trusted for mixtures of components of these streams when mixed with large quantities of hydrogen, the classic cubic equations of state Peng-Robinson and Soave-Redlich-Kwong which are very simple to use and are reliable for various mixtures regardless their simplicity, a more complicated statistical model such as Perturbed-Chain SAFT equation of state and lastly the UMR-PRU predictive model which is the PR EoS coupled with UNIFAC through the Universal Mixing Rule.

After a detailed searched on the available online literature, various experimental data points referring the abovementioned systems of pure hydrogen and hydrogen-containing binary mixtures were collected. The data available for pure hydrogen were plenty, they were reliable and lead to safe conclusions as it comes to the model accuracy comparison. This was not the case for the data available for the binary mixtures. The thermophysical property data have been extracted mainly from rather old sources, since there were no up-to-date data found, and have a clear focus on single phase density values for the systems of hydrogen mixed with methane, carbon dioxide or nitrogen for very low concentration of hydrogen in the mixtures. Based on such data, it is not possible to draw safe conclusions regarding modern processes

related to hydrogen production, since these will be based on high hydrogen concentrations. The available vapor-liquid equilibrium data led to safer results.

From the thermodynamic model comparison, it was concluded that the GERG-2008 EoS can be used as a reference equation for pure hydrogen since it gave the best results in all of the calculations. GERG-2008 EoS can also be trusted for the single-phase density and the sound velocity calculations of the six binary mixtures regarding the experimental data. Since the data fail to cover a wide range of hydrogen compositions, GERG-2008 EoS was used to extend the existing database for single-phase density and speed of sound data in higher hydrogen compositions and it was found that the rest of the thermodynamic models give similar results for a composition range from 0 % to 100 % hydrogen, with SRK EoS being the most reliable comparing to the GERG-2008 EoS. Both in case of pure hydrogen and hydrogen-containing binary mixtures, no model can predict well enough the residual part of heat capacities or the Joule-Thomson coefficient. The vapor-liquid equilibrium calculations were better performed by UMR-PRU EoS.

It is a fact now that for these six binary mixtures the models that can predict satisfactorily their thermophysical properties do not succeed on vapor-liquid equilibrium and vice versa. Due to this fact, the binary interaction parameters of the mixtures for, indicatively, PR EoS were properly determined, after carrying out fittings to the bubble point pressure experimental data in order to realize if this technique can lead the equations of state to achieve better accuracy for both property and vapor-liquid equilibrium calculations.

Finally, it was concluded that if a certain model should be proposed for each one of the examined systems these models would be; GERG-2008 EoS for pure hydrogen, hydrogen-propane and hydrogen-carbon monoxide, UMR-PRU EoS for hydrogen-ethane and hydrogen-carbon dioxide and lastly PR EoS with fitted acentric factor for hydrogen and fitted binary interaction parameters for hydrogen-methane and hydrogen-nitrogen.

**Key Words:** Data evaluation for hydrogen-containing systems, Thermodynamic modeling of pure hydrogen, Thermodynamic modeling of hydrogen-containing binary systems, GERG-2008 EoS evaluation of hydrogen-containing systems

## Περίληψη

Δεδομένου ότι ο κόσμος οδεύει προς μια νέα εποχή που βασίζεται σε μηδενικές εκπομπές αερίων θερμοκηπίου στην ατμόσφαιρα και στις ανανεώσιμες πηγές ενέργειας, θα πρέπει να δοθεί έμφαση σε μια εναλλακτική λύση για τα ορυκτά καύσιμα: το υδρογόνο. Το καθαρό υδρογόνο, το οποίο παράγεται κυρίως με αναμόρφωση ατμού μεθανίου και δευτερευόντως με ηλεκτρόλυση νερού σε σημαντικά λιγότερες ποσότητες, μπορεί να είναι το «πράσινο όπλο» ενάντια στη σημερινή περιβαλλοντική κρίση. Ωστόσο, για να επιτευχθεί η μετάβαση από τα ορυκτά καύσιμα στο υδρογόνο, είναι σημαντικό να ελεγχθεί εάν το υπάρχον σύστημα αγωγών και το σύστημα αποθήκευσης που χρησιμοποιείται για ρεύματα φυσικού αερίου μπορεί να εφαρμοστεί και σε ρεύματα που περιέχουν υδρογόνο.

Στην εργασία αυτή έμφαση δίνεται κυρίως στις ιδιότητες που σχετίζονται με το σχεδιασμό των αγωγών μεταφοράς αερίων και τον προσδιορισμό των συνθηκών αποθήκευσης για τις περιπτώσεις καθαρού υδρογόνου και δυαδικών μιγμάτων μεταξύ υδρογόνου και βασικών συστατικών φυσικού αερίου. Πιο συγκεκριμένα, αρκετά θερμοδυναμικά μοντέλα έχουν αξιολογηθεί ως προς την ικανότητα πρόβλεψής τους σε σύγκριση με τα διαθέσιμα διαδικτυακά πειραματικά δεδομένων των επιθυμητών εξεταζόμενων ιδιοτήτων.

Οι ιδιότητες μείζονος σημασίας όσον αφορά τη μεταφορά και την αποθήκευση είναι: οι τάσεις ατμών, όσον αφορά τα καθαρά συστατικά, ή οι πληροφορίες ισορροπίας ατμού-υγρού, όσον αφορά τα μείγματα, που μπορούν να χρησιμοποιηθούν για τον σωστό προσδιορισμό των συνθηκών λειτουργίας σε μία αλυσίδα παραγωγής για τις επιθυμητές φάσεις μείγματος, η πυκνότητα του συστήματος, η οποία είναι σημαντική για τον υπολογισμό της απώλειας πίεσης τριβής μέσα σε έναν σωλήνα, τα υπολειμματικά μέρη των ενεργειακών ιδιοτήτων της μοριακής θερμοχωρητικότητας και της ενθαλπίας, καθώς και ο συντελεστής JT, που είναι σημαντικοί για τον προσδιορισμό των μεταβολών της θερμοκρασίας ενός ρευστού, και τέλος η ταχύτητα του ήχου, που είναι σημαντική για τον καθορισμό της ροής κρίσιμης μάζας των ροών του αγωγού.

Επιπλέον, τα συστατικά που θεωρήθηκαν ως συστατικά ενδιαφέροντος και εξετάστηκαν όταν βρίσκονται αναμεμειγμένα με υδρογόνο ήταν τα κύρια συστατικά του φυσικού αερίου που μπορούν να βρεθούν στην αλυσίδα παραγωγής υδρογόνου μέσω της διαδικασίας αναμόρφωσης ατμού και αυτά είναι: το μεθάνιο, το οποίο είναι το πιο σημαντικό, το αιθάνιο, το προπάνιο, το μονοξείδιο του άνθρακα, το διοξείδιο του άνθρακα και το άζωτο. Μελετήθηκαν μόνο δυαδικά μείγματα και όχι τριαδικά ή πολυσυστατικά συστήματα.

Τέλος, τα θερμοδυναμικά μοντέλα που έχουν δοκιμαστεί για τους παραπάνω υπολογισμούς είναι: η GERG-2008 EoS που είναι η εξίσωση αναφοράς για το φυσικό αέριο και για παρόμοια ρεύματα αερίων και είναι σημαντικό να δούμε αν μπορεί να είναι αξιόπιστη για μείγματα συστατικών αυτών των ρευμάτων όταν αναμιγνύονται με μεγάλες ποσότητες υδρογόνου, οι κλασικές κυβικές καταστατικές εξισώσεις Peng-Robinson και Soave-Redlich-Kwong που είναι πολύ απλές στη χρήση τους και είναι αξιόπιστες για διάφορα μείγματα ανεξάρτητα από την απλότητά τους, ένα πιο περίπλοκο στατιστικό μοντέλο όπως η καταστατική εξίσωση Perturbed-Chain SAFT και τέλος το μοντέλο πρόβλεψης UMR-PRU που είναι το PR EoS σε συνδυασμό με την UNIFAC μέσω του Universal Mixing Rule.

Μετά από λεπτομερή αναζήτηση στη διαθέσιμη διαδικτυακή βιβλιογραφία, συλλέχθηκαν διάφορα σημεία πειραματικών δεδομένων που αναφέρονται στα προαναφερθέντα συστήματα καθαρού υδρογόνου και δυαδικών μιγμάτων που περιέχουν υδρογόνο. Τα διαθέσιμα δεδομένα για το καθαρό υδρογόνο ήταν πολλά, ήταν αξιόπιστα και οδηγούσαν σε



ασφαλή συμπεράσματα όσον αφορά τη σύγκριση της ακρίβειας των μοντέλων. Αυτό δεν ίσχυε για τα διαθέσιμα δεδομένα σε ό,τι αφορά στα δυαδικά μείγματα. Τα δεδομένα θερμοφυσικών ιδιοτήτων έχουν εξαχθεί κυρίως από παλιές πηγές, δεδομένου ότι δεν βρέθηκαν πιο σύγχρονα δεδομένα, και έχουν σαφή εστίαση στην πυκνότητα μιας φάσης για τα συστήματα υδρογόνου αναμειγμένου με μεθάνιο, διοξείδιο του άνθρακα ή άζωτο και για πολύ χαμηλή συγκέντρωση υδρογόνου στα μείγματα αυτά. Με βάση τέτοια δεδομένα, δεν είναι δυνατό να εξαχθούν ασφαλή συμπεράσματα σχετικά με τις σύγχρονες διεργασίες που σχετίζονται με την παραγωγή υδρογόνου, καθώς αυτές θα βασίζονται σε υψηλές συγκεντρώσεις υδρογόνου. Τα διαθέσιμα δεδομένα ισορροπίας ατμού-υγρού οδήγησαν σε ασφαλέστερα αποτελέσματα.

Από τη σύγκριση των θερμοδυναμικών μοντέλων, συνήχθη το συμπέρασμα ότι το GERG-2008 EoS μπορεί να χρησιμοποιηθεί ως εξίσωση αναφοράς για το καθαρό υδρογόνο, καθώς έδωσε τα καλύτερα αποτελέσματα σε όλους τους υπολογισμούς. Η GERG-2008 EoS είναι επίσης αξιόπιστη για τους υπολογισμούς της μονοφασικής πυκνότητας και της ταχύτητας ήχου των έξι δυαδικών μιγμάτων με βάση τα πειραματικά δεδομένα. Εφόσον τα διαθέσιμα δεδομένα αποτυγχάνουν να καλύψουν ένα ευρύ φάσμα συγκεντρώσεων υδρογόνου, η GERG-2008 EoS χρησιμοποιήθηκε για την επέκταση της υπάρχουσας βάσης δεδομένων για την μονοφασική πυκνότητα και την ταχύτητα ήχου σε υψηλότερες συγκεντρώσεις υδρογόνου και βρέθηκε ότι τα υπόλοιπα θερμοδυναμικά μοντέλα δίνουν παρόμοια αποτελέσματα για ένα εύρος συγκεντρώσεων που κυμαίνονται από 0 % έως 100 % υδρογόνο, με την SRK EoS να είναι η πιο αξιόπιστη εξίσωση σε σύγκριση με τη GERG-2008 EoS. Τόσο στην περίπτωση καθαρού υδρογόνου όσο και σε αυτή των δυαδικών μιγμάτων που περιέχουν υδρογόνο, κανένα μοντέλο δεν μπορεί να προβλέψει αρκετά καλά το υπολειπόμενο μέρος της θερμοχωρητικότητας ή τον συντελεστή Joule-Thomson. Οι υπολογισμοί ισορροπίας ατμού-υγρού πραγματοποιήθηκαν καλύτερα με τη UMR-PRU EoS.

Είναι γεγονός πλέον ότι για αυτά τα έξι δυαδικά μείγματα τα μοντέλα που μπορούν να προβλέψουν ικανοποιητικά τις θερμοφυσικές τους ιδιότητες δεν επιτυγχάνουν στην πρόβλεψη της ισορροπίας ατμού-υγρού και το αντίστροφο. Λόγω αυτού του γεγονότος, οι παράμετροι αλληλεπίδρασης των δυαδικών μιγμάτων για, ενδεικτικά, την PR EoS προσδιορίστηκαν εκ νέου. Πραγματοποιήθηκαν προσαρμογές αυτών των παραμέτρων βάσει των πειραματικών δεδομένων για τις πιέσεις σημείου φυσαλίδας, προκειμένου να γίνει αντιληπτό εάν αυτή η τεχνική μπορεί να οδηγήσει τις καταστατικές εξισώσεις στην επίτευξη καλύτερης ακρίβειας. για υπολογισμούς ιδιοτήτων και για υπολογισμούς ισορροπίας ατμού-υγρού ταυτόχρονα.

Τέλος, συνήχθη το συμπέρασμα ότι εάν έπρεπε να προταθεί ένα συγκεκριμένο μοντέλο για κάθε ένα από τα εξεταζόμενα συστήματα αυτά τα μοντέλα θα ήταν: η GERG-2008 EoS για καθαρό υδρογόνο, υδρογόνο-προπάνιο και μονοξείδιο υδρογόνου-άνθρακα, η UMR-PRU EoS για υδρογόνο-αιθάνιο και υδρογόνο-διοξείδιο του άνθρακα και τέλος η PR EoS με προσαρμοσμένο ακεντρικό παράγοντα του υδρογόνου και προσαρμοσμένες παραμέτρους δυαδικής αλληλεπίδρασης για υδρογόνο-μεθάνιο και υδρογόνο-άζωτο.

**Key Words:** Αξιολόγηση πειραματικών δεδομένων για συστήματα που περιέχουν υδρογόνο, Θερμοδυναμική μοντελοποίηση για δυαδικά συστήματα που περιέχουν υδρογόνο, Θερμοδυναμική μοντελοποίηση για το καθαρό, Αξιολόγηση της GERG-2008 EoS για συστήματα που περιέχουν υδρογόνο

## Table of Contents

Acknowledgements.....	i
Abstract .....	ii
Περίληψη.....	iv
Table of Contents .....	vi
List of Tables.....	ix
List of Figures.....	xii
Nomenclature.....	xiv
1. Introduction.....	1
1.1 European energy transition.....	1
1.2 Pure Hydrogen.....	1
1.3 Hydrogen in natural gas streams.....	2
1.4 Hydrogen’s energy and economy.....	3
2. Thermodynamic models.....	4
2.1 Thermodynamic models.....	4
2.1.1 GERG-2008 EoS.....	4
2.1.2 Peng Robinson EoS .....	5
2.1.3 UMR-PRU EoS .....	6
2.1.4 Soave-Redlich-Kwong EoS .....	6
2.1.5 Perturbed-Chain EoS .....	7
2.2 Mathematical formulas .....	8
2.2.1 Vapor Pressure .....	8
2.2.2 Thermophysical Properties.....	8
2.2.3 Vapor-Liquid Equilibrium.....	11
3. Pure hydrogen data and comparison .....	13
3.1 Vapor pressures and thermophysical properties model comparison.....	14
3.2 Alpha functions.....	20
3.3 Discussion .....	20
4. Binaries data and comparison .....	22
4.1 VLE Data evaluation.....	22
4.1.1 Binary mixture of H <sub>2</sub> -CH <sub>4</sub> .....	23
4.1.2 Binary mixture of H <sub>2</sub> -C <sub>2</sub> H <sub>6</sub> .....	28
4.1.3 Binary mixture of H <sub>2</sub> -C <sub>3</sub> H <sub>8</sub> .....	29
4.1.4 Binary mixture of H <sub>2</sub> -CO .....	31

4.1.5 Binary mixture of H <sub>2</sub> -CO <sub>2</sub> .....	33
4.2 Model comparison on VLE calculations.....	40
4.2.1 Binary mixture of H <sub>2</sub> -CH <sub>4</sub> .....	41
4.2.2 Binary mixture of H <sub>2</sub> -C <sub>2</sub> H <sub>6</sub> .....	42
4.2.3 Binary mixture of H <sub>2</sub> -C <sub>3</sub> H <sub>8</sub> .....	43
4.2.4 Binary mixture of H <sub>2</sub> -CO .....	43
4.2.5 Binary mixture of H <sub>2</sub> -CO <sub>2</sub> .....	44
4.2.6 Binary mixture of H <sub>2</sub> -N <sub>2</sub> .....	44
4.3 Thermophysical Data evaluation.....	45
4.3.1 Binary mixture of H <sub>2</sub> -CH <sub>4</sub> .....	45
4.3.2 Binary mixture of H <sub>2</sub> -C <sub>2</sub> H <sub>6</sub> .....	51
4.3.3 Binary mixture of H <sub>2</sub> -C <sub>3</sub> H <sub>8</sub> .....	51
4.3.4 Binary mixture of H <sub>2</sub> -CO .....	51
4.3.5 Binary mixture of H <sub>2</sub> -CO <sub>2</sub> .....	55
4.3.6 Binary mixture of H <sub>2</sub> -N <sub>2</sub> .....	58
4.4 Model comparison on thermophysical properties data.....	61
4.5 Thermophysical properties data extension using GERG-2008 .....	63
4.5.1 Binary mixture of H <sub>2</sub> -CH <sub>4</sub> .....	64
4.5.2 Binary mixture of H <sub>2</sub> -C <sub>2</sub> H <sub>6</sub> .....	66
4.5.3 Binary mixture of H <sub>2</sub> -C <sub>3</sub> H <sub>8</sub> .....	67
4.5.4 Binary mixture of H <sub>2</sub> -CO .....	67
4.5.5 Binary mixture of H <sub>2</sub> -CO <sub>2</sub> .....	68
4.5.6 Binary mixture of H <sub>2</sub> -N <sub>2</sub> .....	68
4.6 Discussion .....	69
5. Determination of the optimum interaction parameters on Peng - Robinson EoS.....	72
5.1.1 k <sub>ij</sub> Regression for the binary mixture of H <sub>2</sub> -CH <sub>4</sub> .....	73
5.1.2 k <sub>ij</sub> Regression for the binary mixture of H <sub>2</sub> -C <sub>2</sub> H <sub>6</sub> .....	75
5.1.3 k <sub>ij</sub> Regression for the binary mixture of H <sub>2</sub> -C <sub>3</sub> H <sub>8</sub> .....	76
5.1.4 k <sub>ij</sub> Regression for the binary mixture of H <sub>2</sub> -CO .....	77
5.1.5 k <sub>ij</sub> Regression for the binary mixture of H <sub>2</sub> -CO <sub>2</sub> .....	78
5.1.6 k <sub>ij</sub> Regression for the binary mixture of H <sub>2</sub> -N <sub>2</sub> .....	79
5.2 Discussion .....	80
6. Conclusions and future work.....	84
References.....	87
Appendices .....	A
Appendix A .....	A

Appendix B..... B  
Appendix C..... D  
Appendix D ..... F  
Appendix E..... H  
Appendix F..... K

## List of Tables

Table 1: Binary mixtures between hydrogen and the main components that can be found in hydrogen's production processes .....	2
Table 2: Table of calculating tools used for the model comparison .....	4
Table 3: Constants used for pure hydrogen's vapor pressure calculation on Antoine equation .....	8
Table 4: Constants used for pure hydrogen's vapor pressure calculation proposed by DIPPR 8	
Table 5: The thermophysical properties in this thesis .....	9
Table 6: The tools that have been used to apply each thermodynamic model.....	13
Table 7: Experimental data temperature and pressure range .....	13
Table 8: Description of the thermodynamic models PR EoS 1 and PR EoS 2 .....	14
Table 9: Description of the thermodynamic models MC EoS 1, MC EoS 2 and PR EoS 3.....	15
Table 10: Mathias-Copeman parameters.....	15
Table 11: Description of the thermodynamic models SRK EoS 1 and SRK EoS 2 .....	16
Table 12: PC-SAFT EoS Hydrogen's proposed pure component parameters.....	16
Table 13: Absolute average deviations % occurred in hydrogen's properties – isobaric data	17
Table 14: Absolute average deviations % occurred in hydrogen's vapor pressure .....	17
Table 15: Absolute average deviations % occurred in Cv calculations after excluding the isobaric subcritical data.....	17
Table 16: The most accurate EoS for each one of the examined properties for pure hydrogen .....	21
Table 17: (a) Pure hydrogen's acentric factor and (b) binary interaction parameters used for the cubic equations of state calculation .....	22
Table 18: Experimental binary VLE data available in online literature .....	23
Table 19: Experimental binary VLE data available in literature for the mixture of H <sub>2</sub> -CH <sub>4</sub> ...	24
Table 20: Experimental data that have been considered as reliable for the binary mixture of H <sub>2</sub> -CH <sub>4</sub> regarding VLE .....	27
Table 21: Experimental binary VLE data available in literature for the mixture of H <sub>2</sub> - C <sub>2</sub> H <sub>6</sub> ..	28
Table 22: Experimental data that have been considered as reliable for the binary mixture of H <sub>2</sub> -C <sub>2</sub> H <sub>6</sub> regarding VLE .....	29
Table 23: Experimental binary VLE data available in literature for the mixture of H <sub>2</sub> -CH <sub>4</sub> ...	30
Table 24: Experimental binary VLE data available in literature for the mixture of H <sub>2</sub> -CO .....	31
Table 25: Experimental data that have been considered as reliable for the binary mixture of H <sub>2</sub> -CO regarding VLE .....	33
Table 26: Experimental binary VLE data available in literature for the mixture of H <sub>2</sub> -CO <sub>2</sub> ...	34
Table 27: Experimental data that have been considered as reliable for the binary mixture of H <sub>2</sub> -CO <sub>2</sub> regarding VLE .....	36
Table 28: Experimental binary VLE data available in literature for the mixture of H <sub>2</sub> -N <sub>2</sub> .....	37
Table 29: Experimental data that have been considered as reliable for the binary mixture of H <sub>2</sub> -N <sub>2</sub> regarding VLE .....	40
Table 30: The number of experimental points that have been used for the evaluation of the thermodynamic models regarding the VLE .....	40
Table 31: Model results for pressure and hydrogen's vapor phase composition of binary mixture of H <sub>2</sub> -CH <sub>4</sub> compared to five thermodynamic models.....	41
Table 32: Model results for pressure and hydrogen's vapor phase composition of binary mixture of H <sub>2</sub> -C <sub>2</sub> H <sub>6</sub> compared to five thermodynamic models.....	42

Table 33: Model results for pressure and hydrogen’s vapor phase composition of binary mixture of H <sub>2</sub> -C <sub>3</sub> H <sub>8</sub> compared to five thermodynamic models.....	43
Table 34: Model results for pressure and hydrogen’s vapor phase composition of binary mixture of H <sub>2</sub> -CO compared to five thermodynamic models.....	43
Table 35: Model results for pressure and hydrogen’s vapor phase composition of binary mixture of H <sub>2</sub> -CO <sub>2</sub> compared to five thermodynamic models.....	44
Table 36: Model results for pressure and hydrogen’s vapor phase composition of binary mixture of H <sub>2</sub> -N <sub>2</sub> compared to five thermodynamic models.....	44
Table 37: Experimental binary thermophysical properties data available in literature .....	45
Table 38: Experimental binary thermophysical properties data available in literature for the mixture of H <sub>2</sub> -CH <sub>4</sub> .....	46
Table 39: Experimental data that have been considered as reliable for the binary mixture of H <sub>2</sub> -CH <sub>4</sub> regarding thermophysical properties .....	51
Table 40: Experimental binary thermophysical properties data available in literature for the mixture of H <sub>2</sub> -CO.....	51
Table 41: Experimental data that have been considered as reliable for the binary mixture of H <sub>2</sub> -CO regarding thermophysical properties .....	55
Table 42: Experimental binary thermophysical properties data available in literature for the mixture of H <sub>2</sub> -CO <sub>2</sub> .....	55
Table 43: Experimental data that have been considered as reliable for the binary mixture of H <sub>2</sub> -CO <sub>2</sub> regarding thermophysical properties .....	58
Table 44: Experimental binary thermophysical properties data available in literature for the mixture of H <sub>2</sub> -N <sub>2</sub> .....	59
Table 45: Experimental data that have been considered as reliable for the binary mixture of H <sub>2</sub> -N <sub>2</sub> regarding thermophysical properties .....	61
Table 46: The number of experimental points that have been used for the evaluation of the thermodynamic models regarding the thermophysical properties.....	62
Table 47: Model accuracy regarding to the available thermophysical-properties experimental data.....	62
Table 48: Model results for the thermophysical properties of binary mixture of H <sub>2</sub> -CH <sub>4</sub> compared to GERG-2008 reference equation.....	65
Table 49: Model results for the thermophysical properties of binary mixture of H <sub>2</sub> -C <sub>2</sub> H <sub>6</sub> compared to GERG-2008 reference equation.....	67
Table 50: Model results for the thermophysical properties of binary mixture of H <sub>2</sub> -C <sub>3</sub> H <sub>8</sub> compared to GERG-2008 reference equation.....	67
Table 51: Model results for the thermophysical properties of binary mixture of H <sub>2</sub> -CO compared to GERG-2008 reference equation.....	68
Table 52: Model results for the thermophysical properties of binary mixture of H <sub>2</sub> -CO <sub>2</sub> compared to GERG-2008 reference equation.....	68
Table 53: Model results for the thermophysical properties of binary mixture of H <sub>2</sub> -N <sub>2</sub> compared to GERG-2008 reference equation.....	69
Table 54: The most accurate EoS for each one of the examined properties for each one of the binary mixtures .....	71
Table 55: Aspen HYSYS’ proposed binary interaction parameters used for the calculations with PR equation of state .....	72
Table 56: Experimental data that have been considered as reliable for the binary mixture of H <sub>2</sub> -CH <sub>4</sub> .....	73

Table 57: The %ARD and AAD for the examined $k_{ij}$ parameters for the binary mixture of H <sub>2</sub> -CH <sub>4</sub> .....	73
Table 58: Experimental data that have been considered as reliable for the binary mixture of H <sub>2</sub> -C <sub>2</sub> H <sub>6</sub> .....	75
Table 59: The %ARD and AAD for the examined $k_{ij}$ parameters for the binary mixture of H <sub>2</sub> -C <sub>2</sub> H <sub>6</sub> .....	76
Table 60: Experimental data that have been considered as reliable for the binary mixture of H <sub>2</sub> -C <sub>3</sub> H <sub>8</sub> .....	76
Table 61: The %ARD and AAD for the examined $k_{ij}$ parameters for the binary mixture of H <sub>2</sub> -C <sub>3</sub> H <sub>8</sub> .....	76
Table 62: Experimental data that have been considered as reliable for the binary mixture of H <sub>2</sub> -CO .....	77
Table 63: The %ARD and AAD for the examined $k_{ij}$ parameters for the binary mixture of H <sub>2</sub> -CO .....	77
Table 64: Experimental data that have been considered as reliable for the binary mixture of H <sub>2</sub> -CO <sub>2</sub> .....	78
Table 65: The %ARD and AAD for the examined $k_{ij}$ parameters for the binary mixture of H <sub>2</sub> -CO <sub>2</sub> .....	79
Table 66: Experimental data that have been considered as reliable for the binary mixture of H <sub>2</sub> -N <sub>2</sub> .....	80
Table 67: The %ARD and AAD for the examined $k_{ij}$ parameters for the binary mixture of H <sub>2</sub> -N <sub>2</sub> .....	80
Table 68: Proposed and regressed binary interaction parameters for the six binary mixtures .....	81
Table 69: Model accuracy regarding to the thermophysical properties experimental data ..	81
Table 70: Model accuracy regarding to the VLE experimental data .....	82
Table 71: The most accurate EoS for each one of the examined properties for pure hydrogen .....	85
Table 72: The most accurate EoS for the calculations regarding pure hydrogen .....	85
Table 73: The most accurate EoS for each one of the examined properties for each one of the binary mixtures .....	85
Table 74: Model selection for the calculations regarding each binary mixture.....	86

## List of Figures

Figure 1: Comparison of PR's predictions of residual isobaric heat capacity with NIST's experimental data in subcritical state .....	18
Figure 2: Comparison of PR EoS 2 and GERG-2008 EoS predictions of vapor pressure with NIST's and DIPPR's experimental data .....	18
Figure 3: Comparison of GERG-2008 EoS, PR EoS 2 and SRK EoS 1 regarding molar density data of pure H <sub>2</sub> .....	19
Figure 4: Comparison of GERG-2008 EoS, PR EoS 2 and SRK EoS 1 regarding isobaric residual molar heat capacity data of pure H <sub>2</sub> .....	19
Figure 5: Temperature behavior of the alpha functions evaluated in this work .....	20
Figure 6: Comparison of Freeth 1931 and Kirk and Ziegler 1967 to the ones of Tsang, Clancy, Street and Calado 1980 at 91.0 K .....	24
Figure 7: Comparison of Augood 1957, Hong and Kobayashi 1981, Hu Lin, Gu and Li 2014 and Kirk and Ziegler 1967 to the ones of Tsang, Clancy, Street and Calado 1980 at 110.0 K.....	25
Figure 8: Comparison of Yorizane, Yoshimura, Masuoko and Toyama 1967 and Sagara, Arai and Saito 1972 to the ones of Tsang, Clancy, Street and Calado 1980 at 142.0 K.....	26
Figure 9: Comparison of Benham 1957 and Sagara, Arai and Saito 1972 to the ones of Hong and Kobayashi 1981 at a temperature of 173.2 K.....	27
Figure 10: Comparison of Cohen, Hipnick 1967, Hiza, Heck, Kidney 1968, Sagara, arai, saito 1972 and Heintz and Street 1982 at two different isotherms of (a) 148.2 K and (b) 173.2 K.	29
Figure 11: Comparison of (a) Buriss, Hsu, Reamer, Sage 1953 at two different isotherms of 277.6 K and 344.3 K and (b) Trust, Kurata 1971 at two different isotherms of 173.2 K and 248.2 K.....	31
Figure 12: Comparison of Akers, Eubanks 1960 and Yorizane, Yoshimura, Masuoko, Toyama 1968 to the ones of Tsang, Clancy, Street and Calado 1980 at a temperature of 122.0 K.....	32
Figure 13: Comparison of Augood 1957 and Verschole 1931 to the ones of Tsang, Clancy, Street and Calado 1980 at a temperature of 83.2 K .....	33
Figure 14: Comparison of Augood 1957 and Spano, Heck, Barrick 1968 to the ones of Tsang, Clancy, Street and Calado 1980.....	34
Figure 15: Comparison of Augood 1957 and Spano, Heck, Barrick 1968 to the ones of Tsang, Clancy, Street and Calado 1980.....	35
Figure 16: Comparison of K. Bezanhtak, G. B. Combes, F. Dehghani, N. R. Foster, and D. L. Tomasko 2002 to the ones of Tsang, Clancy, Street and Calado 1980 .....	36
Figure 17: Comparison of Akers, Eubanks 1960 and Gonikberg, Fastowski, Gurwitsch 1939 to the ones of Street and Calado 1978 at a temperature of 100.0 K .....	38
Figure 18: Comparison of (a) Augood 1957 and Gonikberg, Fastowski, Gurwitsch 1939 and (b) Maimoni 1961, Verschoyle 1931 and Yoshimura, Yorizane, Naka 1971 to the ones of Street and Calado 1978 at a temperature of 77.6 K .....	39
Figure 19: Model comparison regarding the experimental VLE data of the mixture H <sub>2</sub> -CH <sub>4</sub> at 91.0K.....	42
Figure 20: Comparison of Jett, Fleyfel, Kobayashi 1994, Jett 1990 and Hernández-Gómez et al. 2018 at hydrogen composition of 0.05 and (a) 240 K and (b) 275 K.....	47
Figure 21: Comparison of Magee et al. 1985, Jett 1990 and Hernández-Gómez et al. 2018 at (a) 325 K and 170 bar, (b) 325 K and 190 bar and (c) 275 K and 190 bar.....	48
Figure 22: Comparison of Machado 1988 and Hernández-Gómez et al. 2018 at composition of hydrogen equal to 0.1 and (a) 120 bar (b) 190 bar .....	49
Figure 23: Machado 1988 data at two different temperature and pressure conditions.....	50



Figure 24: Comparison of Townend, Bhatt, and Bone 1931 and Scott and Bone 1929 at composition of hydrogen equal to 0.333 and 300 K .....	52
Figure 25: Comparison of Cipollina et al.2007, Scott and Bone 1929 and Townend, Bhatt, and Bone 1931 at 300 K and (a) 170 bar and (b) 200 bar .....	53
Figure 26: Cipollina et al. 2007 data at two different pressure and hydrogen molar composition conditions .....	54
Figure 27: Comparison of Cipollina et al. 2007 and Souissi, Kleinrahm, Yang and Richter 2017 at composition of hydrogen equal to 0.05 and 325 K.....	56
Figure 28: Comparison of Bezanhtak et al. 2002 and Souissi, Kleinrahm, Yang and Richter 2017 at 290 K and hydrogen's composition equal to 0.05.....	57
Figure 29: Bezanhtak et al. 2002 data at a specific pressure and hydrogen molar composition condition.....	57
Figure 30: Comparison of Ababio and McElroy 1993 and Zhang et al. 2002 at 290 K and hydrogen's composition equal to 0.05.....	58
Figure 31: Comparison of Jaeschke and Humphreys 1991, Hernández-Gómez et al. 2017 and Bartlett, Cupples, and Tremearne 1927 at 325 K and a composition of hydrogen equal to (a) 0.25 and (b) 0.50 .....	60
Figure 32: Comparison of Deming and Shupe 1931 and Bartlett et al. 1930 at a composition of hydrogen equal to 0.75 and (a) 203 K and (b) 295 K.....	61
Figure 33: Model comparison with the available datasets in the binary mixture of H <sub>2</sub> -CH <sub>4</sub> . 63	
Figure 34: Comparison of the GREG-2008 equation with the equations of state in the binary mixture of H <sub>2</sub> -CH <sub>4</sub> .....	66
Figure 35: Regression of kij for the mixture of H <sub>2</sub> -CH <sub>4</sub> paired with PR EoS .....	74
Figure 36: Comparison of UMR-PRU EoS and PR EoS with the regressed kij parameter for H <sub>2</sub> -Ch <sub>4</sub> mixture at 91.0 K.....	75
Figure 37: Regression of kij for the mixture of H <sub>2</sub> -CO paired with PR EoS.....	78
Figure 38: Regression of kij for the mixture of H <sub>2</sub> -CO <sub>2</sub> paired with PR EoS.....	79

## Nomenclature

### Latin letters

Symbol	Description	Unit
m	Mass	kg
$\rho$	Molar density	moles/m <sup>3</sup>
$\rho_m$	Mass density	kg/m <sup>3</sup>
T	Temperature	K
P	Pressure	bar
V	Volume	m <sup>3</sup>
T <sub>c</sub>	Critical temperature	K
P <sub>c</sub>	Critical pressure	bar
V <sub>c</sub>	Critical volume	m <sup>3</sup>
R	Global gas constant	J/(moles K)
v	Molar volume	m <sup>3</sup> /moles
MW	Molecular weight	g/moles
u	Fluid velocity	m/sec
w	Speed of sound	m/sec
C <sub>P</sub>	Molar isobaric heat capacity	J/(moles K)
C <sub>V</sub>	Molar isochoric heat capacity	J/(moles K)
H	Molar enthalpy	J/moles
C <sub>1</sub> , C <sub>2</sub> , C <sub>3</sub>	Mathias-Copeman parameters	-
p <sup>s</sup>	Vapor pressure	Bar
k <sub>ij</sub>	Binary interaction parameter	-
m	Number of segments – PC SAFT EoS	-
b	Co-volume in cubic EoS	m <sup>3</sup> /moles
a <sup>i</sup>	Helmholtz energy	J
A <sub>1</sub> -A <sub>2</sub>	PC-SAFT parameters	-
A <sub>mn</sub> , B <sub>mn</sub> , C <sub>m</sub>	UNIFAC fitting parameters	-
G <sup>E</sup>	Gibbs free energy	J
x	Molar fraction in liquid phase	moles/moles
y	Molar fraction in vapor phase	moles/moles
f	Fugacity	bar
K	Equilibrium constant	bar (or Pa)
$\Delta P$	Pressure difference	bar
$\Delta T$	Temperature difference	K
F	Feed flow	kg/h
z	Composition	Moles/moles

## Greek letters

Symbol	Description	Unit
$\alpha$	Attractive parameter in cubic EoS	bar (m <sup>3</sup> /moles) <sup>2</sup>
$\tau$	Reduced temperature	-
$\delta$	Reduced density	-
$\omega$	Acentric factor	-
$\varepsilon$	Energy of segments – PC SAFT EoS	J/moles
$\sigma$	Diameter of segment – PC SAFT EoS	Å
$\kappa^{A_i B_i}$	Volume of association – PC SAFT EoS	-
$\varepsilon^{A_i B_j}$	Energy of association – PC SAFT EoS	J/moles
$\phi$	Fugacity coefficient	-
$\mu_{JT}$	Joule-Thomson coefficient	K/Pa
v	Included data	-
x	Excluded data	-

## Abbreviations

Symbol	Description
NG	Natural gas
RE	Renewable energy
EoS	Equation of state
PR	Peng and Robinson
MC	Mathias-Copeman
UMR-PRU	Universal mixing rules – Peng Robinson UNIFAC
SRK	Soave, Redlich and Kwong
PC	Perturbed chain
SAFT	Statistical associating fluid theory
MSVS	Microsoft Visual Studio
H <sub>2</sub>	Hydrogen
CH <sub>4</sub>	Methane
C <sub>2</sub> H <sub>6</sub>	Ethane
C <sub>3</sub> H <sub>8</sub>	Propane
CO	Carbon monoxide
CO <sub>2</sub>	Carbon dioxide
N <sub>2</sub>	Nitrogen
VLE	Vapor-liquid equilibrium
JT	Joule-Thomson
AAD	Average absolute deviation
ARD	Average absolute relative deviation
BPP	Bubble point pressure

### Subscripts

Symbol	Description
r	Reduced
c	Critical
l	Liquid
v	Vapor
res	Residual part
id	Ideal part
Tot	Total property
<i>i</i>	Component
<i>ij</i>	Cross parameter
calc	Calculated value
exp	Experimental value

### Superscripts

Symbol	Description
o	Ideal part
i	component
AiBi	
l	Liquid
v	Vapor
s	Saturated

### Formulas

Symbol	Description
$f(x)$	Function of variable x
$dx$ or $\Delta x$	Difference of variable x
$\sum_i x_i$	Sum of variable x for I components
$\frac{\partial x}{\partial y}$ or $\frac{dx}{dy}$	First partial or total derivative of variable x with respect to variable y
$\frac{\partial^2 x}{\partial y^2}$ or $\frac{d^2 x}{dy^2}$	Second partial or total derivative of variable x with respect to variable y

# 1. Introduction

## 1.1 European energy transition

The anthropogenic activities of the last decades are causing a continuous increase in the emissions of greenhouse gases into the atmosphere. The gases that are responsible for this phenomenon and are related to global warming and climate change are carbon dioxide, methane, nitrogen dioxide, chlorofluorocarbons and ozone [1]. In December of 2019, the European Commission announced some new environmental targets related to the emission of greenhouse gases. The first goal of the European Union is to achieve a reduction of emissions by 55% (compared to 1990) until 2030 which will lead to the second goal of net-zero emissions and decarbonization by 2050. These targets are aimed to limit the global temperature rise to 1.5 °C [2].

This has led the scientific community to look for sustainable alternatives to energy resources and production. The transition towards a decarbonized energy system is mainly based on renewable energy resources. An idea that has been introduced in recent years is the use of hydrogen as an emerging source of clean energy and as an energy carrier. Hydrogen can be the ideal sustainable substitute for fossil fuels. However, hydrogen isn't always environmentally friendly because in some cases its production processes create unwanted emissions[3].

Renewable or green hydrogen is most commonly produced by water electrolysis powered by renewable energy sources. There have, also, been introduced pathways to produce green hydrogen from biomass. Low-carbon or blue hydrogen is produced via steam reforming of oil, coal or natural gas hydrocarbons, followed by carbon capture and storage[4]. In case of lack of carbon capture and storage technologies, greenhouse gas emissions are directly released into the atmosphere and produced hydrogen is called grey or brown. Today, 96% of hydrogen used as feedstock is produced via steam reforming of light hydrocarbons, and mostly methane, or natural gas (reformers with or without carbon capture and storage) and the remaining 4% is produced by water electrolysis [5].

Including hydrogen into the energy supply chain seems like a very tempting solution to the current environmental crisis. Nevertheless, there are various significant technical, economic and geopolitical challenges that should be considered further; hydrogen's generation costs, storage and transport methods should be examined very carefully.

## 1.2 Pure Hydrogen

Hydrogen, whose critical point is found at 33.15 K and 12.96 bar [6], is one of the most interesting elements on earth. Diatomic hydrogen ( $H_2$ ) is the lightest molecule and at standard conditions it exists in its gaseous form [7]. It is abundant in nature as it is found in various molecular forms with the main forms being water and organic compounds. Diatomic hydrogen normally occurs in two isomeric forms, the ortho- and the para-hydrogen whose equilibrium is temperature dependent. At normal conditions gaseous hydrogen consists of 75% orthohydrogen and the remaining 25% parahydrogen and liquid hydrogen consists of 99.79% parahydrogen and 0.21% orthohydrogen [8]. Due to their different rotational quantum states the two spin isomers differ in some of their physical and thermal properties. Cooling hydrogen gas from room temperature to temperatures close to zero Kelvin degrees make it spontaneously and slowly convert from its normal form to almost 100 % para-hydrogen. The conversion rate can be improved by the use of catalysts and it is practically not affected by

pressure changes. The conversion of ortho to para-hydrogen is also an exothermic conversion. A problem that can be occurred while storing hydrogen in cryogenic vessels is that the unconverted normal hydrogen would release heat while converting spontaneously to para-hydrogen which would evaporate the liquid hydrogen [9]. This phenomenon is called 'boil-off' and is occurred because normal hydrogen's heat of conversion is greater than its heat of vaporization at normal boiling point. This problem can be solved by the addition of catalysts during ortho-hydrogen's liquefaction process.

Something unpleasant about normal hydrogen is its low volumetric density. When it is found in its gaseous form its density value is only around  $0.08 \text{ kg/m}^3$  at normal temperature and pressure conditions but even when it is liquified at temperature set to  $252.9^\circ\text{C}$  and normal pressure (hydrogen's boiling point at normal pressure) hydrogen's density is  $71 \text{ kg/m}^3$ . Comparing to LNG density which normally is between  $430 \text{ kg/m}^3$  and  $470 \text{ kg/m}^3$  it is obvious that larger storage equipment is necessary for the transition to hydrogen energy [8].

Even if hydrogen is a non-toxic, odorless, tasteless, colorless, highly combustible gas, it is highly flammable when mixed with small amounts of oxygen (ordinary air) and this makes it pretty unsafe. Due to hydrogen's physical shape, its leaks are untraceable [7].

### 1.3 Hydrogen in natural gas streams

Even though hydrogen is a very promising substitute of fossil fuels, which are the largest source of global energy at the moment, the transition from natural gas to hydrogen cannot happen immediately. Usually, in natural gas mixtures the molar composition of hydrogen is found as trace or up to 0.05%. The transition to hydrogen energy could be achieved by gradually increasing its composition in natural gas or in similar gases. This occurs because current pipeline and storing vessels have to be tested in order to see if they can be safely used for pure hydrogen's transportation. Pure hydrogen's storage will require gigawatt-scale equipment and pipelines [3], [10].

This is why, apart from detailed examination of pure hydrogen, the mixtures of interest in this current work are the binary systems between hydrogen and methane, ethane, propane, carbon monoxide, carbon dioxide and nitrogen.

*Table 1: Binary mixtures between hydrogen and the main components that can be found in hydrogen's production processes*

Binary mixtures of interest
$\text{H}_2\text{-CH}_4$
$\text{H}_2\text{-C}_2\text{H}_6$
$\text{H}_2\text{-C}_3\text{H}_8$
$\text{H}_2\text{-CO}$
$\text{H}_2\text{-CO}_2$
$\text{H}_2\text{-N}_2$

For this purpose, detailed examination of the available thermodynamic models' accuracy on energy and transport related properties' calculations, relevant to pure hydrogen and mixtures of hydrogen with natural gas or similar gases, should be performed. In this work, focus is placed on the thermophysical behavior of pure hydrogen and on transport and energetic properties of binary mixtures containing hydrogen and components commonly found in NG

or similar gases, such as methane, ethane, propane, nitrogen and carbon monoxide and dioxide. Attention should be paid also to the vapor-liquid equilibrium of the same binary mixtures as it is of major importance as it comes to storage conditions. Based on experimental data that can be found in online literature, the predictive accuracy of several thermodynamic models will be evaluated and better knowledge about the models' behavior will be stated.

#### 1.4 Hydrogen's energy and economy

Hydrogen as an energy carrier could significantly limit the footprint of energy use in a global basis. Energy to hydrogen to energy system includes the steps of production, storage path, scale and method, safety handling regulations and utilization and defines how these stages interact. This system can be illustrated as a square whose corners are covered by the abovementioned four stages and indicates their interaction [3]. It is important to state that hydrogen's production mainly depends on the end-point wanted purity.

In order to achieve the transition towards zero-carbon emissions, huge amounts of hydrogen need to be produced. This process is rather costly and certainly less economically viable compared to the cost of producing and distributing natural gas. Additionally, to achieve energy to hydrogen to energy system, many technical "steps" have to be reached and examined thoroughly in order to achieve the desired production of hydrogen, which also cost economically and environmentally. The transition towards low and then zero carbon emissions supply chain is a very tempting solution to the current environmental crisis. However, to overcome the economic and technical obstacles and achieve a low-carbon hydrogen economy, international standards and targets must be set [3].

## 2. Thermodynamic models

### 2.1 Thermodynamic models

An equation of state is a functional relationship that correlates the state variables of a fluid and is used to perform various thermodynamic-related calculations. Thermodynamic models usually contain some empirical parameters that are fitted to experimental data in order to improve their predictive accuracy. No one of the existing equations of state can predict with significantly high accuracy every pure component's or mixture's behavior for every property in all of the potential conditions. This is why it is important to carefully evaluate each model's behavior for every different case. A general form of an equation of state can be presented as:

$$f(P, V, T) = 0$$

Several thermodynamic models are used in the work to perform calculations regarding to pure hydrogen's and mixtures' containing hydrogen properties. Starting with the cubic equations of state, Peng Robinson[11], Soave Redlich Kwong [12] with hydrogen's experimental acentric factor combined with Soave's alpha function [13] both combined with van der Waals mixing rules[14] and UMR-PRU [15] which is the PR EoS coupled with UNIFAC through the Universal Mixing Rule[16]. Also, the soft equation PC-SAFT [17], [18] is evaluated in terms of pure hydrogen and binary mixtures containing hydrogen. Last but not least, equation GERG-2008[19] is evaluated bellow.

PC-SAFT calculations for the thermophysical properties were performed via Aspen HYSYS. GERG-2008 calculations for the thermophysical properties were performed via the software package AGA8 which is available by NIST. Aspen HYSYS was also used for vapor pressure and vapor-liquid equilibrium calculations with PC-SAFT and GERG-2008. Calculations with PR EoS, SRK EoS and UMR-PRU are accessible via the software package ThermoCalc. A list of the software tools used for the calculations regarding the different thermodynamic models is presented below.

Table 2: Table of calculating tools used for the model comparison

Thermodynamic Model	Tool
GERG-2008 EoS	Aspen HYSYS
Peng Robinson EoS	ThermoCalc-MSVS
Soave Redlich Kwong EoS	ThermoCalc-MSVS
UMR-PRU EoS	ThermoCalc-MSVS
PC-SAFT EoS	Aspen HYSYS

#### 2.1.1 GERG-2008 EoS

GERG-2008 is a multi-fluid mixture model which can be used for temperatures between 60 K and 700 K and pressures up to 70 MPa. It is usually used as a reference equation of state for natural gases and similar mixtures. The GERG-2008 equation consists of an ideal part, a pure components' contribution part and a departure function and can be written as:

$$\alpha(\delta, \tau, \bar{x}) = \alpha^o(\rho, T, \bar{x}) + \sum_{i=1}^N x_i \alpha_{oi}^r(\delta, \tau) + \Delta\alpha^r(\delta, \tau, \bar{x}) \quad (1)$$

where  $\delta$  and  $\tau$  stand for the reduced density and temperature of the mixture and they only depend on the mixture's composition  $\bar{x}$ .



$$\delta = \frac{\rho}{\rho_r(\bar{x})} \quad (2) \quad \text{and} \quad \tau = \frac{T}{T_r(\bar{x})} \quad (3)$$

The departure function contains the sum of binary specific and generalized departure functions, which can be developed for single binary mixtures or for a group of binary mixtures and is expressed as shown below:

$$\Delta\alpha^r(\delta, \tau, \bar{x}) = \sum_{j=i+1}^N \sum_{i=1}^{N-1} \Delta\alpha_{ij}^r(\delta, \tau, \bar{x}) \quad (4)$$

The calculations of thermophysical properties and vapor-liquid equilibrium of a mixture are based on the derivatives of  $\alpha$  with respect to reduced density, reduced temperature and the mixture's composition.

Pure component and interaction parameters used by GERG-2008 EoS are presented in Appendix B.

### 2.1.2 Peng Robinson EoS

The PR EoS can be written as:

$$P = \frac{RT}{v-b} - \frac{a(T)}{v \cdot (v+b) + b \cdot (v-b)} \quad (5)$$

where P stands for pressure, T for temperature, v for molar volume and R for the universal gas constant. Parameters b and a(T) arise from the components' critical point as written below:

$$b = \frac{0.0780 \cdot R \cdot T_c}{P_c} \quad (6)$$

$$a(T) = \left[ \frac{0.45724 \cdot R^2 \cdot T_c^2}{P_c} \right] \alpha(T) \quad (7)$$

where  $T_c$  and  $P_c$  stand for critical temperature and pressure. The original PR alpha function,  $\alpha(T)$ , proposed by Soave is presented by equations 8 and 9.

$$\alpha(T) = \left[ 1 + \kappa \cdot \left( 1 - \left( \frac{T}{T_c} \right)^{0.5} \right) \right]^2 \quad (8)$$

$$\kappa = 0.37464 + 1.54226 \cdot \omega - 2.6992 \cdot \omega^2 \quad (9)$$

where  $\omega$  stands for every component's acentric factor.

In order to achieve better representation of the thermodynamic properties different alpha function models can be used. A commonly used model, especially in supercritical conditions, is the alpha function introduced by Mathias and Copeman (1983).

$$\alpha(T) = \left[ 1 + C_1 \cdot \left( 1 - \left( \frac{T}{T_c} \right)^{0.5} \right) + C_2 \cdot \left( 1 - \left( \frac{T}{T_c} \right)^{0.5} \right)^2 + C_3 \cdot \left( 1 - \left( \frac{T}{T_c} \right)^{0.5} \right)^3 \right]^2 \quad (10)$$

where  $C_1$ ,  $C_2$  and  $C_3$  are parameters for each component.

If the value of temperature is greater than the critical temperature, parameters  $C_2$  and  $C_3$  are equal to zero.

In case of mixtures instead of pure components the classical Van der Waals mixing rules are used for the calculation of parameters  $b$  and  $a(T)$  and as a result, equations 11 and 12 are reformulated.

$$b = \sum_i x_i b_i \quad (11)$$

$$a(T) = \sum_i \sum_j x_i x_j (a_i a_j)^{0.5} (1 - k_{ij}) \quad (12)$$

### 2.1.3 UMR-PRU EoS

UMR-PRU is a predictive equation of state originally proposed by Voutsas et al. that couples PR EoS with an original UNIFAC-type  $G^E$  model via the Universal Mixing Rules.

$$\frac{a}{b R T} = \frac{1}{A} \left( \frac{G_{comp}^E}{R T} + G_{res}^E \right) + \sum_i x_i \frac{a_i}{b_i R T} \quad (13)$$

$$b = \sum_i \sum_j x_i x_j \left( \frac{b_i^{0.5} b_j^{0.5}}{2} \right)^2 \quad (14)$$

Parameter  $a$  is the EoS attractive parameter,  $b$  is the co-volume,  $A$  equals to  $-0.53$  for PR EoS and  $G_{comp-SG}^E$  and  $G_{res}^E$  stand for the Staverman-Guggenheim terms of the combinatorial and residual term of the UNIFAC activity coefficient model. The UNIFAC binary interaction parameter  $\Psi_{mn}$  between two groups which is used for the calculation of the residual excess Gibbs energy is presented below:

$$\Psi_{mn} = e^{-\frac{A_{mn} + B_{mn}(T-298.15) + C_{mn}(T-298.15)^2}{T}} \quad (15)$$

where  $A_{mn}$ ,  $B_{mn}$  and  $C_{mn}$  are parameters determined after fitting the model results to binary phase equilibrium data.

The UNIFAC group interaction parameters used for UMR-PRU are presented in Table A-1 in Appendix 1.

The UMR-PRU model is very successful when applied to hydrocarbon mixtures, polar and associating mixtures and mixtures containing mercury. This model performs calculations regarding vapour-liquid equilibrium, dew points, K values and liquid dropouts with comparably high accuracy.

### 2.1.4 Soave-Redlich-Kwong EoS

The SRK EoS is given by the expression:

$$P = \frac{R T}{v - b} - \frac{a(T)}{v \cdot (v + b)} \quad (16)$$

where  $P$  stands for pressure,  $T$  for temperature,  $v$  for molar volume and  $R$  for the universal gas constant. Parameters  $b$  and  $a(T)$  arise from the components' critical point as written below:

$$b = \frac{0.08664 \cdot R \cdot T_c}{P_c} \quad (17)$$

$$\alpha(T) = \left[ \frac{0.42748 \cdot R^2 \cdot T_c^2}{P_c} \right] \alpha(T) \quad (18)$$

where  $T_c$  and  $P_c$  stand for critical temperature and pressure. Soave's expression for the alpha function is written below.

$$\alpha(T) = \left[ 1 + \kappa \cdot \left( 1 - \left( \frac{T}{T_c} \right)^{0.5} \right) \right]^2 \quad (19)$$

$$\kappa = 0.480 + 1.574 \cdot \omega - 0.176 \cdot \omega^2 \quad (20)$$

where  $\omega$  stands for every component's acentric factor.

In case of mixtures instead of pure components mixing rules must be used for the calculation of parameters  $b$  and  $a(T)$  and as a result, equations 17 and 18 are reformulated as established in equations 11 and 12.

### 2.1.5 Perturbed-Chain EoS

The PC-SAFT is a molecular model proposed by Gross and Sadowski in 2001. Molecules are conceived to be chains of freely jointed spherical segments. Perturbation theories define that molecules' interactions can be divided into a reference and a perturbation term. The reference term represents the repulsive forces and the perturbation term represents the attractive forces of the molecules. For the calculation repulsive forces, the reference fluid should be defined as a hard-chained fluid in which no intermolecular attraction is observed. The attractive forces are divided into further contributions, such as dispersion, association and multi-polar contributions.

Most of thermodynamic properties can be obtained by proper differentiation of Helmholtz free energy. This is the reason that statistical thermodynamics (SAFT equations) use the residual Helmholtz energy achieve the requested calculations. Equation 21 analyzes further the residual Helmholtz energy.

$$a^{res} = a^{seg} + a^{chain} + a^{assoc} \quad (21)$$

where  $a^{seg}$  stands for the segment's Helmholtz energy, including hard sphere reference and dispersion term,  $a^{chain}$  is the contribution from chain formation and  $a^{assoc}$  is the contribution from association.

$$\frac{a^{chain}}{R \cdot T} = \sum_i x_i \cdot (1 - m_i) \cdot \ln[g_{ii} \cdot (d_{ii})^{hs}] \quad (22)$$

$$\frac{a^{assoc}}{R \cdot T} = \sum_i x_i \left[ \sum_{A_i} \ln X^{A_i} - \frac{X^{A_i}}{2} \right] + \frac{M_i}{2} \quad (23)$$

$$a^{seg} = (a^{hs} - a^{disp}) \cdot \sum_i x_i \cdot m_i \quad (24)$$

$$\frac{a^{disp}}{k \cdot N \cdot T} = \frac{A_1}{k \cdot N \cdot T} + \frac{A_2}{k \cdot N \cdot T} \quad (25)$$

Equations 22-25 demonstrate the formula of every term's calculation, where  $X^{A_i}$  is the fraction of molecules  $I$  not bonded to  $A$ ,  $M_i$  is the number of association sites on molecule  $I$ ,

$g_{ii}$  is the radial distribution function. The PC-SAFT dispersion term is expressed by the sum of a first order and a second order perturbation term. As presented in equations 26 and 27,  $A_1$  and  $A_2$  have a dependance on molar density, composition and molecule size.

$$\frac{A_1}{k \cdot N \cdot T} = -2\pi\rho m^2 \cdot \frac{\varepsilon}{kT} \cdot \sigma^3 \cdot \int_1^\infty \tilde{u}(x) \cdot g^{hc} \cdot \left(m; x \frac{\sigma}{d}\right) \cdot x^2 dx \quad (26)$$

$$\frac{A_2}{k \cdot N \cdot T} = -\pi\rho m \cdot \left(1 + Z^{hc} + \rho \cdot \frac{\partial Z^{hc}}{\partial \rho}\right)^{-1} \cdot m^2 \cdot \left(\frac{\varepsilon}{kT}\right)^2 \cdot \sigma^3 \cdot \frac{\partial}{\partial \rho} \cdot \left[\rho \int_1^\infty \tilde{u}(x)^2 \cdot g^{hc} \cdot \left(m; x \frac{\sigma}{d}\right) \cdot x^2 dx\right] \quad (27)$$

where  $x$  is the reduced radial distance around segment,  $\tilde{u}(x)$  is the reduced potential function and  $g^{hc} \cdot \left(m; x \frac{\sigma}{d}\right)$  is the average segment-segment radial distribution function of hard-chain fluid with temperature dependent segment diameter  $d$ .

In SAFT EoS every component is characterized by the following pure component parameters: the number of segments ( $m$ ), diameter of segment ( $\sigma$ ), energy of segment ( $\varepsilon$ ), volume of association ( $\kappa^{A|Bj}$ ) and energy of association ( $\varepsilon^{A|Bj}$ ).

## 2.2 Mathematical formulas

### 2.2.1 Vapor Pressure

For the vapor pressure calculation two different expressions are used; equation 28, Antoine equation, and equation 29, a fit equation proposed by DIPPR (DIPPR 101) [20][21].

$$\log(P^s) = A - \frac{B}{T + C} \quad (28)$$

where  $T$  is measured in Kelvin degrees and  $P^s$  in bar and

$$\ln(P^s) = a + \frac{b}{T} + c \cdot \ln(T) + d \cdot T^e \quad (29)$$

where  $T$  is measured in Kelvin degrees and  $P^s$  in Pascal.

The constants proposed by NIST and DIPPR for pure Hydrogen are as follows:

Table 3: Constants used for pure hydrogen's vapor pressure calculation on Antoine equation

Antoine constants for pure hydrogen		
A	B	C
3.54314	99.395	7.726

Table 4: Constants used for pure hydrogen's vapor pressure calculation proposed by DIPPR

DIPPR constants for pure hydrogen				
A	b	c	d	e
12.752	-95.133	1.0974	0.000336	2

### 2.2.2 Thermophysical Properties

As it comes to fuels' production, storage and transport, the prediction of pure components' and mixtures' thermophysical properties is of major importance. In this work emphasis will be

placed on the molar density, which is important for calculating the frictional pressure loss inside a pipe, the residual parts of the energetic properties of molar heat capacity and enthalpy and also JT coefficient, which are important for determining temperature changes of a fluid, and lastly the speed of sound, which is important for defining the critical mass flux of pipeline flows.

Table 5: The thermophysical properties in this thesis

Evaluated properties
Single-phase molar density
Molar residual isobaric heat capacity
Molar residual isochoric heat capacity
Molar residual enthalpy
Speed of sound
Joule-Thomson coefficient

Molar density can be calculated as indicated below:

$$\rho = \frac{1}{v} = \frac{P}{z R T} \quad (30)$$

where z stands for the fluids' compressibility factor at conditions of temperature T and pressure P, R for the global gas constant and v for fluid's molar volume.

Mass density is defined as:

$$\rho_m = \frac{m}{V} \quad (31)$$

where m stands for the mass and V for the volume of the fluid.

Detailed knowledge of isobaric heat capacity can be utilized in processes that are affected by enthalpy change and in the design of isobaric processes. It is defined as the enthalpy derivative with respect to temperature under constant pressure as indicated in equation 32

$$C_P = \left( \frac{\partial H}{\partial T} \right)_P \quad (32)$$

Total isobaric heat capacity results from the sum of the ideal isobaric heat capacity (ideal part) and the deviation from the ideal isobaric heat capacity in given conditions (residual part).

$$C_P = C_{P,id} + C_{P,res} \quad (33)$$

In terms of pure components  $C_{P,id}$  is calculated as a third-degree polynomial as indicated in equation 34.

$$C_{P,id} = a + b T + c T^2 + d T^3 \quad (34)$$

Isochoric heat capacity is defined as the internal energy derivative with respect to temperature under constant volume as indicated in equation 35.

$$C_V = \left( \frac{\partial U}{\partial T} \right)_V \quad (35)$$

Similar to total isobaric heat capacity, total isochoric heat capacity results from the sum of the ideal isochoric heat capacity (ideal part) and the deviation from the ideal isochoric heat capacity in given conditions (residual part).

$$C_V = C_{V,id} + C_{V,res} \quad (36)$$

The relationship between  $C_{p,id}$  and  $C_{V,id}$  is given below:

$$C_{p,id} = C_{V,id} + R \quad (37)$$

Enthalpy is an extensive property which is calculated as the sum of the system's internal energy and the product of its pressure and volume. For inhomogeneous systems, the total enthalpy can be measured as the sum of the enthalpies of the subsystems.

$$H(S, p) = U + p V \quad (38)$$

Combining the first and second law of thermodynamics, the calculation of the enthalpy change can be easily achieved as shown below.

$$dH(S, p) = T dS + V dp \quad (39)$$

The total enthalpy changes for pure components (as a function of temperature and pressure) is defined as follows:

$$dH = \left(\frac{\partial H}{\partial T}\right)_P dT + \left(\frac{\partial H}{\partial P}\right)_T dP \quad (40)$$

Total enthalpy results from the sum of the ideal enthalpy (ideal part) and the deviation from the ideal enthalpy in given conditions (residual part).

$$H = H_{id} + H_{res} \quad (41)$$

Sound velocity is an important physical variable for the energy industry as it is used to detect hydrates and other physical obstacles in gas pipelines.

The resulting wave equation if infinite number of low-frequency sound waves is assumed is presented below:

$$\frac{\partial^2 u_x}{\partial t^2} = w \frac{\partial^2 u_x}{\partial x^2} \quad (42)$$

Where a fluid's speed velocity,  $w$ , is given from the equation 42

$$w^2 = \left(\frac{\partial P}{\partial \rho_m}\right)_S \quad (43)$$

Where  $P$  is the fluid's pressure and  $\rho_m$  its mass density.

Equation (43) is valid if:

- i. Pressure changes are small
- ii. The effect of viscosity is neglected
- iii. The speed of the fluid is small relative to the sound velocity

Another expression for the calculation of speed of sound is;

$$w^2 = \frac{1}{MW} \frac{C_p}{C_v} \left(\frac{\partial P}{\partial \rho}\right)_T \quad (44)$$

Where  $V$  stands for the fluid's volume and  $MW$  for its molar weight

For a fluid to be determined as compressible or incompressible it is of major importance to know the speed of sound value. Sound velocity is used to perform Mach's number calculation. If Mach's number is smaller or equal to 3 a fluid's flow is defined as incompressible. Mach's number,  $M$ , is calculated as:

$$M = \frac{u}{w} \quad (45)$$

In thermodynamics, the Joule–Thomson effect describes the temperature change of a real gas or liquid when it is forced through a valve or porous plug while keeping it insulated so that no heat is exchanged with the environment. Accurate prediction of JT coefficient is of major importance for the determination of pipeline, throttling process and as liquefaction process conditions.

At the event of temperature decrease while performing throttling process (cooling) JT coefficient turns negative and vice versa. In terms of ideal gases, JT coefficient equals zero as the temperature of an ideal gas does not change during an isenthalpic process.

$$\mu_{JT} = \left( \frac{\partial T}{\partial H} \right)_P \quad (46)$$

Combining equations (40) and (46);

$$\mu_{JT} = \frac{-\left( \frac{\partial H}{\partial P} \right)_T}{C_p} \quad (47)$$

### 2.2.3 Vapor-Liquid Equilibrium

Gibbs phase rule relates the effect of the least number of independent variables upon the various phases that exist in an equilibrium system containing a given number of components.

When two phases of a mixture are at thermodynamic equilibrium the fugacities of all of its components are also in equilibrium;

$$f_i^v = f_i^L \quad (48)$$

Where fugacity is a function of temperature, pressure and composition of a given mixture.

To determine the fugacity term in vapor state;

$$f_i^v = \phi_i^v y_i P \quad (49)$$

And for the liquid state;

$$f_i^L = \phi_i^L x_i f_i^o = \gamma_i x_i P_i^s \quad (50)$$

Where  $\gamma$  stands for the activity factor,  $y_i$  and  $x_i$  for the vapor and liquid component compositions and  $P_i^s$  for the vapor pressure.

After the assumption of ideal behavior in vapor and liquid phase, the simplified Raoult's law is presented;

$$f_i^v = y_i P \quad (51) \quad \text{and} \quad f_i^L = x_i P_i^s \quad (52)$$

Or

$$y_i P = x_i P_i^s \quad (53)$$

In normal temperature and pressure conditions, vapor phase is close to the ideal behavior in contrast to the liquid phase, thus in high pressure condition nor the vapor neither the liquid phase should be assumed to behave ideally. In systems that high pressure is occurred, the balance ration K is determined as presented below;

$$K_i = \frac{y_i}{x_i} = \frac{\varphi_i^L}{\varphi_i^V} \quad (54)$$

The bubble point is the starting point of boiling of the liquid phase with a composition x where it acquires the first bubble with a composition y. The calculation is performed repeatedly until the equation 55 converges.

$$\sum_i y_i = \sum_i K_i x_i \quad (55)$$

The definition and calculation of the dew point is similar. It is defined as the start point of liquefaction of gas when the vapor phase with composition y where it acquires the first drop with composition x.

$$\sum_i x_i = \sum_i \frac{y_i}{K_i} \quad (56)$$

Two phases are formed during the expansion of a fluid: the vapor phase, which moves to the top of the separation vessel (V), and liquid phase, which moves to the bottom (L). For given feed flow (F), composition (z), temperature, and pressure and if the system has reached the thermodynamic equilibrium, the VLE calculations can be performed accurately.

$$y_i = \frac{F K_i z_i}{F + V(K_i - 1)} \quad (57)$$

$$\sum_i (y_i - x_i) = \sum_i \frac{F (K_i - 1) z_i}{F + V(K_i - 1)} = 0 \quad (58)$$

The iterative solutions proposed by various equations of state reveal useful information regarding designing and optimizing processes linked to natural gas supply chain.



### 3. Pure hydrogen data and comparison

In order to be able to evaluate properly hydrogen-containing streams' behavior it is important to have the ability to predict pure hydrogen's behavior with high accuracy. Due to its quantum nature, predicting accurately hydrogen's behavior and properties, especially in low temperature and pressure conditions, can be very challenging. For this purpose, the reference equation of state GERG-2008 along with the classical cubic equations of state Peng-Robinson and Soave-Redlich-Kwong and also the Perturbed-Chain SAFT equation have been used to predict pure hydrogen's behavior. Regarding to the cubic equations of state, it will be evaluated whether the use of hydrogen's experimental acentric factor can lead to satisfactorily accurate results or if a fitted acentric factor, as the one proposed by Aspen HYSYS, could be a better choice. Focusing even more on PR EoS, the effect of the alpha-function that is combined with the EoS will be presented below. It is examined whether Mathias and Copeman alpha-function can be used instead of Soave's alpha-function. Mathias and Copeman alpha-function is a three-parameter equation which, compared to Soave's one-parameter expression for the alpha-function, could give better results after a successful parameter regression.

Table 6: The tools that have been used to apply each thermodynamic model

Thermodynamic Model	Software tool used for the calculations
GERG-2008	AGA8 code / NIST [22]
Peng-Robinson EoS	ThermoCalc-MSVS
Soave-Redlich-Kwong EoS	ThermoCalc-MSVS
PC-SAFT EoS	Aspen HYSYS

In this work, hydrogen's vapor pressures and thermophysical properties will be calculated and compared to experimental data that are available on the NIST and DIPPR Databases[6]. The abovementioned thermodynamic models will be tested on terms of their accuracy in a wide temperature and pressure range for hydrogen in both its subcritical and supercritical state. Specifically, vapor pressure data were collected from NIST and DIPPR Databases for a temperature range between pure hydrogen's triple and critical point and the thermophysical properties were collected from the NIST Database for a temperature between 200 K and 360 K and a pressure range between 1 bar and 2000 bar. The examined thermophysical properties are molar density, the residual part of molar isobaric and isochoric heat capacity, the residual part of molar enthalpy, speed of sound and Joule-Thomson coefficient.

Table 7: Experimental data temperature and pressure range

Property	Temperature range (K)	Pressure range (bar)	Reference
Vapor pressure, $P^s$	21.12 – 32.47	1.2 – 11.8	NIST, DIPPR
Molar density	200 - 360	1.0 – 2000.0	NIST
Molar residual $C_p$	200 - 360	1.0 – 2000.0	NIST
Molar residual $C_v$	200 - 360	1.0 – 2000.0	NIST
Molar residual $H$	200 - 360	1.0 – 2000.0	NIST
Speed of sound	200 – 360	1.0 – 2000.0	NIST
JT coefficient	200 - 360	1.0 – 2000.0	NIST

### 3.1 Vapor pressures and thermophysical properties model comparison

The temperature range in which the calculations for the thermodynamic properties were performed is between 200 K and 360 K and the pressure range is between 1 bar and 2000 bar. At standard conditions hydrogen is in supercritical state, it has an experimental acentric factor equal to  $\omega = -0.215$  and its critical point is at 33.44 K and 13.16 bar. DIPPR and NIST Databases and also Aspen HYSYS all propose the same critical point approximately.

The average absolute relative deviations of the vapor pressure and the thermophysical properties' calculations and the average absolute relative deviations along with the average absolute deviations for hydrogen's vapor pressure, residual  $C_p$  and  $C_v$  and also JT coefficient calculations compared to the experimental data are presented below on Tables 13 and 14.

$$\%ARD = \frac{\sum \left| \frac{\text{experimental value} - \text{calculated value}}{\text{experimental value}} \right| \times 100\%}{\sum \text{Number of values}} \quad (59)$$

$$AAD = \frac{\sum |\text{experimental value} - \text{calculated value}|}{\sum \text{Number of values}} \quad (60)$$

Initially, the reference equation of state GERG-2008 was used to perform pure hydrogen's volumetric density, constant pressure and constant volume heat capacity, molar enthalpy, speed of sound, Joule-Thomson coefficient and vapor pressure calculations. Tables 13 and 14 briefly show the absolute average deviations that occurred. It is shown that GERG-2008, as expected, results in the highest accuracy for all of the abovementioned properties, except from residual  $C_p$ , and gives significantly better results especially for molar density, residual  $C_v$  and speed of sound, compared to the rest of the evaluated thermodynamic models. Nevertheless, it fails predict JT coefficient resulting in significant relative deviations over 100 % and it cannot predict accurately residual  $C_p$  and  $C_v$  resulting in significant relative deviations between 25 % and 30 %.

Using the experimental acentric factor proposed combined with Soave's alpha function, hydrogen's volumetric density, constant pressure and constant volume heat capacity, molar enthalpy, speed of sound and Joule-Thomson coefficient were calculated (PR EoS 1). The calculations were repeated using an acentric factor equal to  $\omega = -0.120$  (2), which was proposed by Aspen HYSYS, in order to reduce the observed errors (PR EoS 2) (see Table 8).

Table 8: Description of the thermodynamic models PR EoS 1 and PR EoS 2

	PR EoS 1	PR EoS 2
Tc (K)	33.44	33.44
Pc (bar)	13.16	13.16
$\omega$	-0.215	-0.12
Thermodynamic model	Peng-Robinson EoS	Peng-Robinson EoS
Alpha function	Soave's expression	Soave's expression

Additionally, hydrogen's vapor pressure was calculated using these two different acentric factors and was compared with the data proposed by NIST and DIPPR. The temperature range for these calculations is between its triple point and its critical point, or between 21.12 K and 32.47 K.

Tables 13 and 14 briefly show the absolute average deviations that occurred. It is obvious that when PR EoS 2 is used instead of PR EoS 1 the properties' behavior is more accurate. The only thermodynamic properties that are predicted better using  $\omega=-0.215$  are constant volume heat capacity only regarding to the isothermal data. PR EoS 1 and PR EoS 2 gave almost the same results at residual molar enthalpy and speed of sound predictions. Regarding to the calculated vapor pressure, the deviation between the experimental and generated data tends to zero when calculated with PR EoS 2.

It was also evaluated whether using Mathias and Copeman expression for the alpha function instead of Soave's expression could result in a better behavior for the abovementioned thermodynamic properties. For this evaluation, the parameters of Mathias-Copeman alpha function were adjusted in order to minimize the deviation between the experimental and calculated values of hydrogen's vapor pressure (MC EoS 1) [23], vapor pressure and total molar enthalpy (MC EoS 2) [23] and between Soave's and Mathias-Copeman's alpha function values (MC EoS 3) using  $\omega=-0.120$ . The Mathias-Copeman parameters are represented in table 10.

Table 9: Description of the thermodynamic models MC EoS 1, MC EoS 2 and PR EoS 3

	MC EoS 1 [23]	MC EoS 2 [23]	MC EoS 3
T <sub>c</sub> (K)	33.44	33.44	33.44
P <sub>c</sub> (bar)	13.16	13.16	13.16
$\omega$	-0.12	-0.12	-0.12
Thermodynamic model	Peng-Robinson EoS	Peng-Robinson EoS	Peng-Robinson EoS
Alpha function	Mathias-Copeman expression	Mathias-Copeman expression	Mathias-Copeman expression
Parameters were fitted to	Vapor pressure data	Vapor pressure and total enthalpy data	PR EoS 2

Table 10: Mathias-Copeman parameters

	C <sub>1</sub>	C <sub>2</sub>	C <sub>3</sub>
MC EoS 1	0.030123	-0.01982	0.002968
MC EoS 2	0.028501	-0.014564	-0.0018776
MC EoS 3	0.191792	0.005291	0.001

Tables 13 and 14 briefly show the absolute average deviations that occurred. As expected, the use of Mathias-Copeman equation (MC EoS 3) instead of Soave (PR EoS 2) results in almost the same values for most of the properties. A different behavior is observed in the calculated molar enthalpy whose absolute average deviation from the experimental data is minimized using the model MC EoS 2. This behavior is expected because the model MC EoS 2 has been chosen to minimize this specific error. Another property that behaves differently is again constant volume heat capacity. Regarding to its isobaric data, PR EoS 2 predicts the property's behavior more accurately. Regarding to the isothermal data, MC EoS 1 gives the shortest deviation which is, however, over 100%.

The same calculations were repeated again using SRK EoS for the properties' predictions. For these calculations two different values of the acentric factor were used;  $\omega=-0.215$  (SRK EoS 1) and  $\omega=-0.120$  (SRK EoS 2).

Table 11: Description of the thermodynamic models SRK EoS 1 and SRK EoS 2

	SRK EoS 1	SRK EoS 2
T <sub>c</sub> (K)	33.44	33.44
P <sub>c</sub> (bar)	13.16	13.16
ω	-0.215	-0.12
Thermodynamic model	Soave-Redlich-Kwong EoS	Soave-Redlich-Kwong EoS
Alpha function	Soave's expression	Soave's expression

Tables 13 and 14 briefly show the absolute average deviations that occurred. As it is shown in table 13, SRK EoS 1 and 2 can predict more accurately than PR EoS the following properties; hydrogen's  $C_p$ ,  $C_v$  and JT coefficient and it also gives very accurate results while predicting the rest of hydrogen's properties. SRK EoS 1 accurately predicts vapor pressure data.

Finally, the calculations of pure hydrogen's molar density, constant pressure heat capacity and molar enthalpy were performed using PC-SAFT EoS using the two sets of parameters proposed by literature [24] shown in Table 12. Pure hydrogen's mass density data were collected for a range of temperature between 200 K and 400 K and a range of pressure between 400 bar and 1000 bar in order to perform a regression for the pure component parameters (PC-SAFT EoS 1). The second set of pure hydrogen's parameters (PC-SAFT EoS 2) is presented after a regression via regression software in Aspen Plus using Maximum Likelihood as the objective function and Britt and Luecke's algorithm.

PC SAFT EoS 1 and 2 failed to predict hydrogen's vapor pressure when it is in liquid phase for a temperature range between the triple and critical point, which is a significant failure of the model. A different set of pure component parameters should be introduced and evaluated in order to predict hydrogen's behavior more accurately with PC SAFT EoS.

Tables 13 and 14 briefly show the absolute average deviations that occurred. It is obvious that this thermodynamic method results in significantly big deviations for the properties' calculations, except from the molar density calculations. Molar density's calculations are accurate, especially while using PC-SAFT 2, due to the fact that the model's parameters were calculated after PC-SAFT's pure component parameters were fitted to mass density data. PC-SAFT 1 gave slightly better results than PC-SAFT 2 only while calculating the residual molar enthalpy of pure hydrogen. In general, PC-SAFT EoS resulted in the least accurate model for the calculation of pure hydrogen's thermodynamic properties. Additionally, the properties' values were more accurately calculated for pressure values between 400 bar and 1000 bar for both PC-SAFT 1 and PC-SAFT 2, because the regressions for the sets of parameters were performed between this range of pressure.

Table 12: PC-SAFT EoS Hydrogen's proposed pure component parameters

	M (g/mol)	m	σ (Å)	ε/k (K)
PC-SAFT EoS 1	2.016	0.8285	2.973	12.53
PC-SAFT EoS 2	2.016	0.935864	2.912599	25.62934

Table 13: Absolute average deviations % occurred in hydrogen's properties – isobaric data

	AADd %	AADC <sub>p,res</sub> %	AADC <sub>v,res</sub> %	AADh <sub,res< sub=""> %</sub,res<>	AADJT %	AADw %
GERG-2008	0.05	33.9	31.8	2.5	104.4	0.5
PR EoS 1	3.4	32.2	91.9	2.4	346.8	3.0
PR EoS 2	1.3	19.4	63.6	3.3	147.5	2.3
MC EoS 1	2.3	32.1	101.9	2.4	336.1	2.7
MC EoS 2	2.7	30.8	87.6	2.4	337.2	2.9
MC EoS 3	1.2	19.1	63.9	3.3	138.1	2.3
SRK EoS 1	1.2	10.5	69.8	3.8	120.7	3.9
SRK EoS 2	2.2	16.5	60.9	5.1	67.5	4.0
PC-SAFT EoS 1	3.1	55.9	-	14.5	-	-
PC-SAFT EoS 2	2.6	21.8	-	16.2	-	-

Table 14: Absolute average deviations % occurred in hydrogen's vapor pressure

	AADPs % NIST database	AADPs % DIPPR database
GERG-2008	0.002	2.6
PR EoS 1	2.7	2.5
PR EoS 2	0.2	0.01
MC EoS 1	3.0	2.8
MC EoS 2	3.1	2.9
MC EoS 3	10.7	10.9
SRK EoS 1	1.6	1.5
SRK EoS 2	10.9	11.1
PC-SAFT EoS 1	-	-
PC-SAFT EoS 2	-	-

It was found that the absolute average deviations when calculating the  $C_v$  at hydrogen's subcritical state were over 100%. These large deviations were observed due to the fact that in low pressure conditions the experimental  $C_v$  values tend to zero. Specifically, the isobaric and isothermal experimental data at 1 and 10 bar are of the order of  $10^{-2}$  or smaller. Excluding these data from the data set, the calculated errors are reduced significantly as it is shown at Table 15.

Table 15: Absolute average deviations % occurred in  $C_v$  calculations after excluding the isobaric subcritical data

	PR EoS 1	PR EoS 2	MC EoS 1	MC EoS 2	MC EoS 3	SRK EoS 1	SRK EoS 2
AADC <sub>v,res</sub> %	90.4	48.8	102.4	85.5	49.5	59.7	39.8

What is important to note is that cubic equations of state fail to predict the behavior of hydrogen's thermodynamic properties in its subcritical state due to its quantum nature. For example, hydrogen's residual  $C_p$  data and PR EoS 1 prediction is presented in Figure 1.

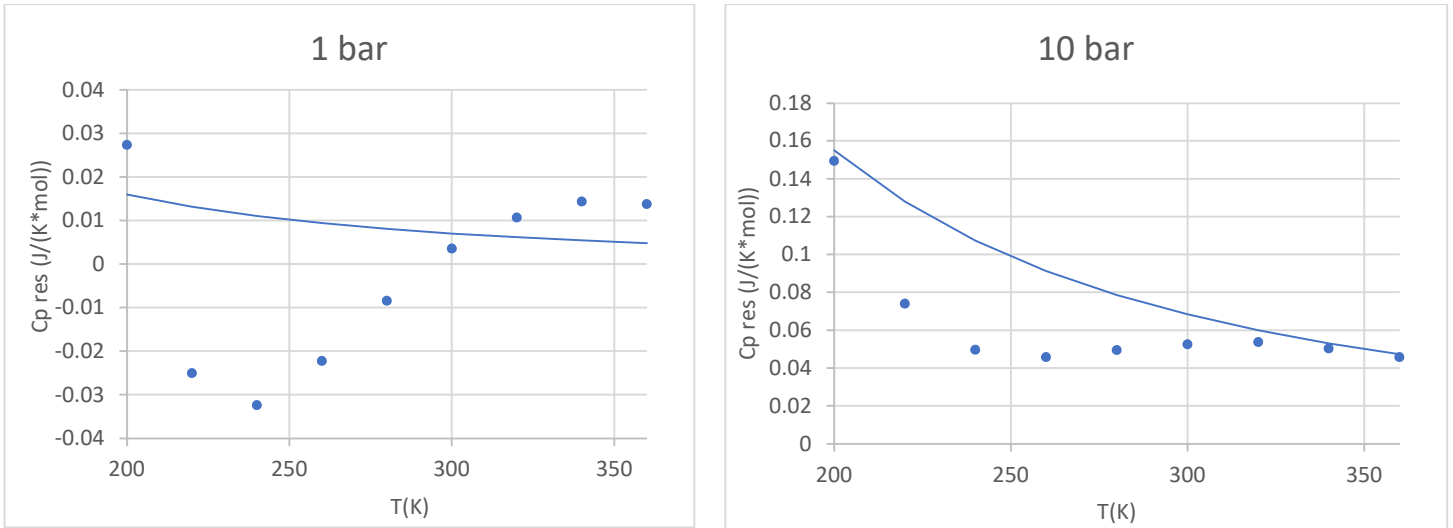


Figure 1: Comparison of PR's predictions of residua isobaric heat capacity with NIST's experimental data in subcritical state

The behavior of the properties using the evaluated thermodynamic models is presented indicatively below. In the following diagrams PR EoS 2 is presented as a continuous line while the rest of the models are presented as dashed lines.

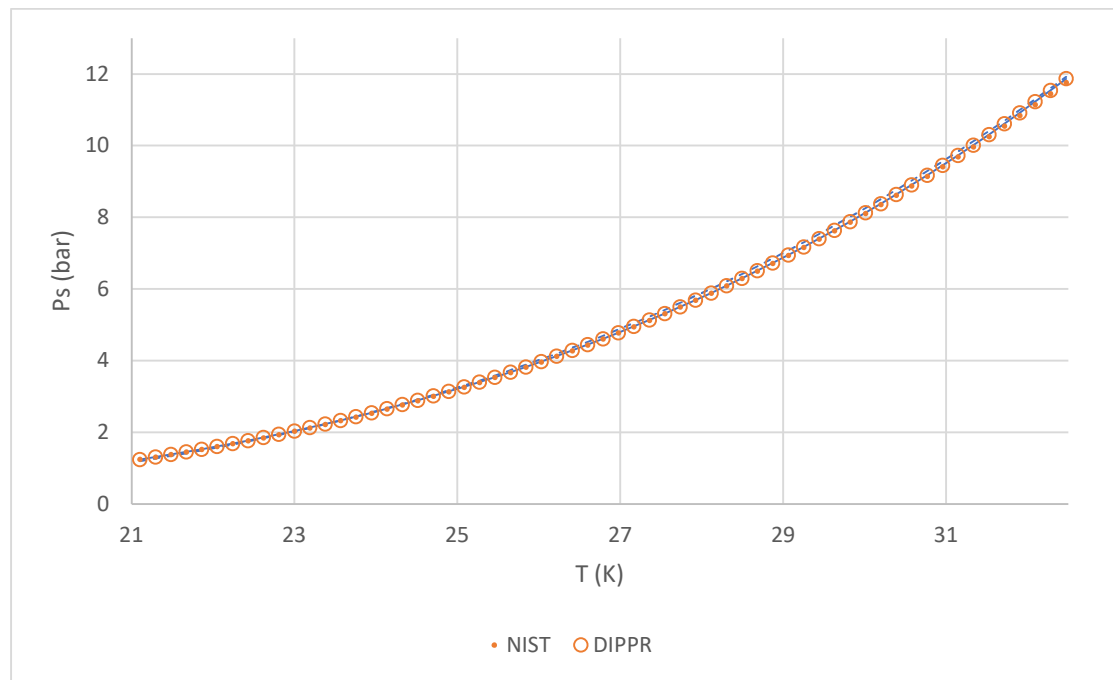


Figure 2: Comparison of PR EoS 2 and GERG-2008 EoS predictions of vapor pressure with NIST's and DIPPR's experimental data

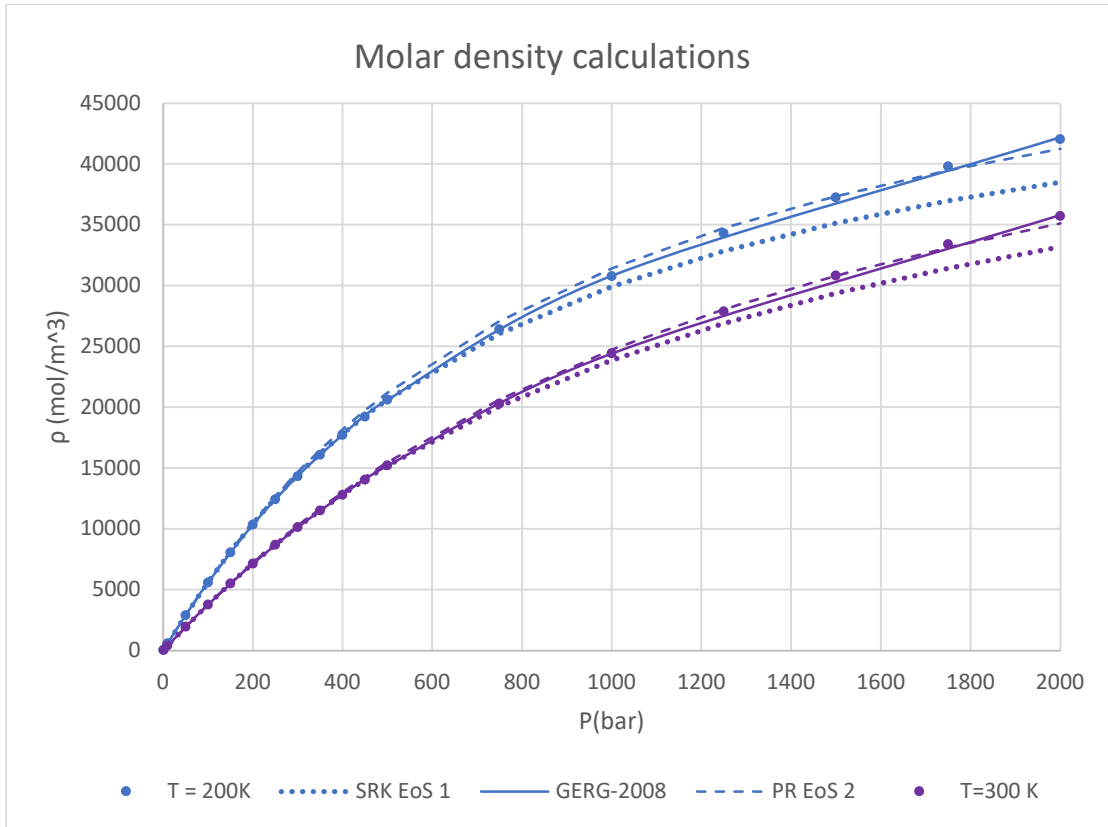


Figure 3: Comparison of GERG-2008 EoS, PR EoS 2 and SRK EoS 1 regarding molar density data of pure H2

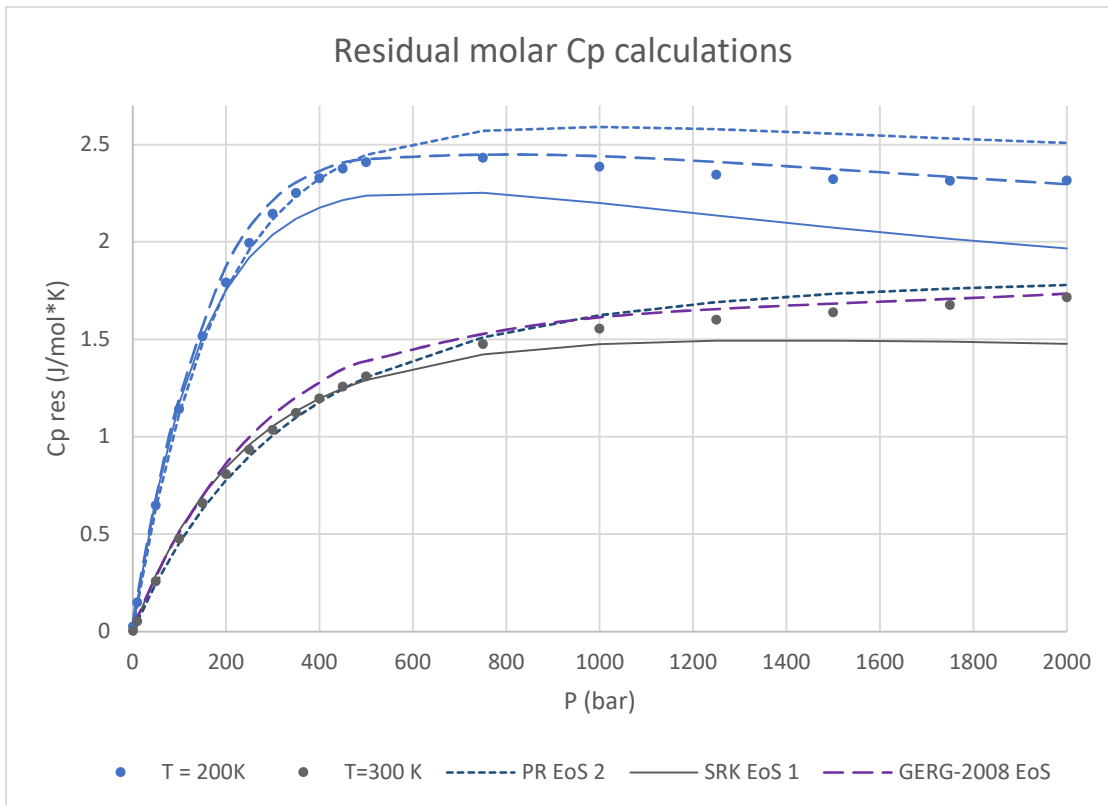


Figure 4: Comparison of GERG-2008 EoS, PR EoS 2 and SRK EoS 1 regarding isobaric residual molar heat capacity data of pure H2

### 3.2 Alpha functions

With a focus on accurate prediction of component's supercritical region, it has been shown that alpha-functions paired with cubic equations of state have to be consistent[25]. In order to achieve this, the alpha-function must agree with the following mathematical criteria. The alpha-function; must be of class  $C^2$  meaning that its first and second derivatives in terms of temperature must be continuous, has to be positive ( $\alpha(T) > 0$ ), monotonically decreasing ( $\frac{d\alpha}{dT} \leq 0$ ) and convex ( $\frac{d^2\alpha}{dT^2} \geq 0$ ) and also satisfy  $\frac{d^2\alpha}{dT^2} \leq 0$  for all of the temperature range. It is important to state that both Soave and Mathias-Copeman alpha-functions, and all of the published alpha-functions, fail the consistency test, which means that inaccuracy is expected while predicting hydrogen's supercritical state.

The expressions of the alpha functions that were used in the thermodynamic properties' calculations are presented in Figure 5. The curve of PR EoS 1 tends to zero at a slow rate while the curve of SRK EoS 2 has the biggest slope of the evaluated curves. Though, the calculated thermodynamic properties were better predicted while using Peng-Robinson EoS combined with the expression of PR EoS 2 for the alpha function or RSK EoS combined with the expression of SRK EoS 1 for the alpha function. The choice of the alpha function that will be combined with the cubic equation of state greatly affects the model's predictions.

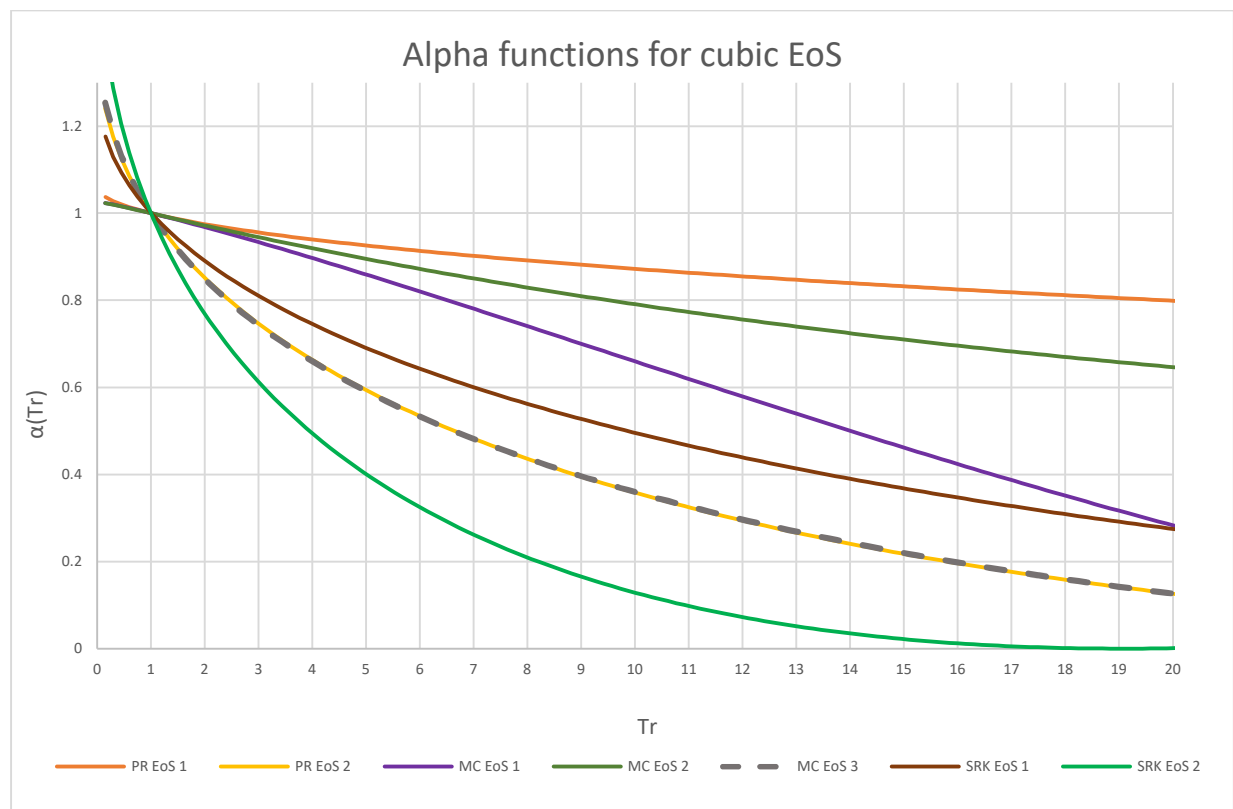


Figure 5: Temperature behavior of the alpha functions evaluated in this work

### 3.3 Discussion

The equation of state GERG-2008 which is a reference equation as it comes to natural gases and similar gases, as expected, performs the most accurate behavior in almost all of the examined calculations. It fails to perform the highest accuracy only when it comes to residual molar  $C_p$ . Even though it is the most accurate of the evaluated models, it cannot be used for the JT coefficient calculations and shouldn't be used for residual molar  $C_p$  and  $C_v$  either



because it performs significantly high errors regarding to the experimental data of these properties.

It is shown that PR EoS with a fitted acentric factor, such as  $\omega=-0.12$  suggested by Aspen HYSYS (PR EoS 2), and SRK EoS combined with hydrogen's experimental acentric factor (SRK EoS 1) can be used to predict accurately hydrogen's thermodynamic properties at its supercritical state. At its subcritical state and at high pressure conditions the results of the thermodynamic models are not so accurate. Hydrogen's quantum nature makes the prediction of its properties in subcritical state quite challenging and inaccurate while using common cubic equations of state.

For the calculations of hydrogen's thermodynamic properties, using PR EoS combined with Soave's expression for the alpha function and an adjusted acentric factor, such as the one proposed by Aspen HYSYS (PR EoS 2), instead of Hydrogen's experimental acentric factor (PR EoS 1) resulted in better calculations. The use of Mathias and Copeman alpha function instead of Soave's expression can also lead to reliable results when the three parameters have been properly adjusted. It is important to note that the choice of the alpha function that will be combined with the cubic equation of state greatly affects the model's predictions.

For the calculations of hydrogen's thermodynamic properties, using SRK EoS combined with Soave's expression for the alpha function and an adjusted acentric factor, such as the one proposed by Aspen HYSYS (SRK EoS 2), instead of Hydrogen's experimental acentric factor (SRK EoS 1) resulted in worse calculations.

Hydrogen's residual molar density, residual  $C_p$ , residual molar enthalpy, speed of sound and vapor pressure can be calculated satisfactorily using PR EoS with fitted acentric factor (PR EoS2) and SRK EoS with the experimental acentric factor (SRK EoS 1). Significant errors are observed in the calculation of constant volume heat capacity and Joule-Thomson coefficient. SRK EoS with a fitted acentric factor gave the best results regarding to constant volume heat capacity and Joule-Thomson coefficient predictions. Nevertheless, SRK with the fitted acentric factor proposed by Aspen HYSYS (SRK EoS 2) fails to predict properly hydrogen's vapor pressures.

Additionally, it is shown that PC-SAFT EoS cannot predict satisfactorily pure hydrogen's thermodynamic properties, except from the molar density. Very accurate prediction of molar density data is expected because the two sets of pure parameters that were evaluated in this work were created after a fit to hydrogen's density data. The biggest failure of the model is that it cannot predict hydrogen's vapor pressures. A different set of pure component parameters should be introduced and evaluated in order to predict hydrogen's behavior more accurately with PC SAFT EoS.

To conclude the abovementioned statements GERG-2008 EoS is the equation that should be preferred for the calculations regarding to pure hydrogen since it's the one that results in the smallest deviations for every property except  $C_{p,res}$ .

Table 16: The most accurate EoS for each one of the examined properties for pure hydrogen

	d	$C_{p,res}$	$C_{v,res}$	$H_{,res}$	w	JT	$p^S$
Thermodynamic Model	GERG-2008	SRK EoS 1	GERG-2008				
Software Tool	AGA8 code / NIST	ThermoCalc	AGA8 code / NIST				

## 4. Hydrogen-containing binary mixtures' data and comparison

The storage equipment and the pipelines that can be applicable to mixtures containing hydrogen are designed based on the physical and thermodynamical properties of the mixtures. These properties reveal important information about the mixtures' behavior in specific temperature and pressure conditions and also reveal how the mixtures are affected from possible changes on these conditions. Additionally, detailed knowledge of the natural gas and similar gas mixtures containing hydrogen VLE's is essential because it can lead to the selection of the optimum storage and transport temperature and pressure conditions.

It is shown that the choice of acentric factor for pure components can widely affect the behavior of cubic equations of state while calculating its properties. To achieve more accurate results when it comes to the cubic equations of state different values of the acentric factor of pure hydrogen are used while performing calculations with PR EoS and SRK EoS. It is found that when using PR EoS the acentric factor of pure hydrogen proposed by ASPEN HYSYS results in more accurate predictions, while in the case of SRK EoS the experimental acentric factor behaves better. What is also worth mentioning is that the binary interaction parameters used for the calculations with PR EoS and SRK EoS have been extracted from ASPEN HYSYS' database.

After performing and evaluating the vapor pressure and thermophysical properties calculations for pure hydrogen of several thermodynamic models it can be concluded that when using PR EoS a fitted acentric factor for hydrogen should be included instead of the experimental one, when using SRK EoS the experimental acentric factor for hydrogen results into better predictions and when using PC-SAFT EoS the second set of pure component parameters proposed in Table 11 should be preferred. These conclusions were taken into consideration while performing the binary mixtures calculations. The model parameters that were used for the thermophysical properties' and VLE calculations are presented in Table 17. The binary parameters used by PC-SAFT EoS are set to zero as proposed by Aspen HYSYS.

Table 17: (a) Pure hydrogen's acentric factor and (b) binary interaction parameters used for the cubic equations of state calculation

(a)

Thermodynamic model	Acentric factor for hydrogen
PR EoS	-0.12
SRK EoS	-0.215

(b)

Binary mixture	PR EoS Kij parameters from Aspen HYSYS	SRK EoS Kij parameters from Aspen HYSYS
H <sub>2</sub> -CH <sub>4</sub>	0.202	0.0001
H <sub>2</sub> -C <sub>2</sub> H <sub>6</sub>	0.2231	0.0001
H <sub>2</sub> -C <sub>3</sub> H <sub>8</sub>	0.2142	0.0001
H <sub>2</sub> -CO	0.0253	-0.0007
H <sub>2</sub> -CO <sub>2</sub>	0.1202	0.1164
H <sub>2</sub> -N <sub>2</sub>	-0.036	-0.001

### 4.1 VLE Data evaluation

Detailed knowledge of the vapor-liquid equilibrium of natural gas mixtures related to operation of natural gas pipelines is essential. It is important to understand the different behavior of the natural gas and relative gas mixtures when they are mixed with hydrogen and the accuracy of the predictions of various thermodynamic models in these mixtures.

The two-phase data that were found in online-literature and will be used for evaluation of the abovementioned thermodynamic models are presented in Table 18. Plenty of vapor-liquid equilibrium datasets regarding to the binaries of H<sub>2</sub>-CH<sub>4</sub>, H<sub>2</sub>-CO, H<sub>2</sub>-CO<sub>2</sub> and H<sub>2</sub>-N<sub>2</sub> were found and evaluated. As for the binaries of H<sub>2</sub>-C<sub>2</sub>H<sub>6</sub>, H<sub>2</sub>-C<sub>3</sub>H<sub>8</sub>, the available datasets are more limited. Since natural gas mixtures mainly contain CH<sub>4</sub> it is of major importance that especially the binary mixture of H<sub>2</sub>-CH<sub>4</sub> should be carefully examined.

Table 18: Experimental binary VLE data available in online literature

Binary mixture	T range (K)	P range (bar)	Number of x points (hydrogen's liquid molar composition)	Number of y points (hydrogen's vapor molar composition)	Reference
H <sub>2</sub> -CH <sub>4</sub>	90.6-183.1	2.2-1379.8	385	386	[26], [27],[28],[29]
H <sub>2</sub> -C <sub>2</sub> H <sub>6</sub>	100.2-280.2	5.8-5595	321	328	[26],[30]
H <sub>2</sub> -C <sub>3</sub> H <sub>8</sub>	98.2-360.9	17.2-551.6	61	82	[26]
H <sub>2</sub> -CO	23.5-298.1	0.3-608.0	274	282	[26], [29]
H <sub>2</sub> -CO <sub>2</sub>	219.9-298.3	1.0-1689.6	213	222	[26], [31], [29]
H <sub>2</sub> -N <sub>2</sub>	63.2-122.0	1.2-293.0	204	192	[26],[32], [29]

It is shown that the choice of acentric factor for pure components can widely affect the behavior of cubic equations of state while calculating its properties. To achieve more accurate results when it comes to PR EoS two different values of the acentric factor of pure hydrogen are used while performing VLE calculations. It is found that when using PR EoS, the acentric factor of pure hydrogen proposed by ASPEN HYSYS results in less accurate predictions, while in the case of the experimental acentric factor the results are better. What is also worth mentioning is that the binary interaction parameters used for the calculations with PR EoS and SRK EoS and the pure component parameters for GERG-2008 EoS and PC-SAFT EoS have been extracted from ASPEN HYSYS' database. The interaction parameters used for UMR-PRU have been extracted from publications related to UMR-PRU[15], [23]. For the binary mixture of hydrogen and carbon monoxide the calculations will not be performed with UMR-PRU EoS because there are no published adjusted parameters yet.

#### 4.1.1 Binary mixture of H<sub>2</sub>-CH<sub>4</sub>

For the binary mixture of H<sub>2</sub>-CH<sub>4</sub> there are nine available datasets regarding to VLE data covering a wide range of experimental temperature and pressure values.

Table 19: Experimental binary VLE data available in literature for the mixture of H<sub>2</sub>-CH<sub>4</sub>

Dataset	T range (K)	P range (bar)	NP x	NP y
Augood 1957	111.700	23.8-180.3	3	2
Benham 1957	116.5-172	33.8-158.6	10	10
Freeth 1931	90.6	17.11-198.34	14	19
Hong and Kobayashi 1980	108.2-183.1	13.9-284.1	132	129
Hu, Lin, Gu and Li 2014	100.1-120.5	2.37-22.7	22	22
Sagara, Arai and Saito 1972	103.1-173.6	10.7-108.3	27	27
Tsang, Clancy, Calado and Street 1980	92.3-150.0	2.2-1379.8	128	128
Yorizane, Yoshimura, Masuoko and Toyama 1967	103.2-163.2	11-152	24	24
Kirk and Ziegler 1967	90.7-110.0	15.3-126.3	25	25

The comparison of the data of the different datasets is to be presented in detail below.

In this case, the dataset of Street and Calado 1980 is the one that covers the widest range of temperature and pressure conditions and it contains a lot of experimental points which helps at the evaluation of the available datasets.

Comparing the data of Freeth 1931 and Kirk and Ziegler 1967 to the ones of Tsang, Clancy, Street and Calado 1980 at a temperature of 91.0 K the data of Freeth 1931 don't seem to be very accurate.

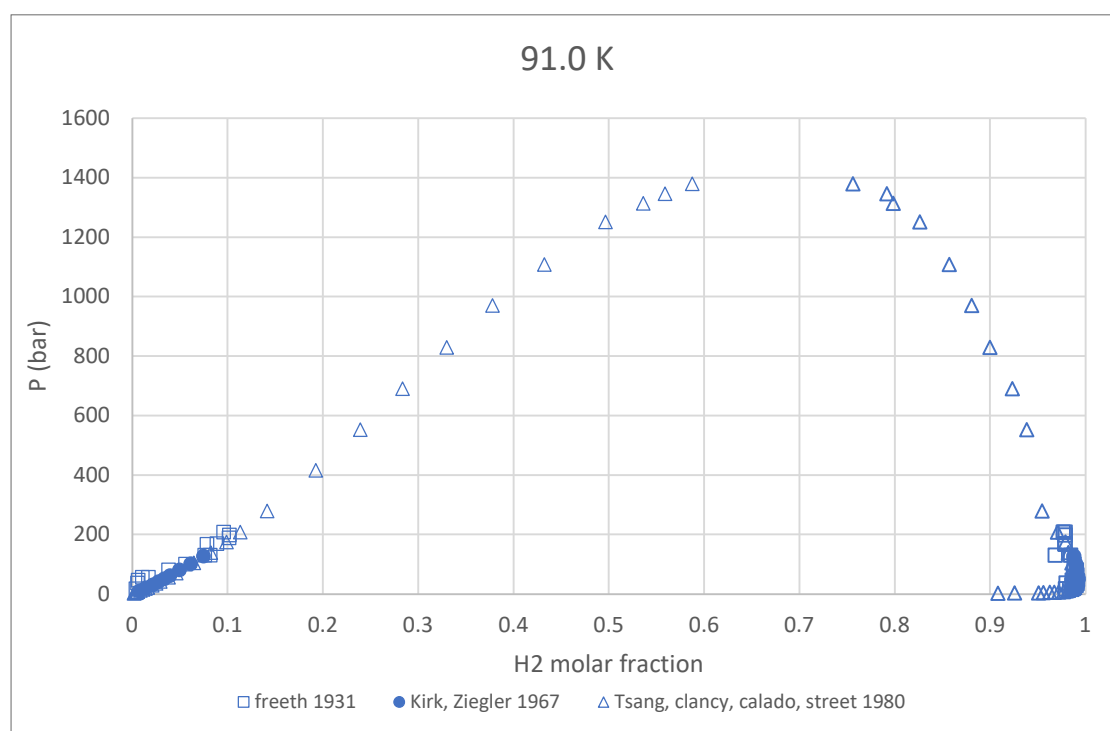


Figure 6: Comparison of Freeth 1931 and Kirk and Ziegler 1967 to the ones of Tsang, Clancy, Street and Calado 1980 at 91.0 K

Comparing the data of Augood 1957, Hong and Kobayashi 1981, Hu Lin, Gu and Li 2014 and Kirk and Ziegler 1967 to the ones of Tsang, Clancy, Street and Calado 1980 at a temperature of 110.0 K the data of Augood 1957 present slightly lower composition values at specific pressures comparing to the rest of the datasets.

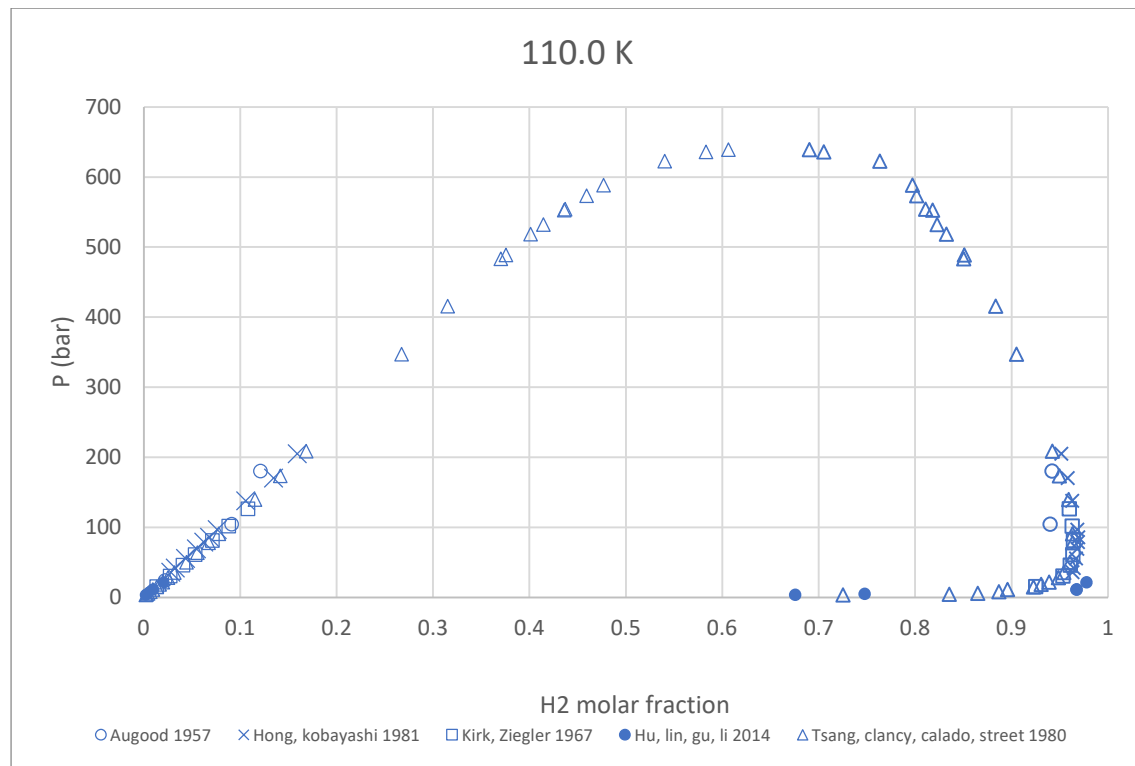


Figure 7: Comparison of Augood 1957, Hong and Kobayashi 1981, Hu Lin, Gu and Li 2014 and Kirk and Ziegler 1967 to the ones of Tsang, Clancy, Street and Calado 1980 at 110.0 K

Comparing the data of Yorizane, Yoshimura, Masuoko and Toyama 1967 and Sagara, Arai and Saito 1972 to the ones of Tsang, Clancy, Street and Calado 1980 at a temperature of 142.0 K The data of both Yorizane, Yoshimura, Masuoko and Toyama 1967 and Sagara, Arai and Saito 1972 present slightly lower vapor composition values for hydrogen at specific pressures comparing to Tsang, Clancy, Street and Calado 1980.

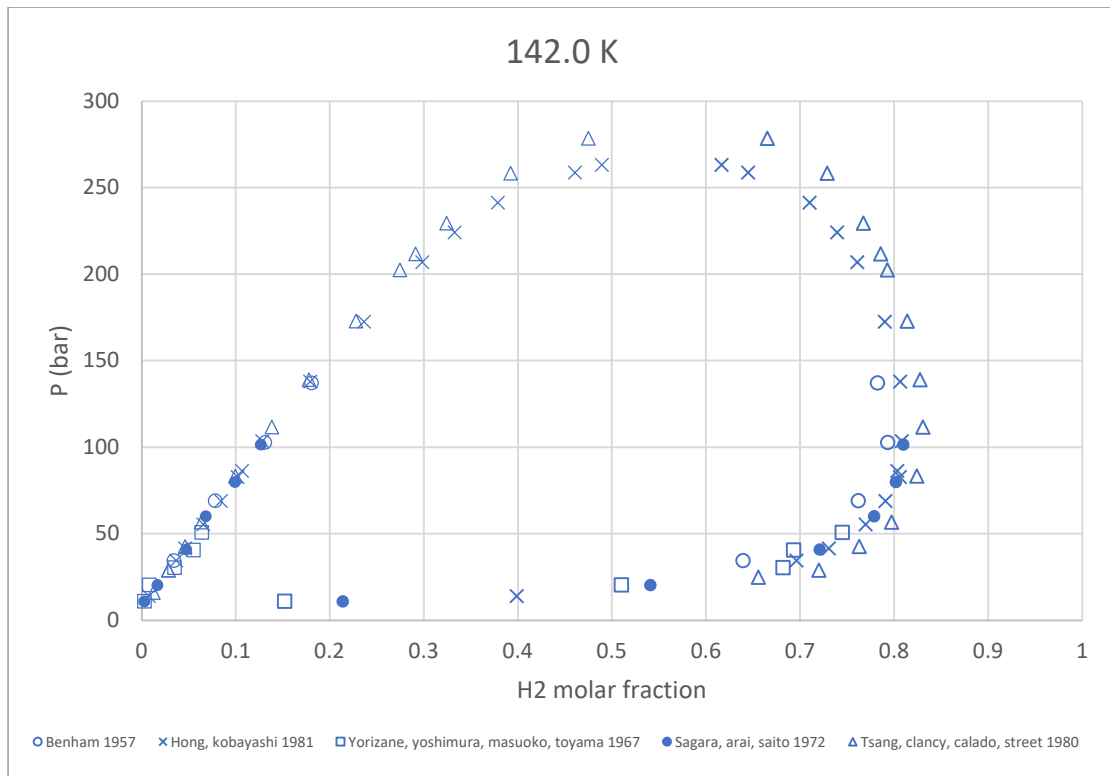


Figure 8: Comparison of Yorzane, Yoshimura, Masuoko and Toyama 1967 and Sagara, Arai and Saito 1972 to the ones of Tsang, Clancy, Street and Calado 1980 at 142.0 K

Comparing the data of Benham 1957 and Sagara, Arai and Saito 1972 to the ones of Hong and Kobayashi 1981 at a temperature of 173.2 K the data of Benham 1957 present lower liquid composition and higher vapor composition values for hydrogen at specific pressures comparing to Hong and Kobayashi 1981.

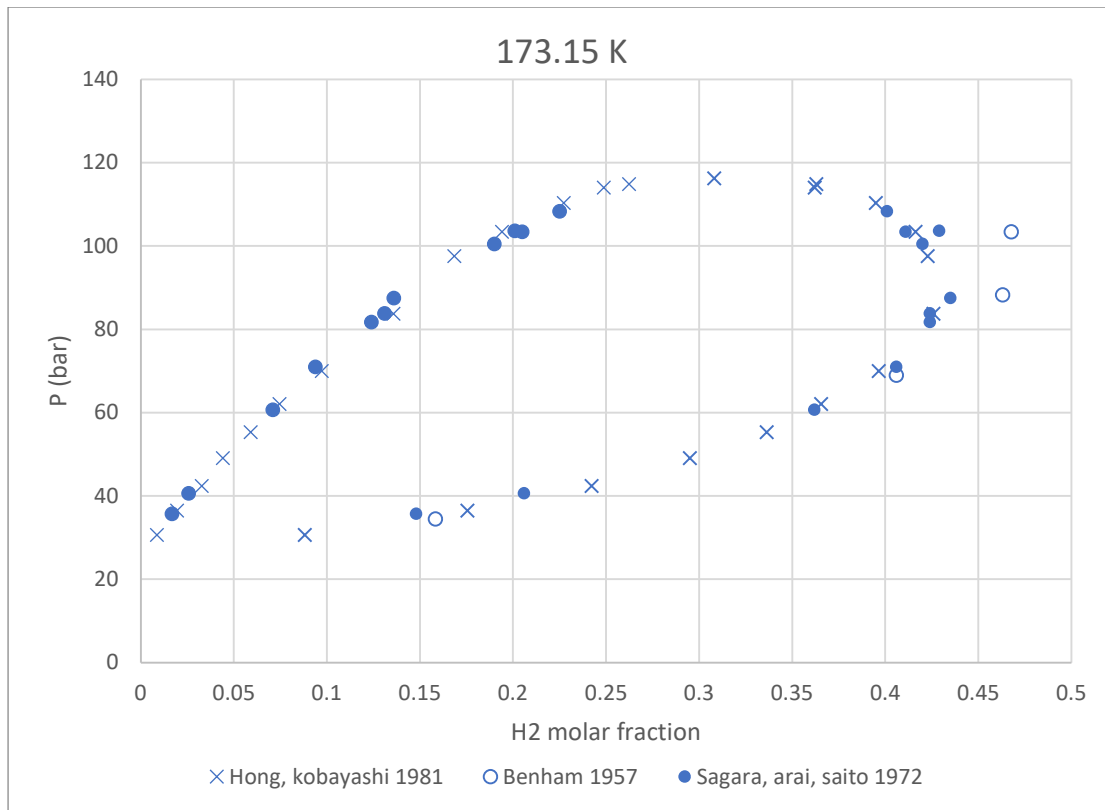


Figure 9: Comparison of Benham 1957 and Sagara, Arai and Saito 1972 to the ones of Hong and Kobayashi 1981 at a temperature of 173.2 K

Concluding the abovementioned statements, the nine datasets compare well to each other with no significant deviations on their behavior. Although the data of Augood 1957, Freeth 1931 and Benham 1957 are not as reliable for the binary of H<sub>2</sub> mixed with CH<sub>4</sub>.

It is also important to note that at higher temperatures both hydrogen’s vapor and liquid molar fraction data at all the available datasets decrease, which is the expected behavior for this binary mixture.

On Table 20 below are stated the datasets that have been excluded from the database due to invalid behavior.

Table 20: Experimental data that have been considered as reliable for the binary mixture of H<sub>2</sub>-CH<sub>4</sub> regarding VLE

Dataset	Included in the database
Augood 1957	x
Benham 1957	x
Freeth 1931	x
Hong and Kobayashi 1980	v
Hu, Lin, Gu and Li 2014	v
Sagara, Arai and Saito 1972	v
Tsang, Clancy, Calado and Street 1980	v
Yorizane, Yoshimura, Masuoko and Toyama 1967	v
Kirk and Ziegler 1967	v

#### 4.1.2 Binary mixture of H<sub>2</sub>-C<sub>2</sub>H<sub>6</sub>

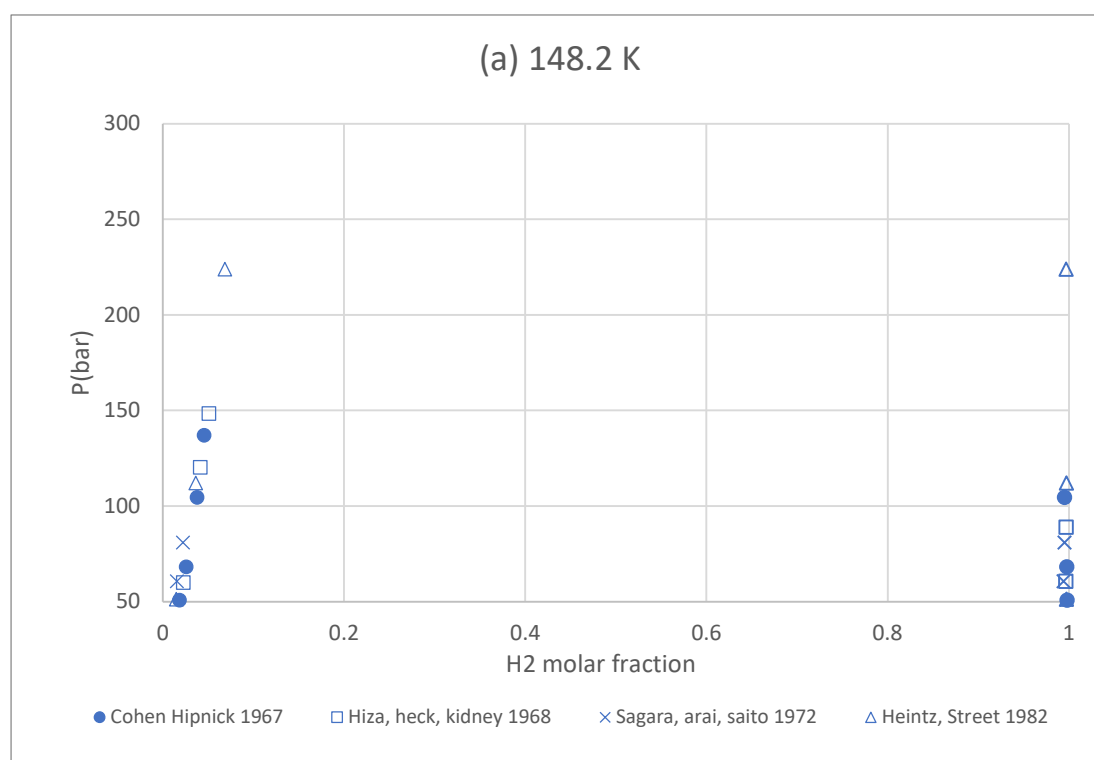
For the binary mixture of H<sub>2</sub>- C<sub>2</sub>H<sub>6</sub> there are four available datasets regarding to VLE data covering a wide range of experimental temperature and pressure values.

Table 21: Experimental binary VLE data available in literature for the mixture of H<sub>2</sub>- C<sub>2</sub>H<sub>6</sub>

Dataset	T range (K)	P range (bar)	NP x	NP y
Cohen and Hipnick 1967	144.2-199.6	9.2-137.9	27	27
Hiza, Heck and Kidney 1968	107.9-189.6	05.83-153.5	29	45
Sagara, arai and Saito 1972	148.2-223.2	20.3-811	15	15
Heintz and Street 1982	100.2-280.2	31.8-5595	250	241

The comparison of the data of the different datasets is to be presented in detail below.

Comparing the data of Cohen, Hipnick 1967, Hiza, Heck, Kidney 1968, Sagara, arai, saito 1972 and Heintz and Street 1982 at two different isotherms of (a) 148.2 K and (b) 173.2 K the data of Sagara, arai, saito 1972 present slightly lower experimental values of hydrogen's composition in both vapor and liquid phase than the other two datasets.





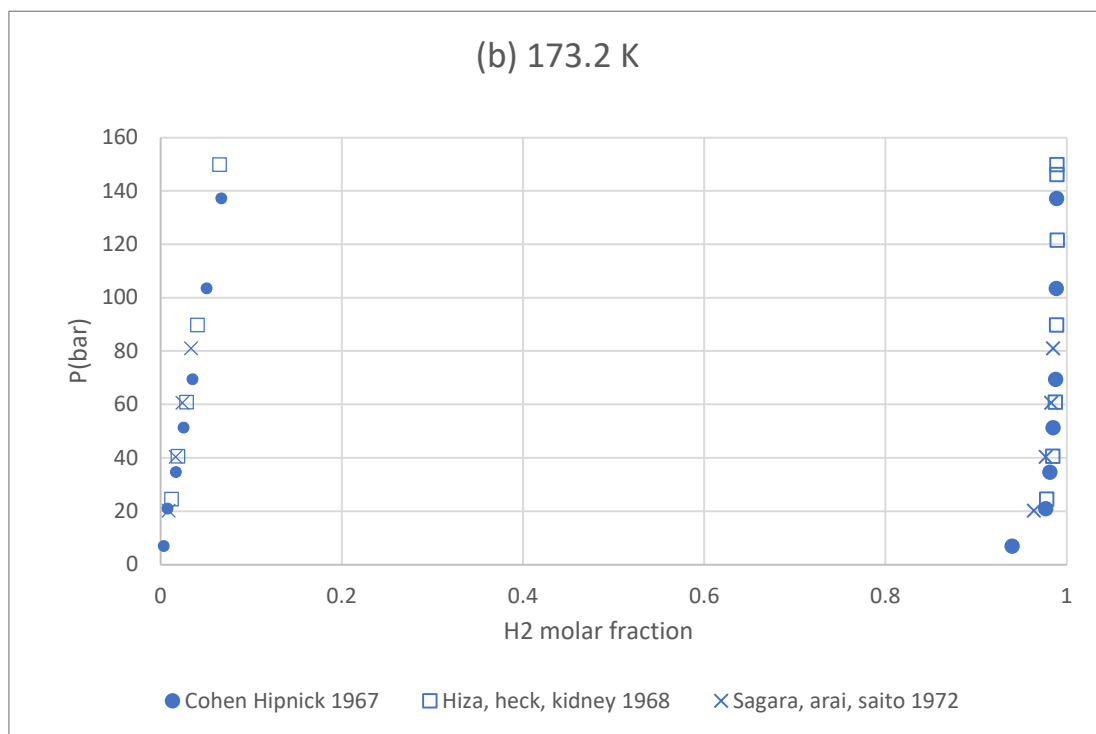


Figure 10: Comparison of Cohen, Hipnick 1967, Hiza, Heck, Kidney 1968, Sagara, arai, saito 1972 and Heintz and Street 1982 at two different isotherms of (a) 148.2 K and (b) 173.2 K

Concluding the abovementioned statements, the four datasets compare well to each other with no significant deviations on their behavior.

On Table 22 below are stated the datasets that have been excluded from the database due to invalid behavior.

Table 22: Experimental data that have been considered as reliable for the binary mixture of H<sub>2</sub>-C<sub>2</sub>H<sub>6</sub> regarding VLE

Dataset	Included in the database
Cohen and Hipnick 1967	v
Hiza, Heck and Kidney 1968	v
Sagara, arai and Saito 1972	v
Heintz and Street 1982	v

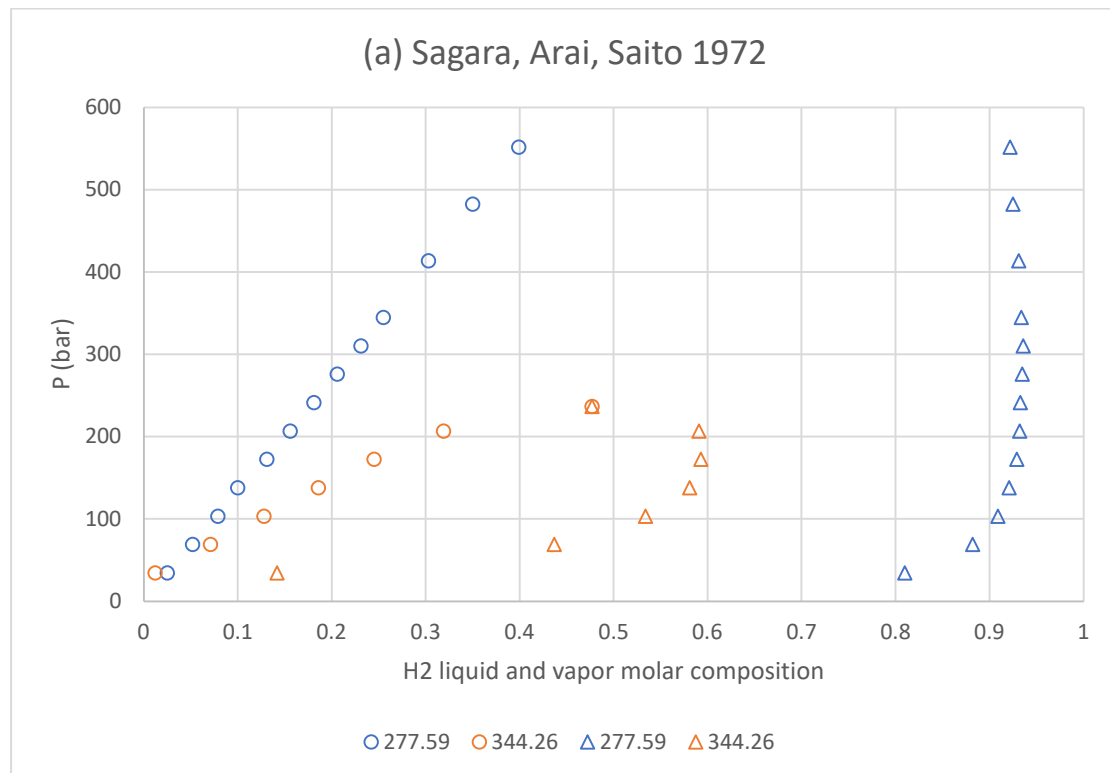
#### 4.1.3 Binary mixture of H<sub>2</sub>-C<sub>3</sub>H<sub>8</sub>

For the binary mixture of H<sub>2</sub>- C<sub>3</sub>H<sub>8</sub> there are two available datasets regarding to VLE data covering a wide range of experimental temperature and pressure values. Unfortunately, in this case the temperature range of the two available datasets differs so it is not possible to compare them with each other.

Table 23: Experimental binary VLE data available in literature for the mixture of H<sub>2</sub>-CH<sub>4</sub>

Dataset	T range (K)	P range (bar)	NP x	NP y
Buriss, Hsu, Reamer, Sage 1953	277.6-360.9	34.5-551.6	36	36
Trust, Kurata 1971	98.2-248.2	17.2-206.8	46	25

Figure 11 demonstrates the behavior two isotherms of (a) Buriss, Hsu, Reamer, Sage 1953 dataset and (b) Trust, Kurata 1971 where it is obvious that for an increase at the temperature conditions of the mixture, both liquid and vapor composition of hydrogen decrease. This decrease is expected since hydrogen is the most volatile component of the mixture.



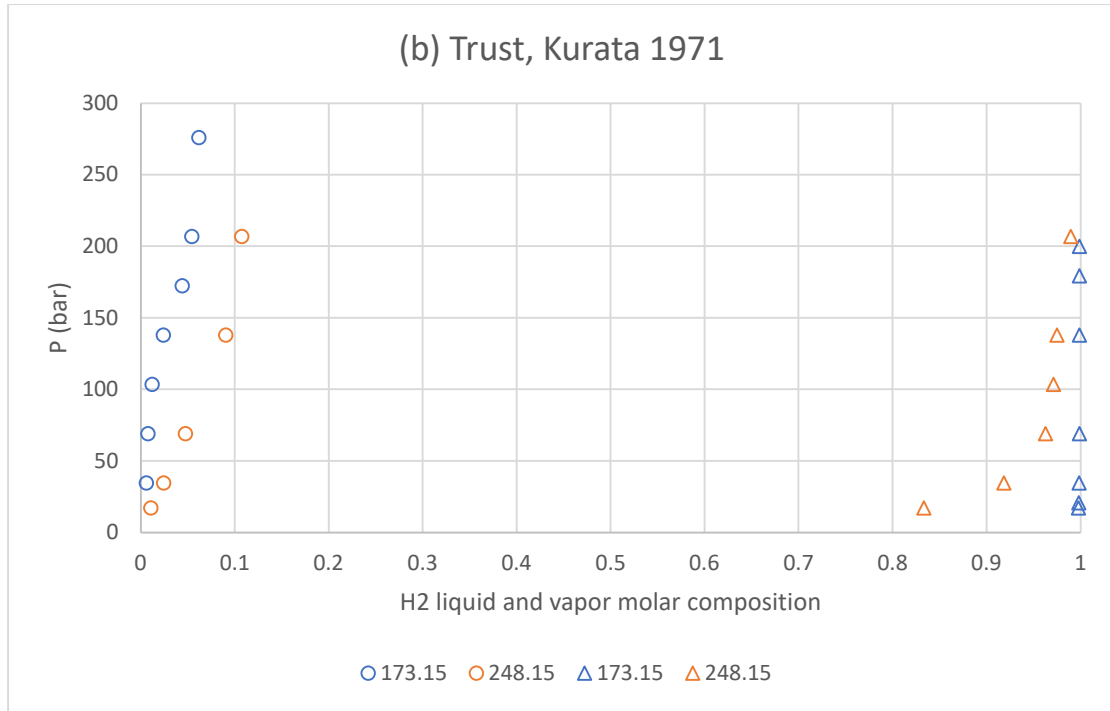


Figure 11: Comparison of (a) Buriss, Hsu, Reamer, Sage 1953 at two different isotherms of 277.6 K and 344.3 K and (b) Trust, Kurata 1971 at two different isotherms of 173.2 K and 248.2 K

#### 4.1.4 Binary mixture of H<sub>2</sub>-CO

For the binary mixture of H<sub>2</sub>-CO five are three available datasets regarding to VLE data covering a wide range of experimental temperature and pressure values.

Table 24: Experimental binary VLE data available in literature for the mixture of H<sub>2</sub>-CO

Dataset	T range (K)	P range (Mpa)	H2 composition range	Number of points
Akers, Eubanks 1960	23.5-122.0	21.7-137.9	10	10
Augood 1957	81.4	96.2-181.7	4	4
Tsang, Clancy, Street and Calado 1980	70-125	4.9-529.4	133	132
Verschole 1931	68.1-88.2	0.33-227.8	69	78
Yorizane, Yoshimura, Masuoko, Toyama 1968	273.1-298.1	122-608	58	58

The comparison of the data of the different datasets is to be presented in detail below.

In this case, the dataset of Tsang, Clancy, Street and Calado 1980 is the one that covers the widest range of temperature and pressure conditions and it contains a lot of experimental points which helps at the evaluation of the available datasets.

Comparing the data of Akers, Eubanks 1960 and Yorizane, Yoshimura, Masuoko, Toyama 1968 to the ones of Tsang, Clancy, Street and Calado 1980 at a temperature of 122.0 K the data of both Akers, Eubanks 1960 and Yorizane, Yoshimura, Masuoko, Toyama 1968 present a slightly different behavior than the experimental points of Tsang, Clancy, Street and Calado 1980 with the largest deviations occur when comparing Akers, Eubanks 1960 and Tsang, Clancy, Street and Calado 1980 vapor composition data.

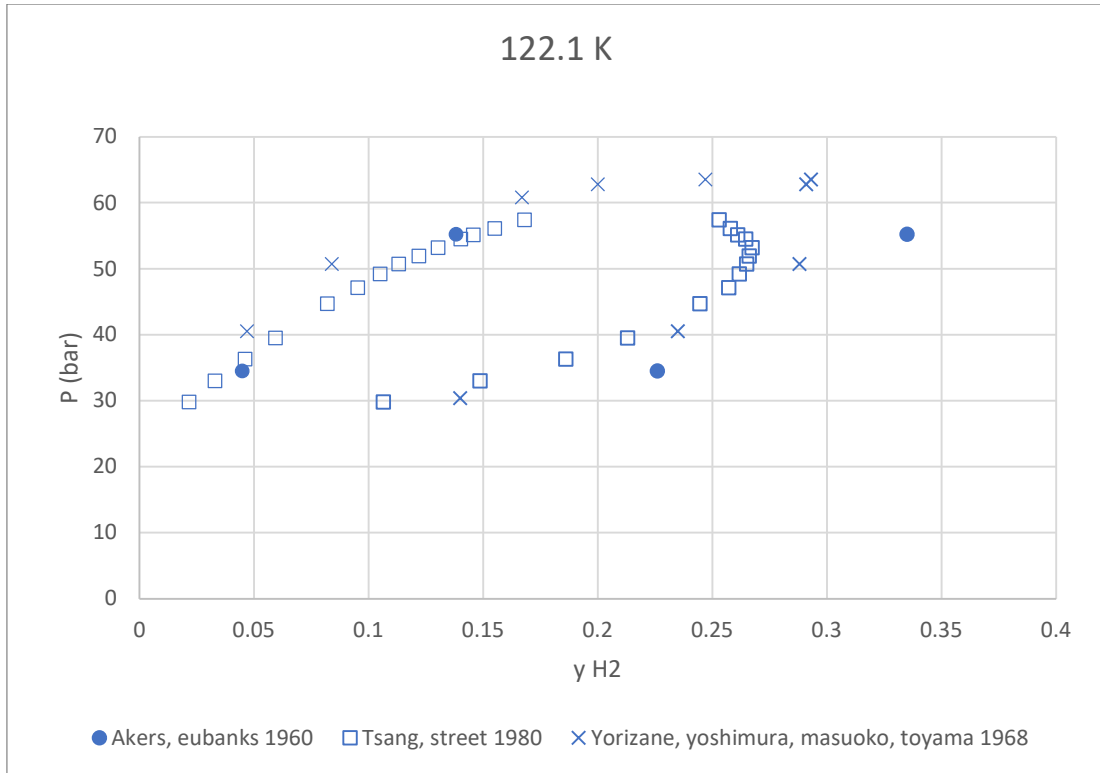


Figure 12: Comparison of Akers, Eubanks 1960 and Yorizane, Yoshimura, Masuoko, Toyama 1968 to the ones of Tsang, Clancy, Street and Calado 1980 at a temperature of 122.0 K

Comparing the data of Augood 1957 and Verschole 1931 to the ones of Tsang, Clancy, Street and Calado 1980 at a temperature of 83.2 K the data of both Augood 1957 and Verschole 1931 present an inaccurate behavior comparing to the experimental points of Tsang, Clancy, Street and Calado 1980 with the largest deviations occur when comparing Verschole 1931 and Tsang, Clancy, Street and Calado 1980 liquid composition data.

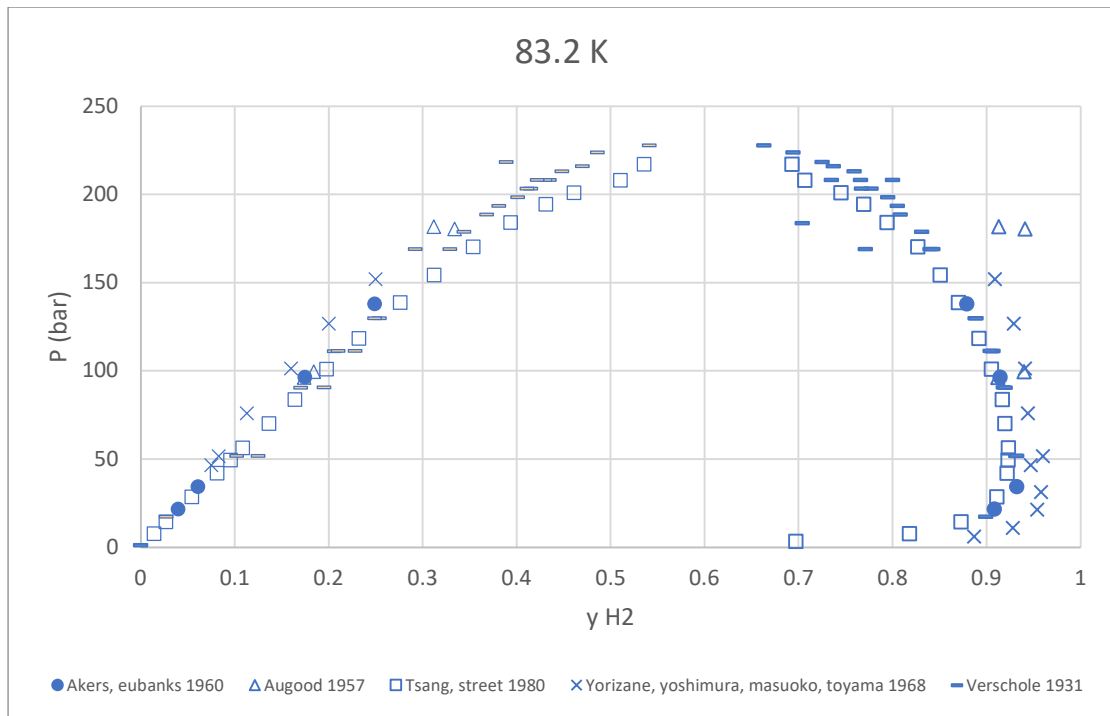


Figure 13: Comparison of Augood 1957 and Verschole 1931 to the ones of Tsang, Clancy, Street and Calado 1980 at a temperature of 83.2 K

Concluding the abovementioned statements, the five datasets do not compare well to each other with the most significant deviations occur when comparing Akers, Eubanks 1960, Verschole 1931 and Augood 1957 experimental data to the other available datasets. Akers, Eubanks 1960, Verschole 1931 and Augood 1957 should be excluded from the database. In terms of H<sub>2</sub>-CO binary mixture, it is important to extend the available dataset in order to ensure the accuracy of the available data.

On Table 25 below are stated the datasets that have been excluded from the database due to invalid behavior.

Table 25: Experimental data that have been considered as reliable for the binary mixture of H<sub>2</sub>-CO regarding VLE

Dataset	Included in the database
Akers, Eubanks 1960	×
Augood 1957	×
Tsang, Clancy, Street and Calado 1980	✓
Verschole 1931	×
Yorizane, Yoshimura, Masuoko, Toyama 1968	✓

#### 4.1.5 Binary mixture of H<sub>2</sub>-CO<sub>2</sub>

For the binary mixture of H<sub>2</sub>-CO<sub>2</sub> there are six available datasets regarding to VLE data covering a wide range of experimental temperature and pressure values.

Table 26: Experimental binary VLE data available in literature for the mixture of H<sub>2</sub>-CO<sub>2</sub>

Dataset	T range (K)	P range (bar)	H <sub>2</sub> composition range	Number of points
Augood 1957	239.7	185.8-192.7	3	3
Kaminishi, Toriumi 1966	233.2-298.2	10.0-200	21	21
Spano, Heck, Barrick 1968	219.9-289.9	10.8-203.2	45	49
Tsang, Street 1980	220-290	9.3-1689.6	134	139
Yorizane, Yoshimura, Masuoka, Toyama 1968	273.2	60.9-374.9	10	10
K. Bezahehtak, G. B. Combes, F. Dehghani, N. R. Foster, and D. L. Tomasko 2002	278.2-290.2	48.1-192.5	41	33

The comparison of the data of the different datasets is to be presented in detail below.

In this case, the dataset of Tsang, Clancy, Street and Calado 1980 is the one that covers the widest range of temperature and pressure conditions and it contains a lot of experimental points which helps at the evaluation of the available datasets.

Comparing the data of Augood 1957 and Spano, Heck, Barrick 1968 to the ones of Tsang, Clancy, Street and Calado 1980 at a temperature of 244.2 K the data of both Augood 1957 don't compare well with the data of Spano, Heck, Barrick 1968.

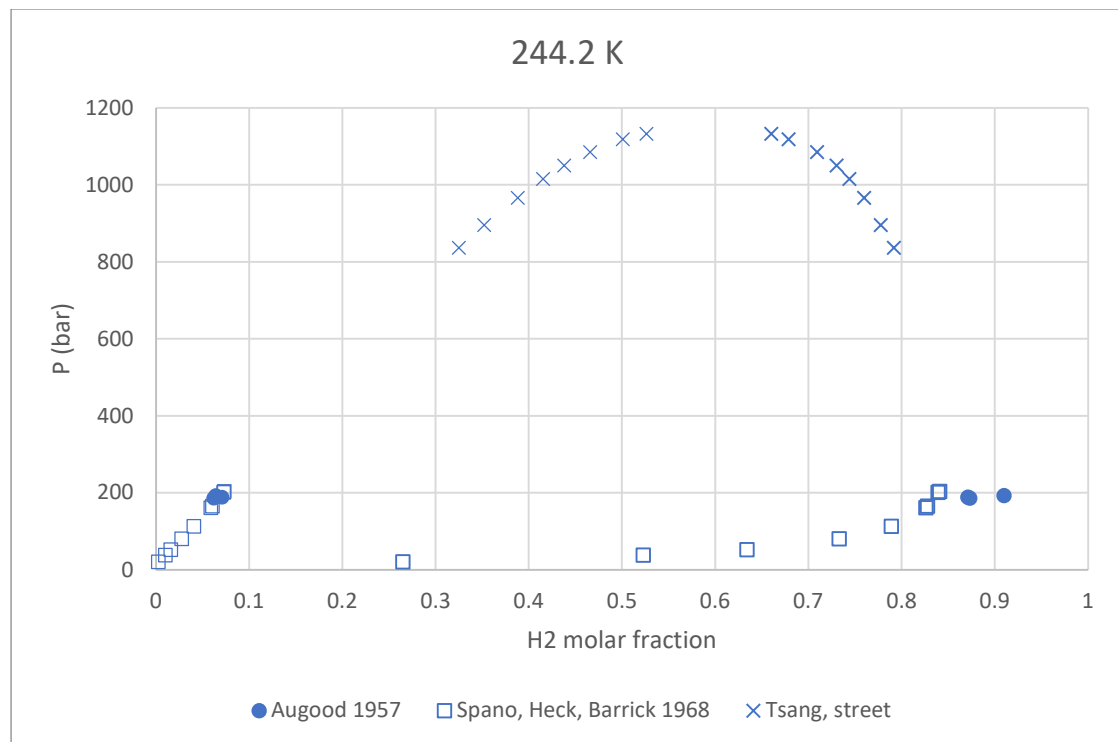


Figure 14: Comparison of Augood 1957 and Spano, Heck, Barrick 1968 to the ones of Tsang, Clancy, Street and Calado 1980

Comparing the data of Yorizane, Yoshimura, Masuoka, Toyama 1968 and Kaminishi, Toriumi 1966 to the ones of Tsang, Clancy, Street and Calado 1980 at a temperature of 273.2 K the data of both Yorizane, Yoshimura, Masuoka, Toyama 1968 present significantly higher hydrogen composition values for pressures over 300 bar comparing with the experimental points of Tsang, Clancy, Street and Calado 1980.

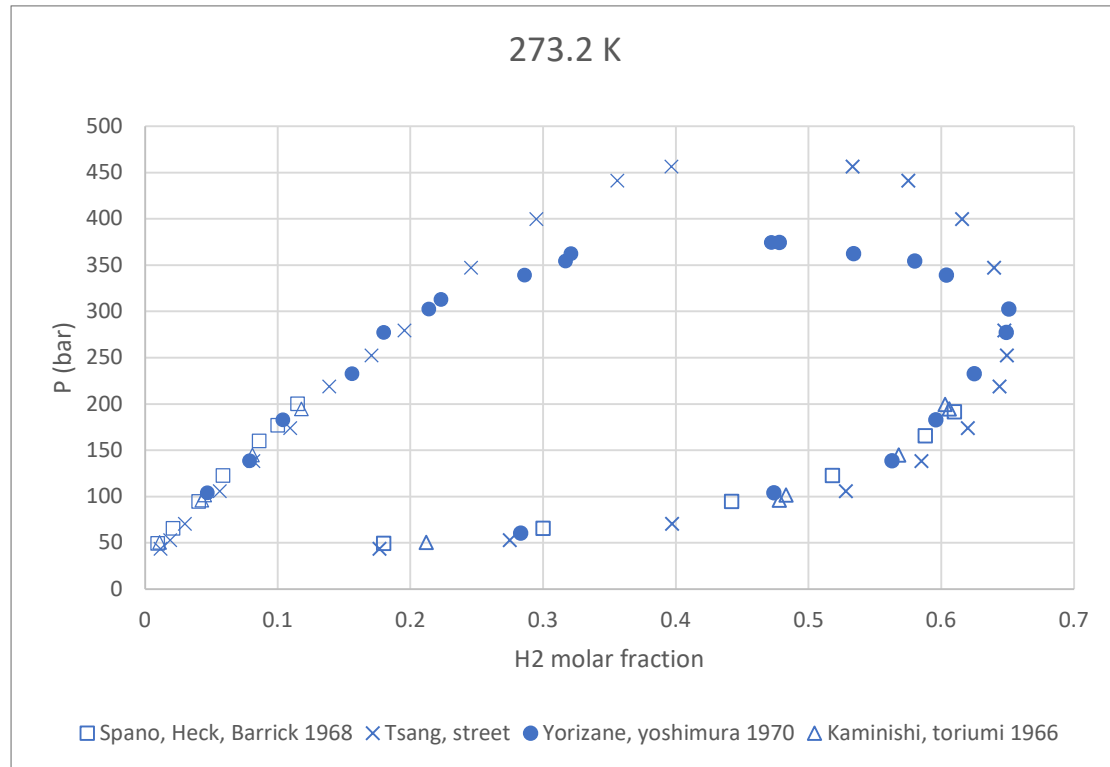


Figure 15: Comparison of Augood 1957 and Spano, Heck, Barrick 1968 to the ones of Tsang, Clancy, Street and Calado 1980

Comparing the data of K. Bezahehtak, G. B. Combes, F. Dehghani, N. R. Foster, and D. L. Tomasko 2002 to the ones of Tsang, Clancy, Street and Calado 1980 at a temperature of 290.0 K the data of K. Bezahehtak, G. B. Combes, F. Dehghani, N. R. Foster, and D. L. Tomasko 2002 present slight deviations in hydrogen's composition on the vapor phase comparing with the experimental points of Tsang, Clancy, Street and Calado 1980. These deviations though are not significant and K. Bezahehtak, G. B. Combes, F. Dehghani, N. R. Foster, and D. L. Tomasko 2002 dataset can be trusted.

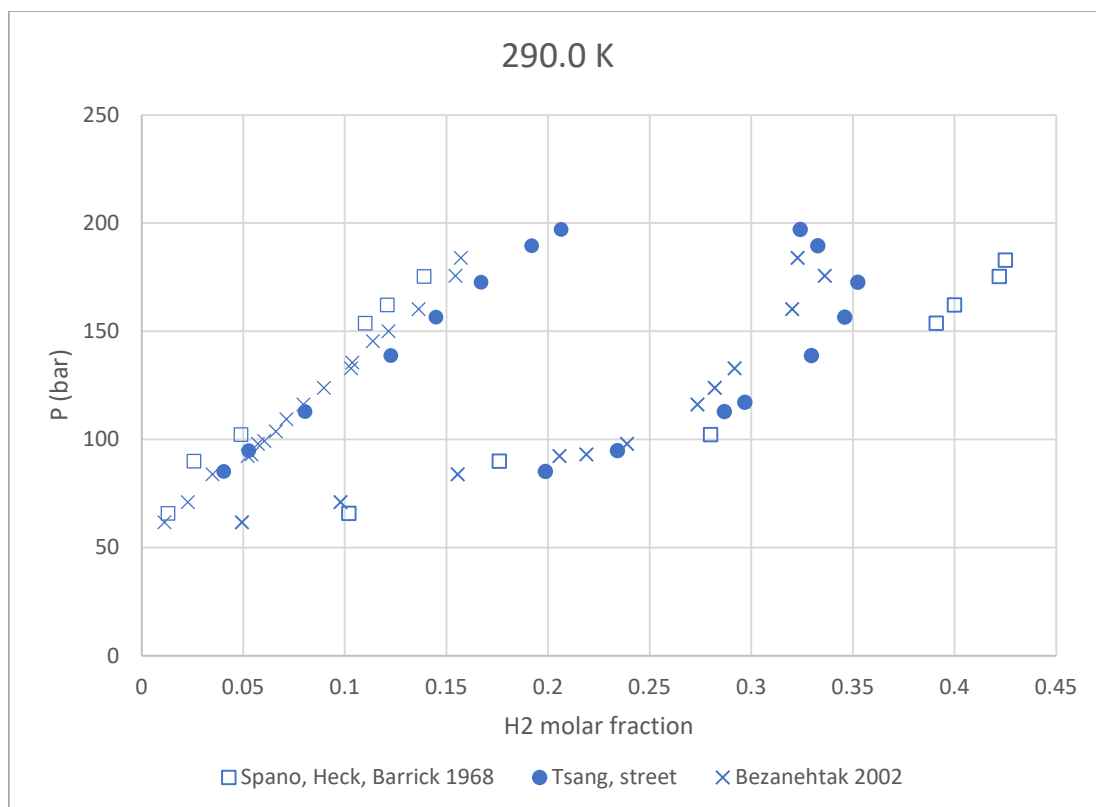


Figure 16: Comparison of K. Bezanehtak, G. B. Combes, F. Dehghani, N. R. Foster, and D. L. Tomasko 2002 to the ones of Tsang, Clancy, Street and Calado 1980

Concluding the abovementioned statements, Yorizane, Yoshimura, Masuoka, Toyama 1968 and Augood 1957 present a significantly different behavior as it comes to VLE data for the binary mixture of H<sub>2</sub> mixed with CO<sub>2</sub>, so these datasets should be excluded from the database.

On Table 27 below are stated the datasets that have been excluded from the database due to invalid behavior.

Table 27: Experimental data that have been considered as reliable for the binary mixture of H<sub>2</sub>-CO<sub>2</sub> regarding VLE

Dataset	Included in the database
Augood 1957	x
Kaminishi, Toriumi 1966	v
Spano, Heck, Barrick 1968	v
Tsang, Street 1980	v
Yorizane, Yoshimura, Masuoka, Toyama 1968	x
K. Bezanehtak, G. B. Combes, F. Dehghani, N. R. Foster, and D. L. Tomasko 2002	v



#### 4.1.6 Binary mixture of H<sub>2</sub>-N<sub>2</sub>

For the binary mixture of H<sub>2</sub>-N<sub>2</sub> there are seven available datasets regarding to VLE data covering a wide range of experimental temperature and pressure values.

Table 28: Experimental binary VLE data available in literature for the mixture of H<sub>2</sub>-N<sub>2</sub>

Dataset	T range (K)	P range (MPa)	H <sub>2</sub> composition range	Number of points
Akers, Eubanks 1960	83.2-122.0	21.7-137.9	10	10
Augood 1957	67.0-77.7	27.2-178.9	10	7
Gonikberg, Fastowski, Gurwitsch 1939	79.0-109.1	1.2-178	38	35
Maimoni 1961	77.4	5.1-152	10	11
Street, Calado 1978	63.2-110.3	13-293	75	74
Verschoyle 1931	63.2-88.2	12.3-227.79	45	39
Yoshimura, Yorizane, Naka 1971	76.4-88.2	16.71-190.49	16	16

The comparison of the data of the different datasets is to be presented in detail below.

In this case, the dataset of Tsang, Clancy, Street and Calado 1980 is the one that covers the widest range of temperature and pressure conditions and it contains a lot of experimental points which helps at the evaluation of the available datasets.

Comparing the data of Akers, Eubanks 1960 and Gonikberg, Fastowski, Gurwitsch 1939 to the ones of Street and Calado 1978 at a temperature of 100.0 K the data of Akers, Eubanks 1960 present significantly different behavior than the experimental points of Street and Calado 1978. Also, the data of Gonikberg, Fastowski, Gurwitsch 1939 seem to be inaccurate as it comes to hydrogen's vapor composition experimental values.

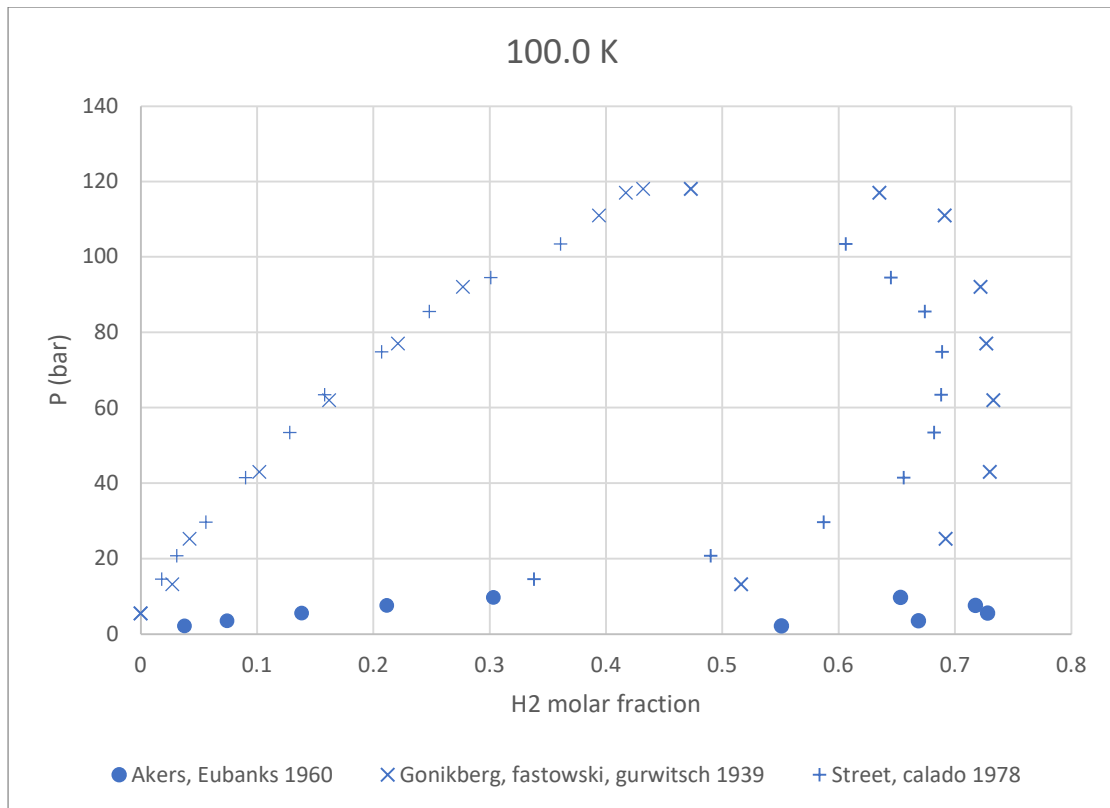


Figure 17: Comparison of Akers, Eubanks 1960 and Gonikberg, Fastowski, Gurwitsch 1939 to the ones of Street and Calado 1978 at a temperature of 100.0 K

Comparing the data of (a) Augood 1957 and Gonikberg, Fastowski, Gurwitsch 1939 and (b) Maimoni 1961, Verschoyle 1931 and Yoshimura, Yorizane, Naka 1971 to the ones of Street and Calado 1978 at a temperature of 77.6 K the data of Augood 1957 present significantly different behavior than the experimental points of Street and Calado 1978. Also, the data of Gonikberg, Fastowski, Gurwitsch 1939 seem to be inaccurate as it comes to hydrogen's liquid and vapor composition experimental values for pressures greater than 150 bar.

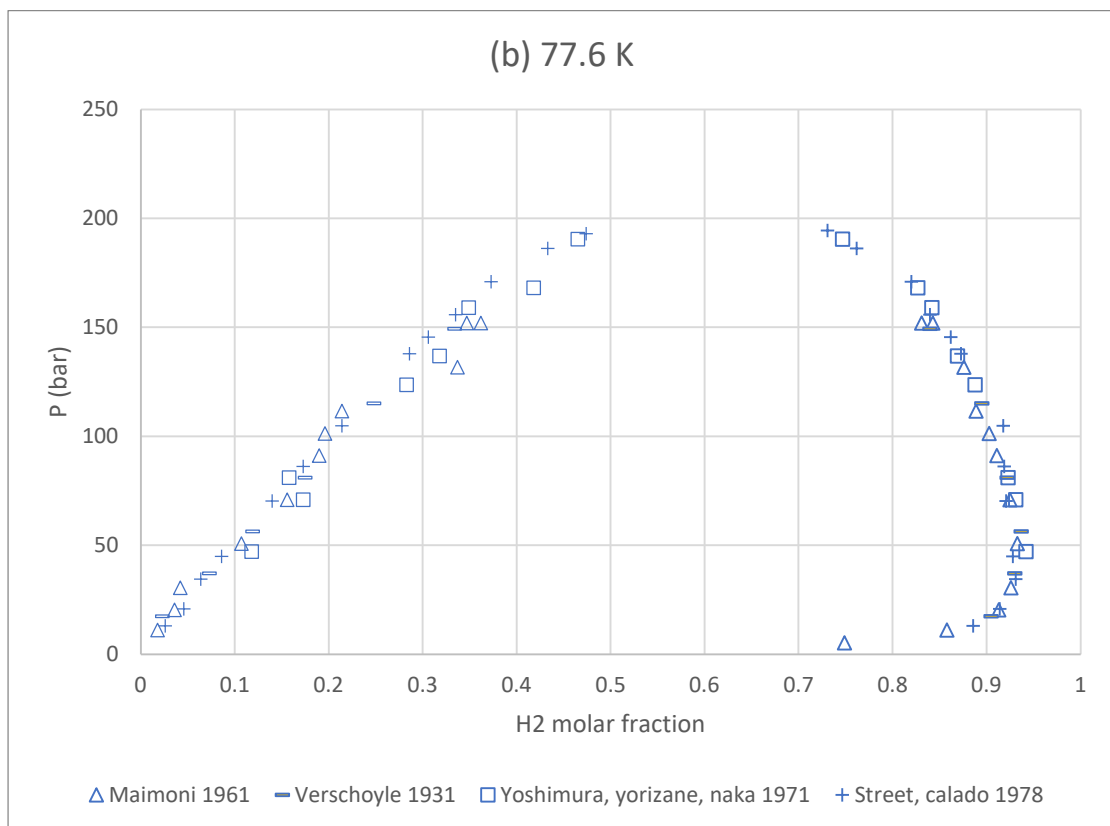
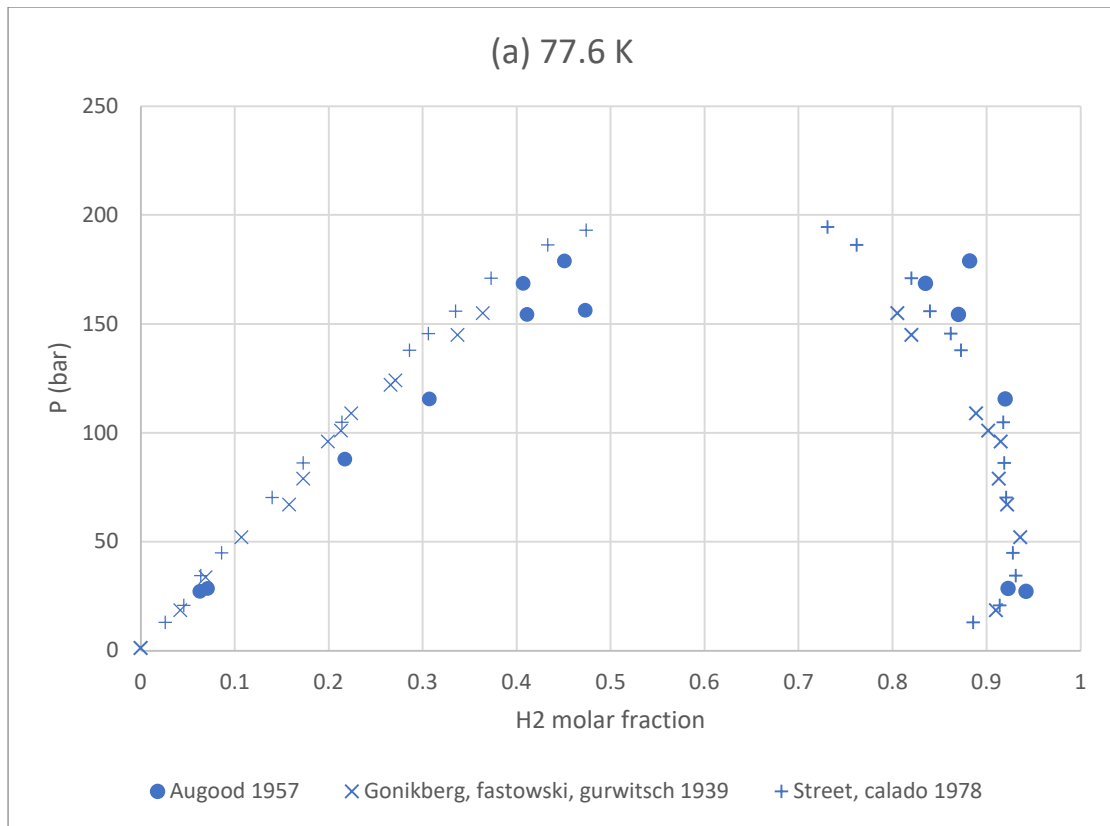


Figure 18: Comparison of (a) Augood 1957 and Gonikberg, Fastowski, Gurwitsch 1939 and (b) Maimoni 1961, Verschoyle 1931 and Yoshimura, Yorizane, Naka 1971 to the ones of Street and Calado 1978 at a temperature of 77.6 K

Concluding the abovementioned statements, Akers, Eubanks 1960 data do not present an accurate behavior as it comes to VLE data for the binary mixture of H<sub>2</sub> mixed with N<sub>2</sub>. It is also obvious that the dataset of Augood 1957 is considered as inaccurate especially for the composition of hydrogen in its vapor phase. Last but not least, Gonikberg, Fastowski, Gurwitsch 1939 is considered as inaccurate especially for the composition of hydrogen in its vapor phase and the deviations of Gonikberg, Fastowski, Gurwitsch 1939 experimental points compared to Street and Calado 1978 points increase as the temperature increases. So the datasets of Akers, Eubanks 1960, Augood 1957 and Gonikberg, Fastowski, Gurwitsch 1939 should be excluded from the database.

On Table 29 below are stated the datasets that have been excluded from the database due to invalid behavior.

Table 29: Experimental data that have been considered as reliable for the binary mixture of H<sub>2</sub>-N<sub>2</sub> regarding VLE

Dataset	Included in the database
Akers, Eubanks 1960	×
Augood 1957	×
Gonikberg, Fastowski, Gurwitsch 1939	×
Maimoni 1961	✓
Street, Calado 1978	✓
Verschoyle 1931	✓
Yoshimura, Yorizane, Naka 1971	✓

#### 4.2 Model comparison on VLE calculations

After the evaluation of the available experimental data is completed, it is important to examine which thermodynamic models should be trusted for the calculation of VLE of these six binary mixtures. The thermodynamic models that are going to be evaluated are; GERG-2008, Peng-Robinson EoS, SRK EoS, PC-SAFT EoS and UMR-PRU. The average absolute relative deviations of the pressure calculations and the average absolute relative deviations along with the average absolute deviations for hydrogen's vapor molar composition calculations compared to the experimental data are presented below for each binary mixture.

Table 30: The number of experimental points that have been used for the evaluation of the thermodynamic models regarding the VLE

Binary mixture	Total number of $x_{H_2}$ experimental data-points used	Total number of $y_{H_2}$ experimental data-points used
H <sub>2</sub> -CH <sub>4</sub>	358 out of 385	355 out of 386
H <sub>2</sub> -C <sub>2</sub> H <sub>6</sub>	321 out of 321	328 out of 328
H <sub>2</sub> -C <sub>3</sub> H <sub>8</sub>	61 out of 61	82 out of 82
H <sub>2</sub> -CO	130 out of 213	130 out of 222
H <sub>2</sub> -CO <sub>2</sub>	261 out of 274	269 out of 282
H <sub>2</sub> -N <sub>2</sub>	146 out of 204	140 out of 192

In the case of PR EoS there were evaluated two values of hydrogen's acentric factor;  $\omega = -0.215$ , which is the experimental value, and  $\omega = -0.12$ , which is proposed by Aspen HYSYS. Using the fitted acentric factor for hydrogen results in lower deviations in terms of thermophysical properties' calculation.

It will be further indicated below that GERG-2008 EoS was not the most accurate thermodynamic model of the VLE calculations for the six evaluated binary mixtures which means that it should not be used as a reference model for these mixtures while at the same time UMR-PRU results into the smallest deviations from the experimental data.

#### 4.2.1 Binary mixture of H<sub>2</sub>-CH<sub>4</sub>

As it is presented in Table 31 UMR-PRU results into the most accurate predictions regarding to pressure predictions and SRK EoS results into the most accurate predictions regarding to hydrogen's vapor phase composition predictions. It is interesting to note that PR EoS with the experimental acentric factor used for pure hydrogen gives significantly better results than when using the Aspen HYSYS' proposed acentric factor. This contradicts the thermophysical properties' calculations, for which the fitted parameter should be used instead of the experimental one due to smaller deviations. Also, PC-SAFT EoS should not be used for the phase equilibrium predictions for the binary mixture of hydrogen and methane. GERG-2008 EoS result in almost 10% deviation for the prediction of bubble point pressure but should not be preferred for vapor phase composition prediction.

Table 31: Model results for pressure and hydrogen's vapor phase composition of binary mixture of H<sub>2</sub>-CH<sub>4</sub> compared to five thermodynamic models

Model	Hydrogen's acentric factor	P (bar)	y H <sub>2</sub>	
			%ARD	AAD
SRK	-0.215	15.1	3.3	0.020
PR	-0.12	308.9	7.1	0.044
PR	-0.215	100.7	4.5	0.030
UMR PRU	-0.215	4.8	3.8	0.026
PC SAFT		71.2	12.7	0.068
GERG		9.9	6.0	0.040

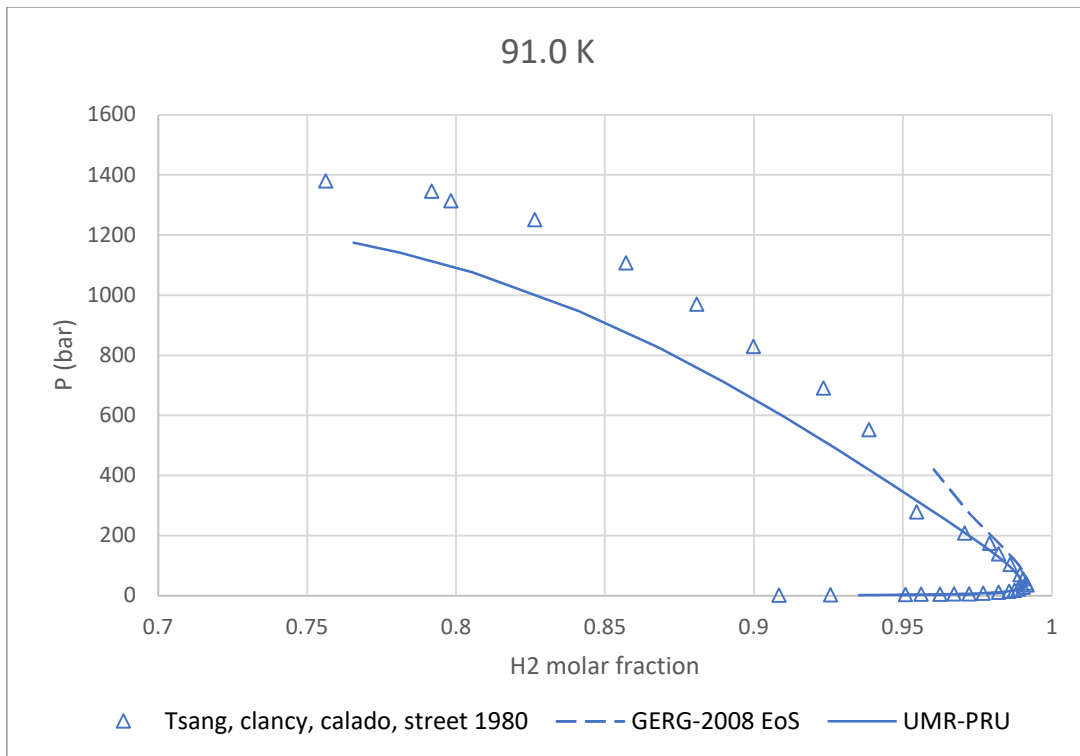


Figure 19: Model comparison regarding the experimental VLE data of the mixture  $H_2-CH_4$  at 91.0K

#### 4.2.2 Binary mixture of $H_2-C_2H_6$

As it is presented in Table 32 UMR-PRU results into the most accurate predictions regarding to pressure predictions and PC-SAFT EoS results into the most accurate predictions regarding to hydrogen's vapor phase composition predictions. It is interesting to note that PR EoS with the experimental acentric factor used for pure hydrogen gives significantly better results than when using the Aspen HYSYS' proposed acentric factor. This contradicts the thermophysical properties' calculations, for which the fitted parameter should be used instead of the experimental one due to smaller deviations. Also, PC-SAFT EoS could be trusted while calculating bubble point pressure for the binary mixture of hydrogen and ethane. GERG-2008 EoS is very accurate while predicting the vapor phase composition of this binary mixture.

Table 32: Model results for pressure and hydrogen's vapor phase composition of binary mixture of  $H_2-C_2H_6$  compared to five thermodynamic models

Model	Hydrogen's acentric factor	P (bar)	y H2	
			%ARD	AAD
SRK	-0.215	16.0	1.4	0.013
PR	-0.12	118.7	2.2	0.037
PR	-0.215	47.4	1.5	0.014
UMR PRU	-0.215	11.2	1.1	0.009
PC SAFT		47.7	0.3	0.005
GERG		15.1	6.3	0.061

#### 4.2.3 Binary mixture of H<sub>2</sub>-C<sub>3</sub>H<sub>8</sub>

As it is presented in Table 33 UMR-PRU results into the most accurate predictions regarding to both bubble point pressure and vapor phase composition predictions. It is interesting to note that PR EoS with the experimental acentric factor used for pure hydrogen gives significantly better results than when using the Aspen HYSYS' proposed acentric factor. This contradicts the thermophysical properties' calculations, for which the fitted parameter should be used instead of the experimental one due to smaller deviations. PR EoS and GERG-2008 EoS can be also preferred for VLE calculations regarding the binary mixture of hydrogen mixed with propane. PC-SAFT EoS and SRK EoS could not be trusted while calculating bubble point pressure for the binary mixture of hydrogen and propane.

Table 33: Model results for pressure and hydrogen's vapor phase composition of binary mixture of H<sub>2</sub>-C<sub>3</sub>H<sub>8</sub> compared to five thermodynamic models

Model	Hydrogen's acentric factor	P (bar)	y H <sub>2</sub>	
			%ARD	AAD
SRK	-0.215	24.2	6.4	0.032
PR	-0.12	70.2	6.7	0.032
PR	-0.215	12.3	2.5	0.014
UMR PRU	-0.215	10.1	1.5	0.011
PC SAFT		35.3	3.9	0.026
GERG		11.2	3.8	0.021

#### 4.2.4 Binary mixture of H<sub>2</sub>-CO

As it is presented in Table 34 PR EoS results into the most accurate predictions regarding to pressure predictions and GERG-2008 EoS results into the most accurate predictions regarding to hydrogen's vapor phase composition predictions. It is interesting to note that PR EoS with the experimental acentric factor used for pure hydrogen gives significantly better results than when using the Aspen HYSYS' proposed acentric factor. This contradicts the thermophysical properties' calculations, for which the fitted parameter should be used instead of the experimental one due to smaller deviations. PC-SAFT EoS and SRK EoS could not be trusted while calculating bubble point pressure for the binary mixture of hydrogen and carbon monoxide. UMR-PRU cannot be used for this binary mixture due to lack of adjusted parameters.

Table 34: Model results for pressure and hydrogen's vapor phase composition of binary mixture of H<sub>2</sub>-CO compared to five thermodynamic models

Model	Hydrogen's acentric factor	P (bar)	y H <sub>2</sub>	
			%ARD	AAD
SRK	-0.215	32.4	7.2	0.039
PR	-0.12	74.0	8.0	0.048
PR	-0.215	21.6	6.5	0.042
PC SAFT		146.7	17.6	0.100
GERG		22.1	5.7	0.035

#### 4.2.5 Binary mixture of H<sub>2</sub>-CO<sub>2</sub>

As it is presented in Table 35 UMR-PRU results into the most accurate predictions regarding to pressure predictions and SRK EoS results into the most accurate predictions regarding to hydrogen's vapor phase composition predictions. It is interesting to note that PR EoS with the experimental acentric factor used for pure hydrogen gives significantly better results than when using the Aspen HYSYS' proposed acentric factor. This contradicts the thermophysical properties' calculations, for which the fitted parameter should be used instead of the experimental one due to smaller deviations. GERG-2008 EoS can be also preferred for VLE calculations regarding the binary mixture of hydrogen mixed with carbon dioxide. PC-SAFT EoS could not be trusted for the binary mixture of hydrogen and carbon dioxide.

Table 35: Model results for pressure and hydrogen's vapor phase composition of binary mixture of H<sub>2</sub>-CO<sub>2</sub> compared to five thermodynamic models

Model	Hydrogen's acentric factor	P (bar)	y H <sub>2</sub>	
			%ARD	AAD
SRK	-0.215	20.4	15.3	0.058
PR	-0.12	63.4	23.2	0.093
PR	-0.215	25.8	17.6	0.088
UMR PRU	-0.215	15.0	17.0	0.082
PC SAFT		119.9	39.7	0.161
GERG		19.4	15.5	0.082

#### 4.2.6 Binary mixture of H<sub>2</sub>-N<sub>2</sub>

As it is presented in Table 36 UMR-PRU results into the most accurate predictions regarding to pressure predictions and PR EoS results into the most accurate predictions regarding to hydrogen's vapor phase composition predictions. In the binary of hydrogen mixed with nitrogen using the fitted acentric factor proposed by Aspen HYSYS for hydrogen while performing VLE calculations results in smaller deviations comparing to PR EoS paired with hydrogen's experimental acentric factor. PC-SAFT EoS could not be trusted for the binary mixture of hydrogen and nitrogen.

Table 36: Model results for pressure and hydrogen's vapor phase composition of binary mixture of H<sub>2</sub>-N<sub>2</sub> compared to five thermodynamic models

Model	Hydrogen's acentric factor	P (bar)	y H <sub>2</sub>	
			%ARD	AAD
SRK	-0.215	29.9	3.3	0.021
PR	-0.12	19.5	2.7	0.019
PR	-0.215	37.8	5.0	0.035
UMR PRU	-0.215	15.7	3.6	0.026
PC SAFT		122.7	10.0	0.081
GERG		35.0	5.2	0.032



### 4.3 Thermophysical Data evaluation

The thermophysical properties' data that were found in literature and will be used for evaluation of the abovementioned thermodynamic models are presented in Table 37. Plenty of single-phase mass density datasets regarding to the binaries of H<sub>2</sub>-CH<sub>4</sub>, H<sub>2</sub>-CO, H<sub>2</sub>-CO<sub>2</sub> and H<sub>2</sub>-N<sub>2</sub> were found and evaluated. Due to lack of data, though, it is not possible to complete evaluation of mass density datasets regarding to the binaries of H<sub>2</sub>-C<sub>2</sub>H<sub>6</sub>, H<sub>2</sub>-C<sub>3</sub>H<sub>8</sub>. There are also a few data available regarding to the thermophysical properties except from mass densities which makes the evaluation other properties' datasets difficult. Since natural gas mixtures mainly contain CH<sub>4</sub> it is of major importance that especially the binary mixture of H<sub>2</sub>-CH<sub>4</sub> should be carefully examined.

Table 37: Experimental binary thermophysical properties data available in literature

Binary mixture	Property	T range (K)	P range (bar)	H2 composition range	Number of points	Reference
H <sub>2</sub> -CH <sub>4</sub>	d	130.0-503.4	1.0-506.6	0.0-1.0	1073	[29], [33]– [38]
	w	273.2-375.0	4.5-20.2	0.05-0.5	232	[39]
	JT	133.6-245.6	34.5-75.8	0.127-0.5657	56	[40]
H <sub>2</sub> -C <sub>2</sub> H <sub>6</sub>	-	-	-	-	-	-
H <sub>2</sub> -C <sub>3</sub> H <sub>8</sub>	-	-	-	-	-	-
H <sub>2</sub> -CO	d	273.2-343.2	8.8-60.8	0.049-0.333	110	[29], [41], [42]
	w	90.0	1.0	0.17-0.72	4	[43]
H <sub>2</sub> -CO <sub>2</sub>	d	278.2-343.2	0.4-48.9	0.003-0.491	119	[29], [42]
H <sub>2</sub> -N <sub>2</sub>	d	203.2-573.2	1.0-148.2	0.05-0.885	839	[29], [44]
	w	90.0	1.0	0.21-0.91	4	[43]
	C <sub>p</sub>	273.2-313.2	30.4-1013.3	0.0-1.0	208	[45]

#### 4.3.1 Binary mixture of H<sub>2</sub>-CH<sub>4</sub>

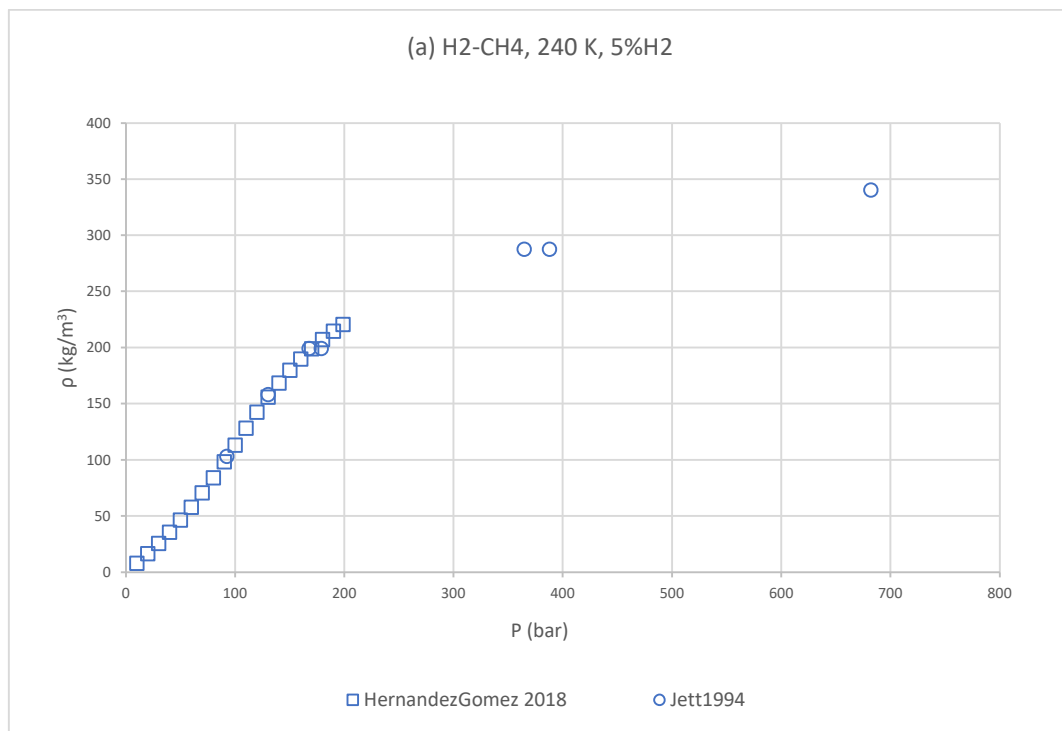
For the binary mixture of H<sub>2</sub>-CH<sub>4</sub> there are six available datasets in online literature regarding to mass density covering a wide range of experimental temperature, pressure and composition values.

Table 38: Experimental binary thermophysical properties data available in literature for the mixture of H<sub>2</sub>-CH<sub>4</sub>

Dataset	T range (K)	P range (bar)	H <sub>2</sub> composition range	Number of points
Hernández-Gómez et al. 2018	240.1-350.0	1.0-19.9	0.05-0.5	391
Jett, Fleyfel, and Kobayashi 1994	142.0-273.2	3.9-68.2	0.0465	109
Jett 1990	273.2	12.8-69.9	0.0465	9
Machado 1988	130.0-159.2	5.3-106.8	0.076-0.91	265
Magee et al. 1985	273.2-503.4	16.4-58.2	0.2005	79
Chuang, Chappellear and Kobayashi 1976	173.2-273.2	4.0-506.6	0.0-1.0	220

The comparison of the data of the different datasets is to be presented in detail below.

Comparing the data of Jett, Fleyfel, Kobayashi 1994 and Jett 1990 to the ones of Hernández-Gómez et al. 2018 in two different temperatures and on low composition of hydrogen a similar behavior is observed. What is also obvious in Figure 1 is that the mass density values increase while pressure increases for each one of the examined datasets, as expected.



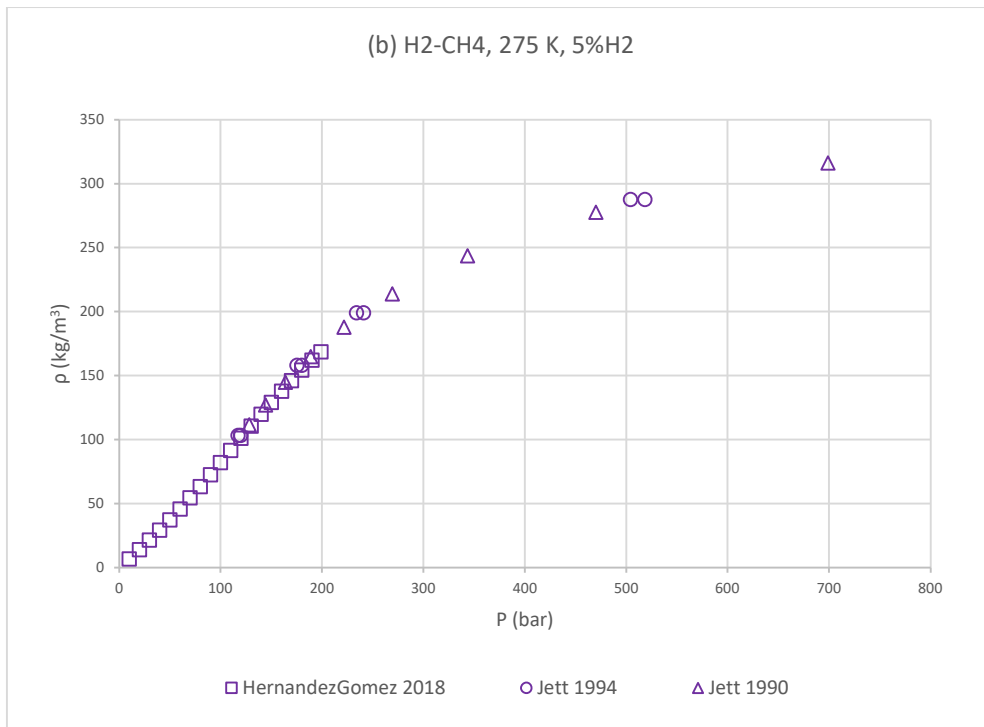
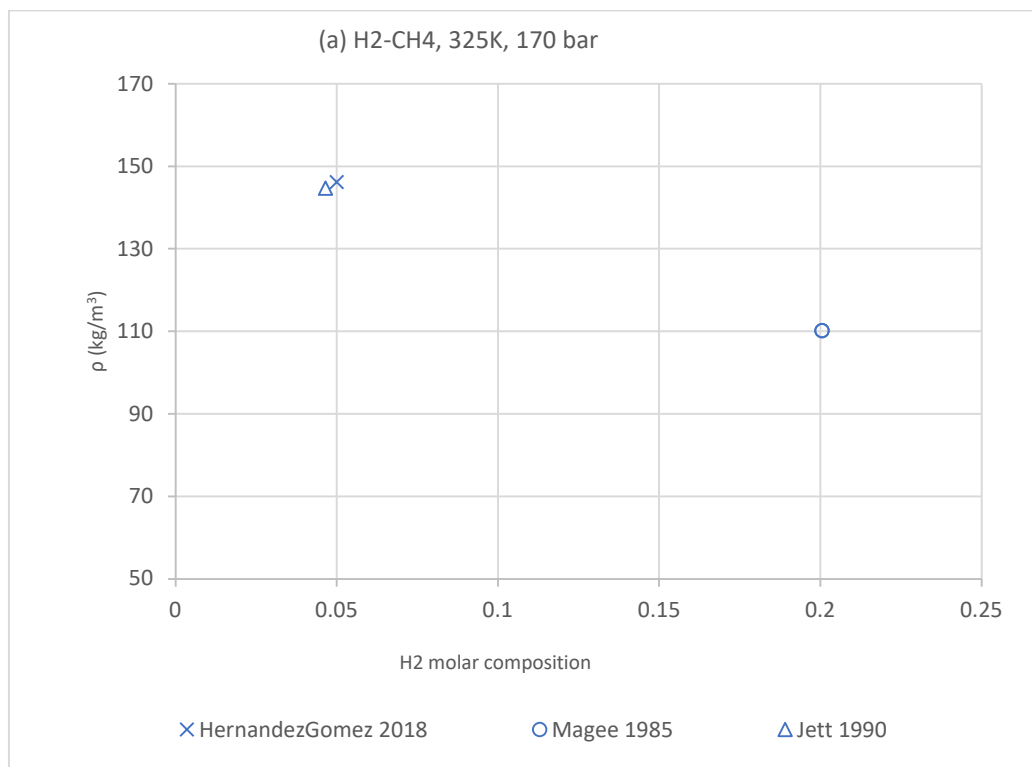


Figure 20: Comparison of Jett, Fleyfel, Kobayashi 1994, Jett 1990 and Hernández-Gómez et al. 2018 at hydrogen composition of 0.05 and (a) 240 K and (b) 275 K

Comparing the data of Magee et al. 1985 and Jett 1990 to the ones of Hernández-Gómez et al. 2018 in two different temperatures and pressures a similar behavior is observed. What is also obvious in Figure 21 is that the mass density values decrease while hydrogen's composition in the mixture increases when combining the data from the datasets, as expected.



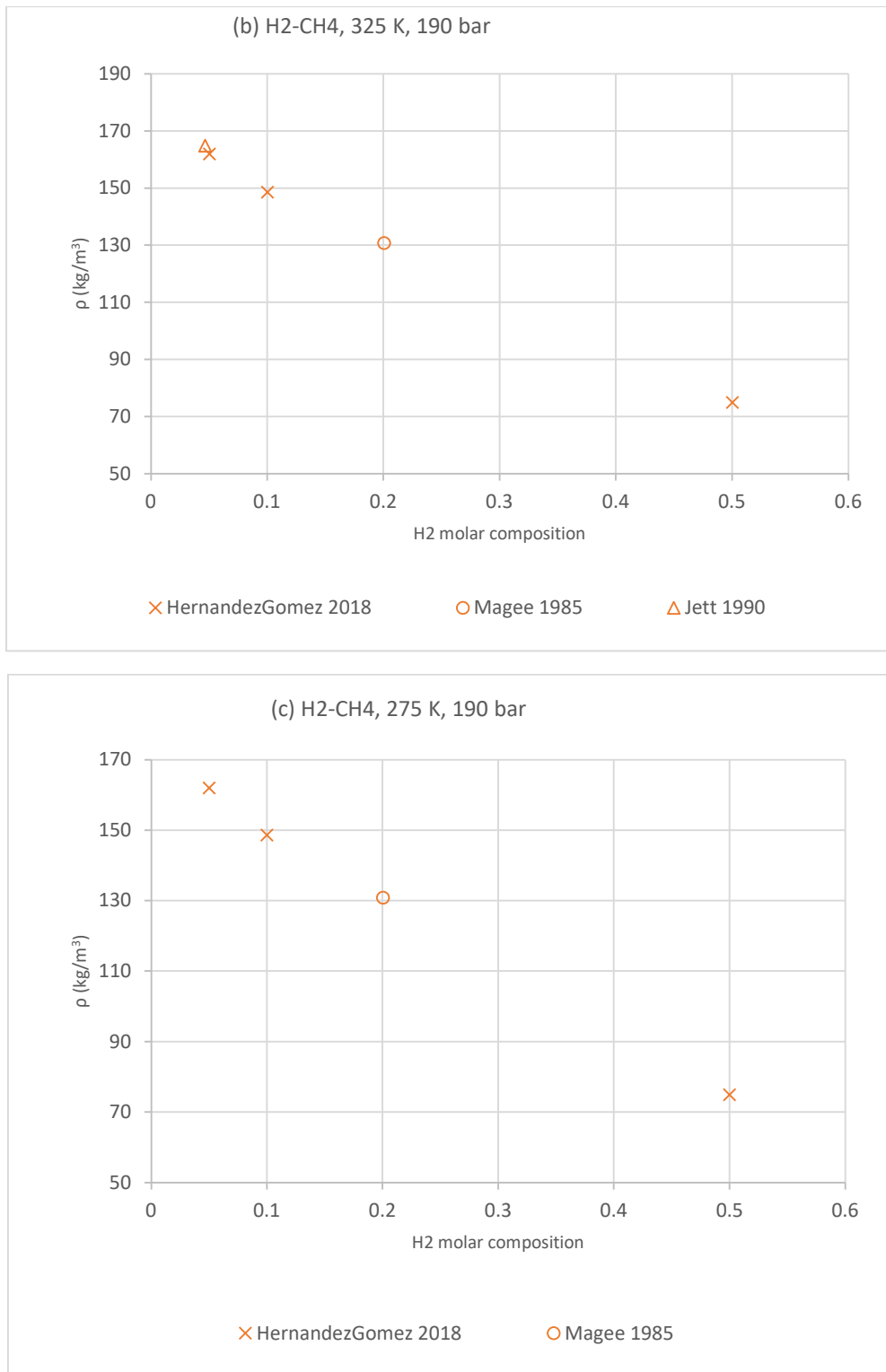


Figure 21: Comparison of Magee et al. 1985, Jett 1990 and Hernández-Gómez et al. 2018 at (a) 325 K and 170 bar, (b) 325 K and 190 bar and (c) 275 K and 190 bar

Comparing the data of Machado 1988 to the ones of Hernández-Gómez et al. 2018 in two different pressures and low composition of hydrogen a similar behavior is observed. It's not clear, though, if they tend to follow the same trendline due to the lack of data for temperatures between 170 K and 230 K. What is also obvious in Figure 22 is that the mass density values decrease while the temperature of the mixture increases for each one of the

examined datasets, as expected. Additionally, in Figure 23 the behavior of Machado 1988 data is presented for two different sets of temperature and pressure values. What is shown in Figure 23 is that for an increase of hydrogen's molar composition from approximately 10% to 80%, the decrease of the mixture's vapor molar density is around  $200 \text{ kg/m}^3$  which is less than the expected decrease which would be around  $600 \text{ kg/m}^3$  depending on the GERG-2008 equation at these temperature and pressure conditions.

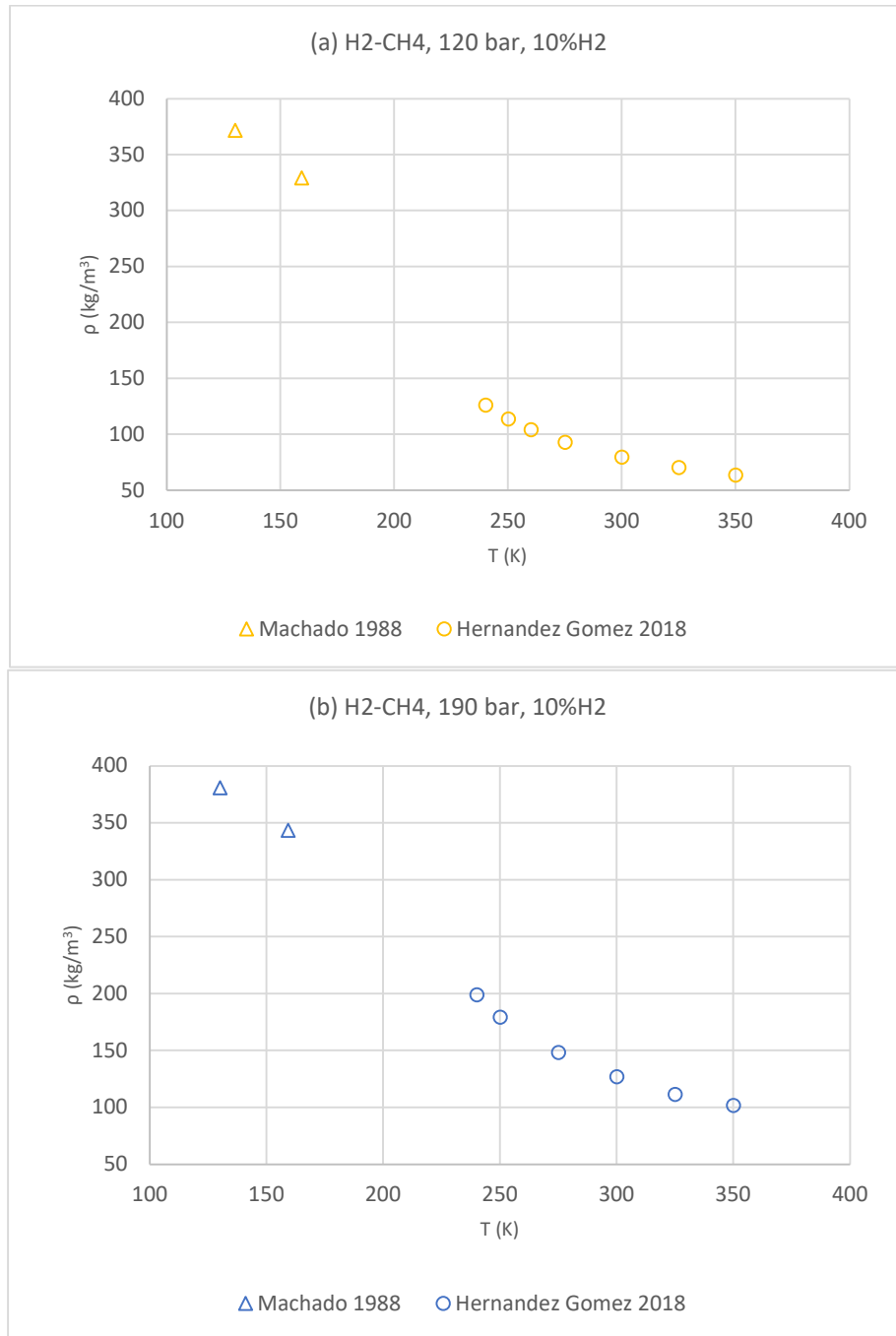


Figure 22: Comparison of Machado 1988 and Hernández-Gómez et al. 2018 at composition of hydrogen equal to 0.1 and (a) 120 bar (b) 190 bar

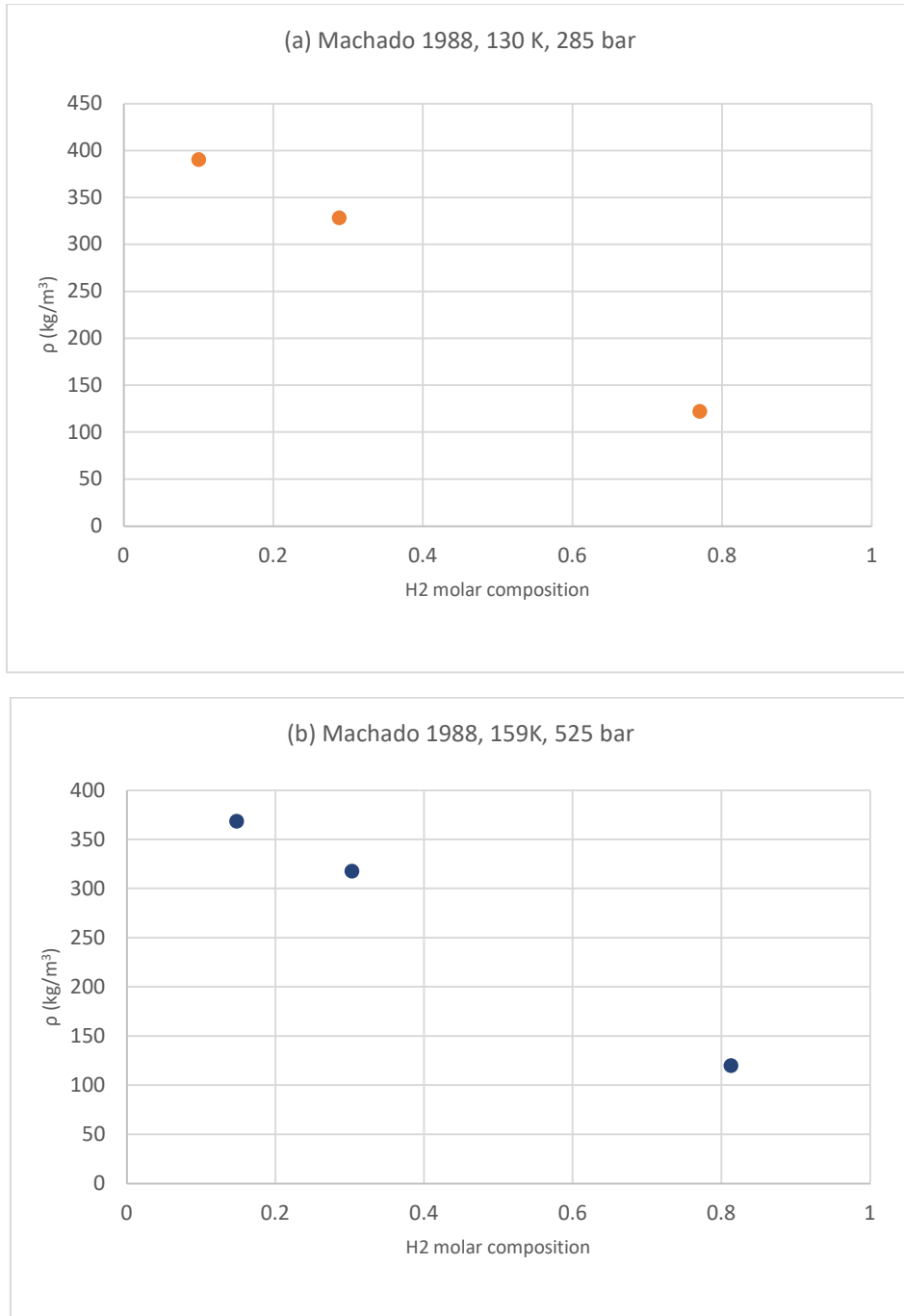


Figure 23: Machado 1988 data at two different temperature and pressure conditions

Concluding the abovementioned statements, the Machado 1988 dataset doesn't behave accurately regarding to the binary of H<sub>2</sub> mixed with CH<sub>4</sub> when comparing to the other available datasets. On Table 39 below are stated the datasets that have been excluded from the database due to invalid behavior.

Table 39: Experimental data that have been considered as reliable for the binary mixture of H<sub>2</sub>-CH<sub>4</sub> regarding thermophysical properties

Dataset	Included in the database
Hernández-Gómez et al. 2018	v
Jett, Fleyfel, and Kobayashi 1994	v
Jett 1990	v
Machado 1988	x
Magee et al. 1985	v
Chuang, Chappellear and Kobayashi 1976	v

#### 4.3.2 Binary mixture of H<sub>2</sub>-C<sub>2</sub>H<sub>6</sub>

For the binary mixture of H<sub>2</sub>- C<sub>2</sub>H<sub>6</sub> there is no available datasets in online literature regarding to mass density which makes the data evaluation impossible.

#### 4.3.3 Binary mixture of H<sub>2</sub>-C<sub>3</sub>H<sub>8</sub>

For the binary mixture of H<sub>2</sub>- C<sub>3</sub>H<sub>8</sub> there is no available datasets in online literature regarding to mass density which makes the data evaluation impossible.

#### 4.3.4 Binary mixture of H<sub>2</sub>-CO

For the binary mixture of H<sub>2</sub>-CO there are three available datasets in online literature regarding to mass density covering a wide range of experimental temperature, pressure and composition values.

Table 40: Experimental binary thermophysical properties data available in literature for the mixture of H<sub>2</sub>-CO

Dataset	T range (K)	P range (MPa)	H <sub>2</sub> composition range	Number of points
Cipollina et al.2007	308.0-343.0	8.8-23.1	0.049-0.112	48
Scott and Bone 1929	298.1	14.2-17.2	0.331	4
Townend, Bhatt, and Bone 1931	273.1-298.1	12.2-60.8	0.333-0.666	58

The comparison of the data of the different datasets is to be presented in detail below.

Comparing the data of Townend, Bhatt, and Bone 1931 to the ones of Scott and Bone 1929 in temperature equal to 300 K and with 33.3% hydrogen in the mixture a similar behavior is observed. What is also obvious in Figure 24 is that the mass density values increase while pressure increases for each one of the examined datasets, as expected.

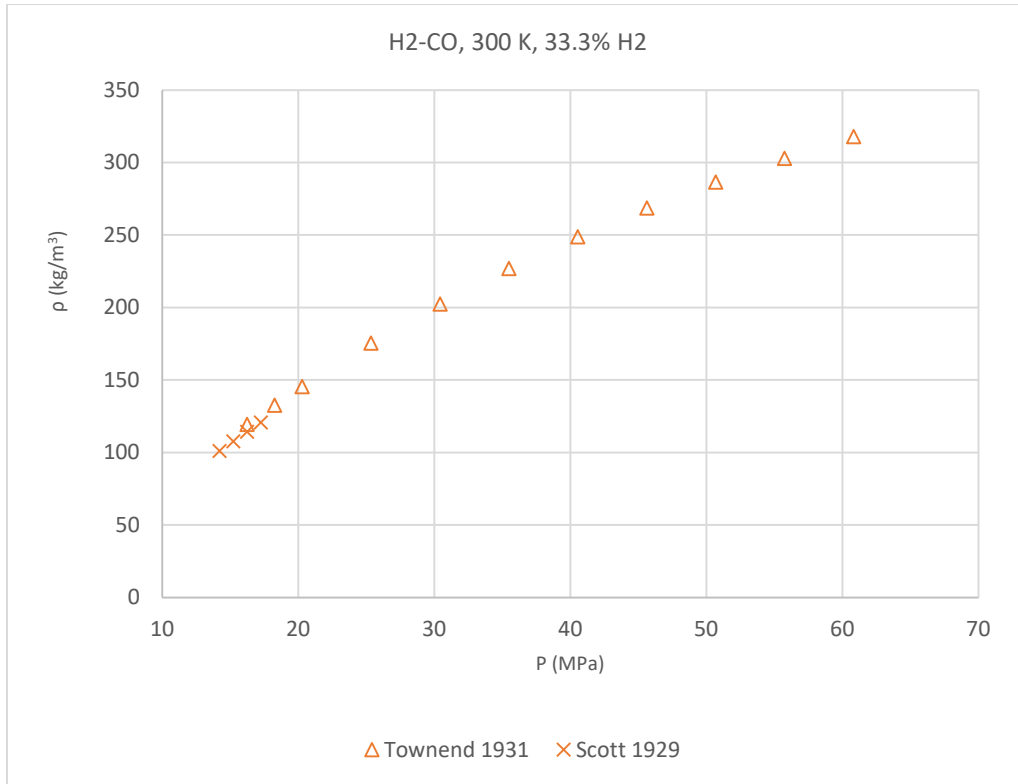


Figure 24: Comparison of Townend, Bhatt, and Bone 1931 and Scott and Bone 1929 at composition of hydrogen equal to 0.333 and 300 K

Comparing the data of Cipollina et al.2007 to the ones of Townend, Bhatt, and Bone 1931 and Scott and Bone 1929 in temperature equal to 300 K and two different pressures it is unclear if a similar behavior is observed. What is also obvious in Figure 25 is that the mass density values decrease while hydrogen's composition in the mixture increases when combining the data from the datasets. The temperature, pressure and composition range of Cipollina et al.2007 dataset is not similar to the other two data sets which make the evaluation of its data impossible. What is also obvious in Figure 26 is that with insignificant increase on the mixture's pressure condition (from 125 to 135 bar in case (a) and from 206 to 216 bar in case (b)), there is no effect on mass density values while temperature increases. What would be the expected behavior of the data is to show a slight decrease while the temperature rises.



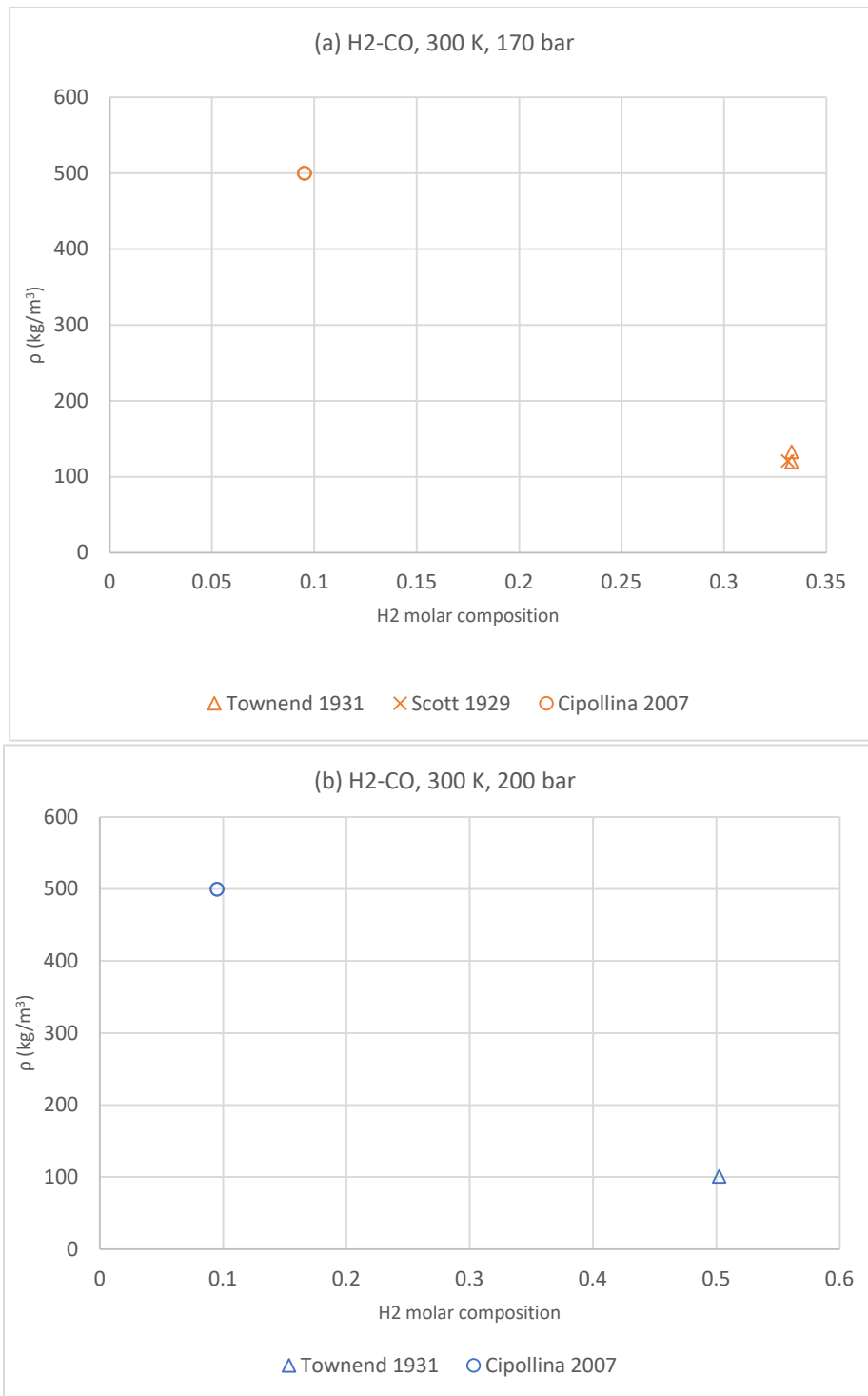


Figure 25: Comparison of Cipollina et al.2007, Scott and Bone 1929 and Townend, Bhatt, and Bone 1931 at 300 K and (a) 170 bar and (b) 200 bar

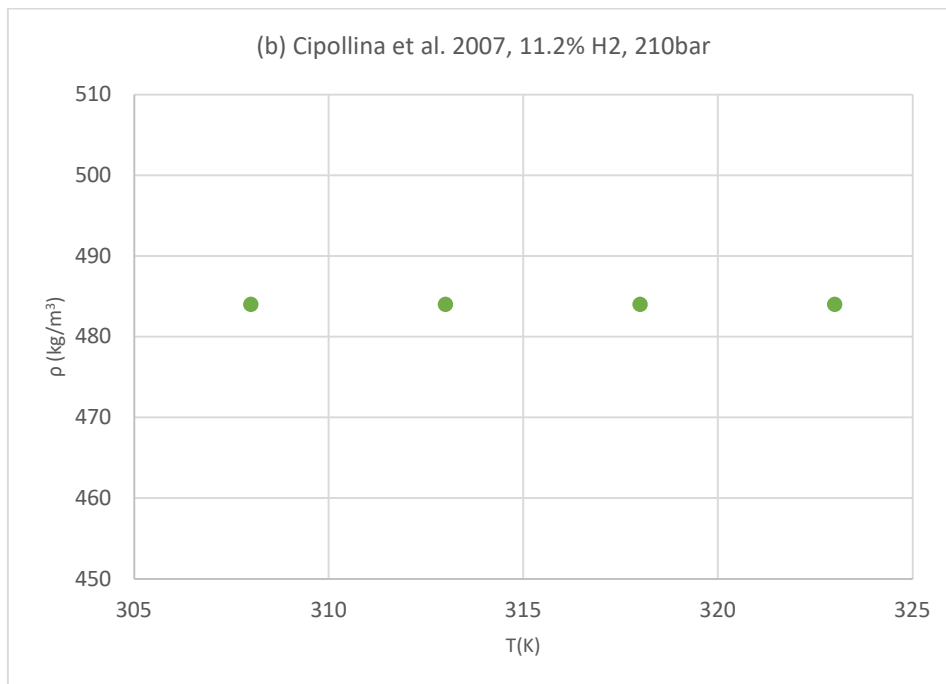
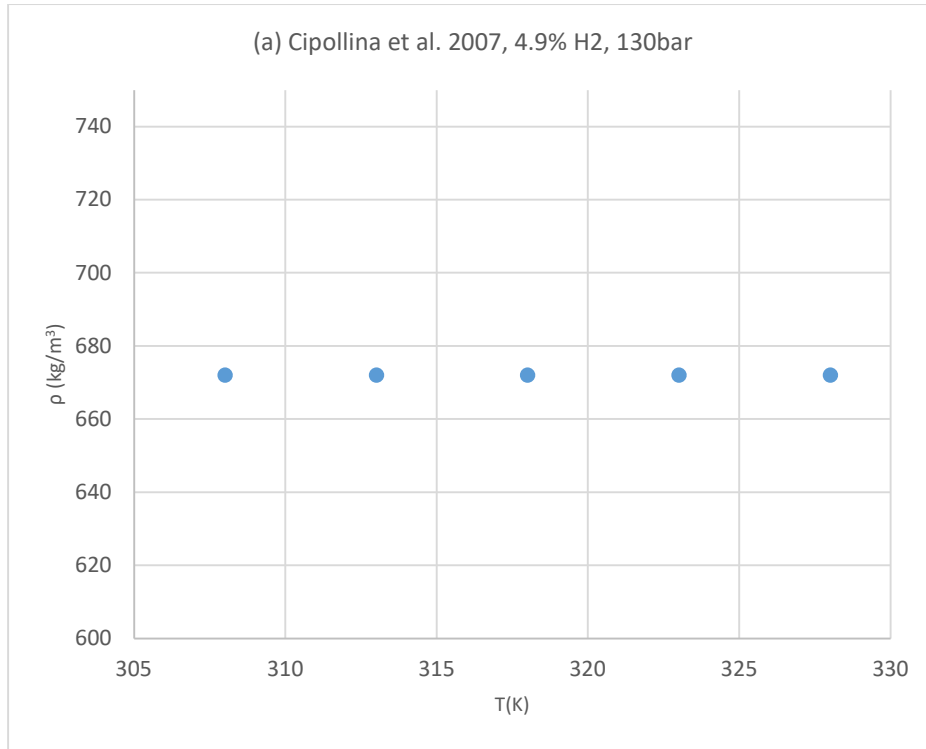


Figure 26: Cipollina et al. 2007 data at two different pressure and hydrogen molar composition conditions

Concluding the abovementioned statements, Cipollina et al.2007 data cannot be considered as a reliable dataset and should be excluded from the database. On Table 41 below are stated the datasets that have been excluded from the database due to invalid behavior.

Table 41: Experimental data that have been considered as reliable for the binary mixture of H<sub>2</sub>-CO regarding thermophysical properties

Dataset	Included in the database
Scott and Bone 1929	v
Townend, Bhatt, and Bone 1931	v
Cipollina et al.2007	x

#### 4.3.5 Binary mixture of H<sub>2</sub>-CO<sub>2</sub>

For the binary mixture of H<sub>2</sub>-CO<sub>2</sub> there are five available datasets in online literature regarding to mass density covering a wide range of experimental temperature, pressure and composition values.

Table 42: Experimental binary thermophysical properties data available in literature for the mixture of H<sub>2</sub>-CO<sub>2</sub>

Dataset	T range (K)	P range (MPa)	H <sub>2</sub> composition range	Number of points
Zhang et al. 2002	308.2	5.5-12.9	0.003	20
Cipollina et al. 2007	308.0-343.0	20.1-48.9	0.045-0.24	48
Ababio and McElroy 1993	303.2-343.2	9.7-12.7	0.3553-0.4906	9
Souissi, Kleinrahm, Yang and Richter 2017	273.2-323.2	0.5-6.0	0.05362	19
Bezanehtak et al. 2002	278.2-298.2	4.8-19.3	0.0088-0.1571	42

The comparison of the data of the different datasets is to be presented in detail below.

Comparing the data of Cipollina et al. 2007 to the ones of Souissi, Kleinrahm, Yang and Richter 2017 in temperature equal to 325 K and with 5% hydrogen in the mixture a strange behavior for Souissi, Kleinrahm, Yang and Richter 2017 data is observed. What is also obvious in Figure 27 is that the mass density values of Souissi, Kleinrahm, Yang and Richter 2017 data do not increase while pressure increases.

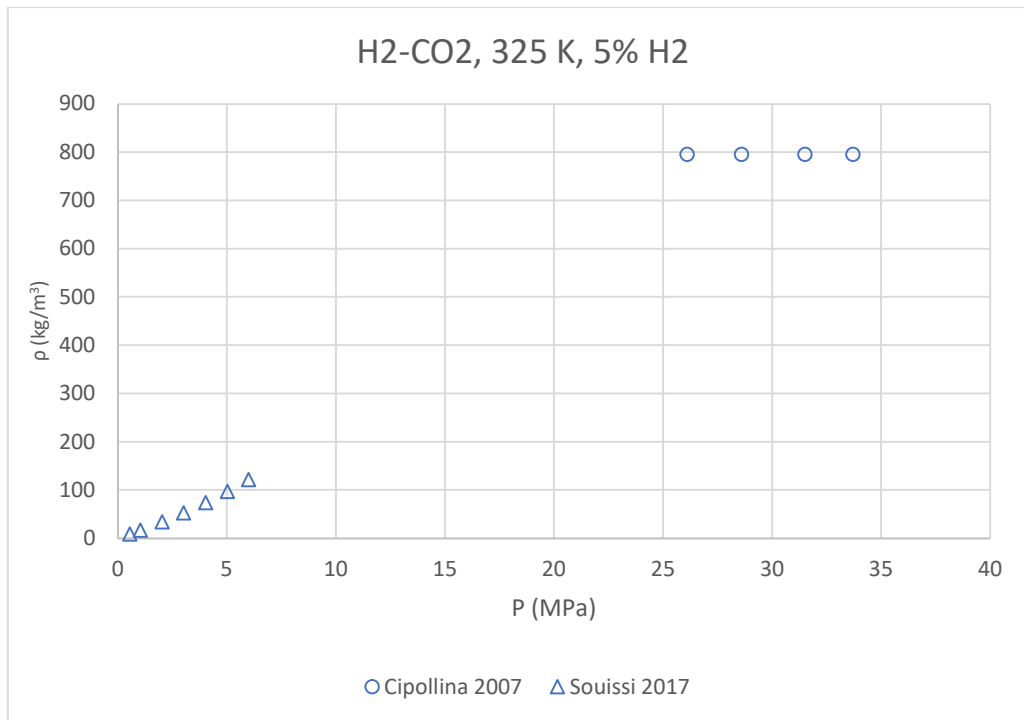


Figure 27: Comparison of Cipollina et al. 2007 and Souissi, Kleinrahm, Yang and Richter 2017 at composition of hydrogen equal to 0.05 and 325 K

Comparing the data of Bezahehtak et al. 2002 to the ones Souissi, Kleinrahm, Yang and Richter 2017 and Scott and Bone 1929 in temperature equal to 290 K and with 5% hydrogen in the mixture similar behavior is observed. What is also obvious in Figure 28 is that the mass density values increase while pressure increases for each one of the examined datasets, as expected. In Figure 29 the behavior of Bezahehtak et al. 2002 data is presented, which is as expected.

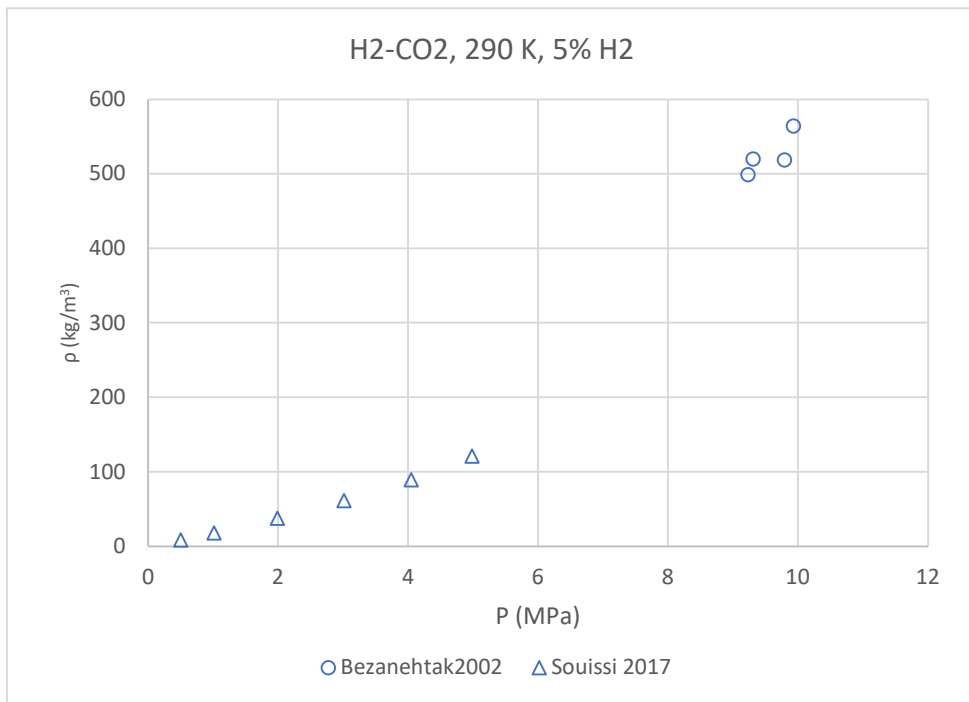


Figure 28: Comparison of Bezanhtak et al. 2002 and Souissi, Kleinrahm, Yang and Richter 2017 at 290 K and hydrogen's composition equal to 0.05

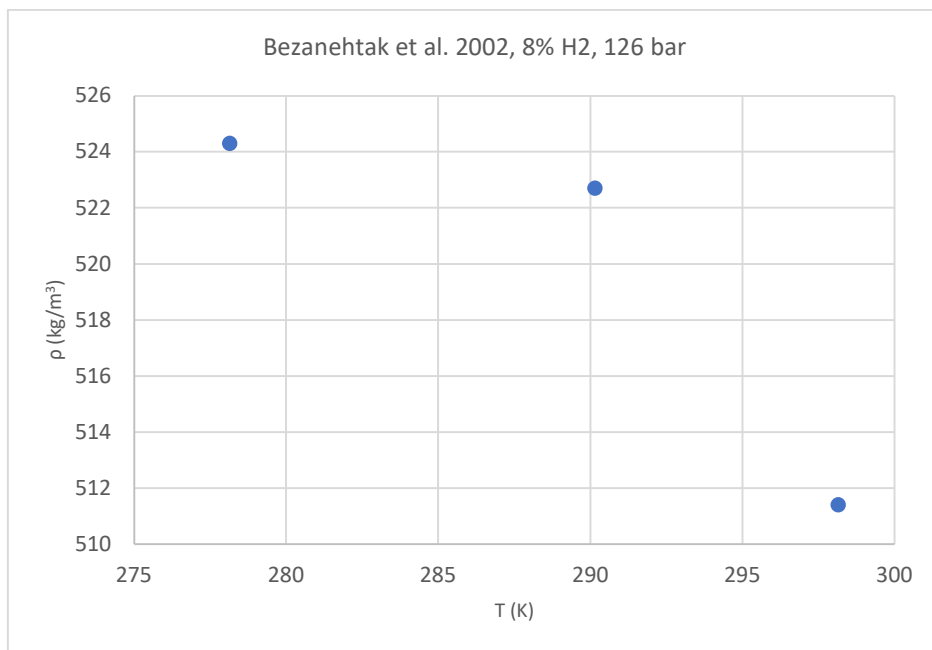


Figure 29: Bezanhtak et al. 2002 data at a specific pressure and hydrogen molar composition condition

Comparing the data of Ababio and McElroy 1993 to the ones Zhang et al. 2002 in temperature equal to 310 K and pressure equal to 115 bar similar behavior is observed. What is also obvious in Figure 30 is that the mass density values decrease while hydrogen's composition in the mixture increases when combining the data from the datasets, as expected.

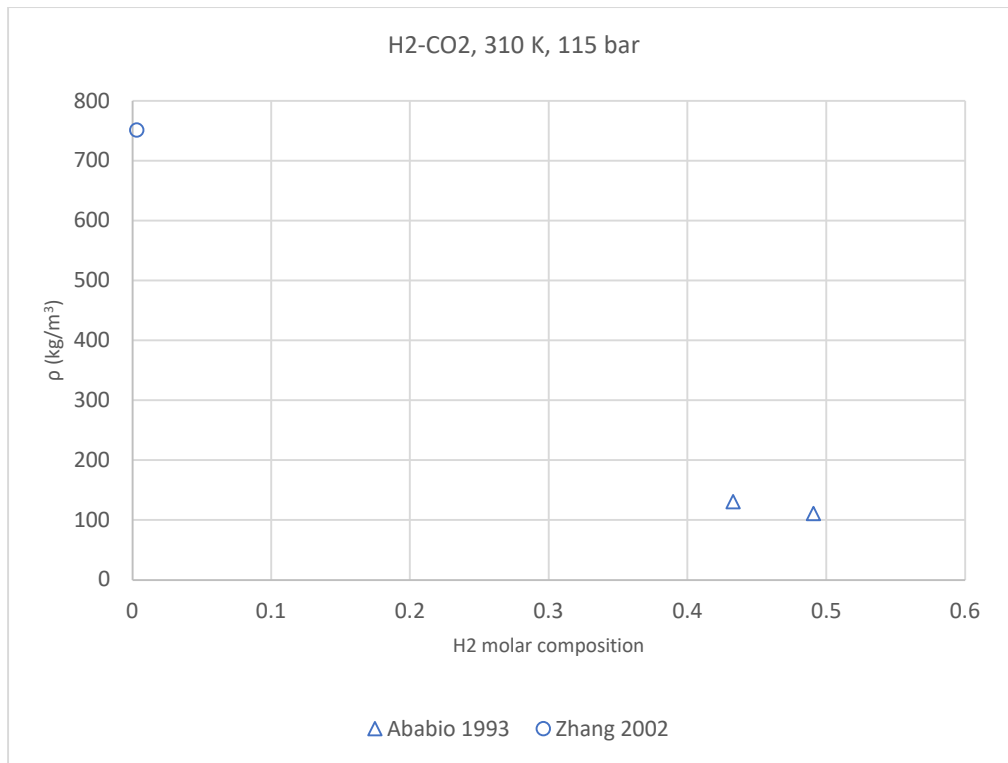


Figure 30: Comparison of Ababio and McElroy 1993 and Zhang et al. 2002 at 290 K and hydrogen's composition equal to 0.05

The comparison of Ababio and McElroy 1993 and Zhang et al. 2002 datasets to Cipollina et al. 2007, Souissi, Kleinrahm, Yang and Richter 2017 and Bezanehtak et al. 2002 is not possible because of their different temperature, pressure and composition spans.

Concluding the abovementioned statements, the Cipollina et al. 2007 data cannot be considered as correct. On Table 43 below are stated the datasets that have been excluded from the database due to invalid behavior.

Table 43: Experimental data that have been considered as reliable for the binary mixture of H<sub>2</sub>-CO<sub>2</sub> regarding thermophysical properties

Dataset	Included in the database
Zhang et al. 2002	v
Cipollina et al. 2007	x
Ababio and McElroy 1993	v
Souissi, Kleinrahm, Yang and Richter 2017	v
Bezanehtak et al. 2002	v

#### 4.3.6 Binary mixture of H<sub>2</sub>-N<sub>2</sub>

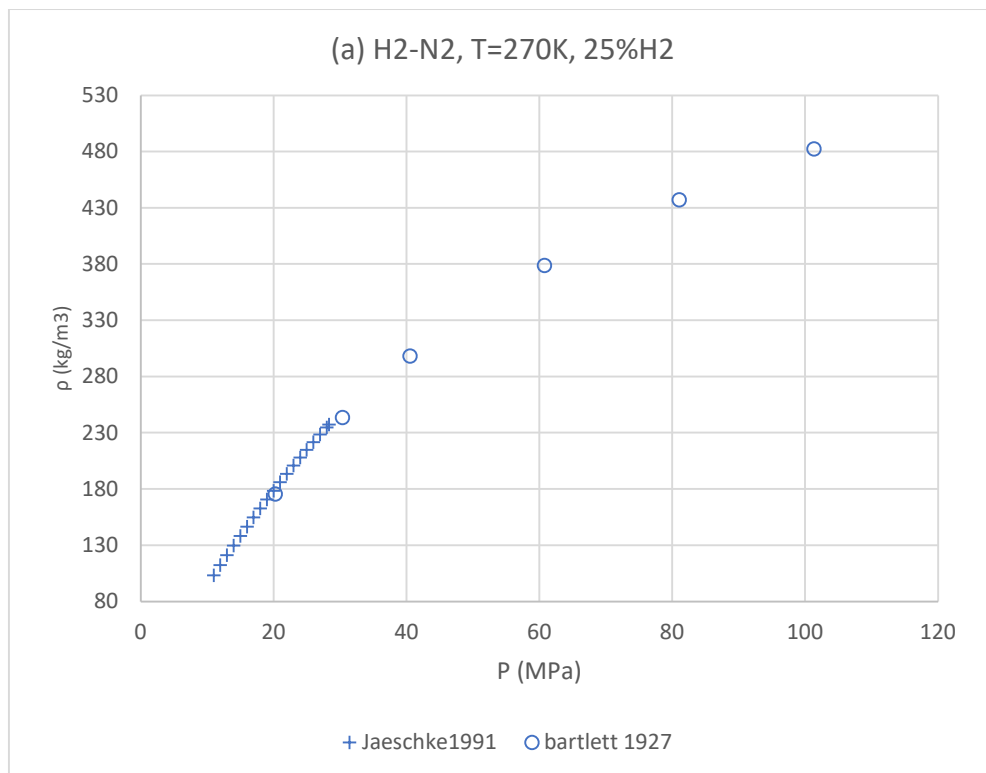
For the binary mixture of H<sub>2</sub>-N<sub>2</sub> there are five available datasets in online literature regarding to mass density covering a wide range of experimental temperature, pressure and composition values.

Table 44: Experimental binary thermophysical properties data available in literature for the mixture of H2-N2

Dataset	T range (K)	P range (MPa)	H2 composition range	Number of points
Jaeschke and Humphreys 1991	270.0-353.2	9.5-30.2	0.1495-0.5002	316
Hernández-Gómez et al. 2017	240.0-349.9	1.0-20.2	0.05-0.5	399
Deming and Shupe 1931	203.2-573.2	23.6-148.2	0.75	57
Bartlett et al. 1930	203.1-293.1	30.4-101.3	0.75	22
Bartlett, Cupples, and Tremearne 1927	273.2	10.1-101.3	0.0-0.885	45

The comparison of the data of the different datasets is to be presented in detail below.

Comparing the data of Jaeschke and Humphreys 1991 and to the ones of Hernández-Gómez et al. 2017 and Bartlett, Cupples, and Tremearne 1927 in temperature equal to 270 K and with 25% and 50% hydrogen in the mixture a similar behavior is observed. What is also obvious in Figure 31 is that the mass density values increase while pressure increases on each one of the datasets, as expected.



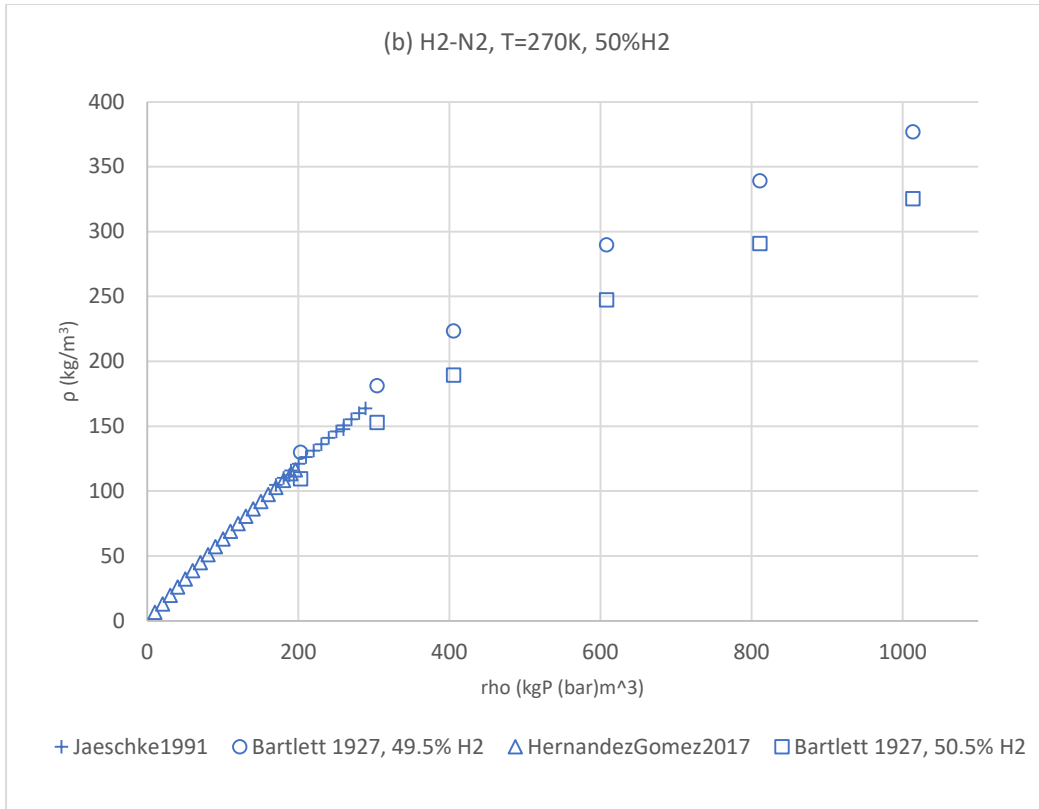
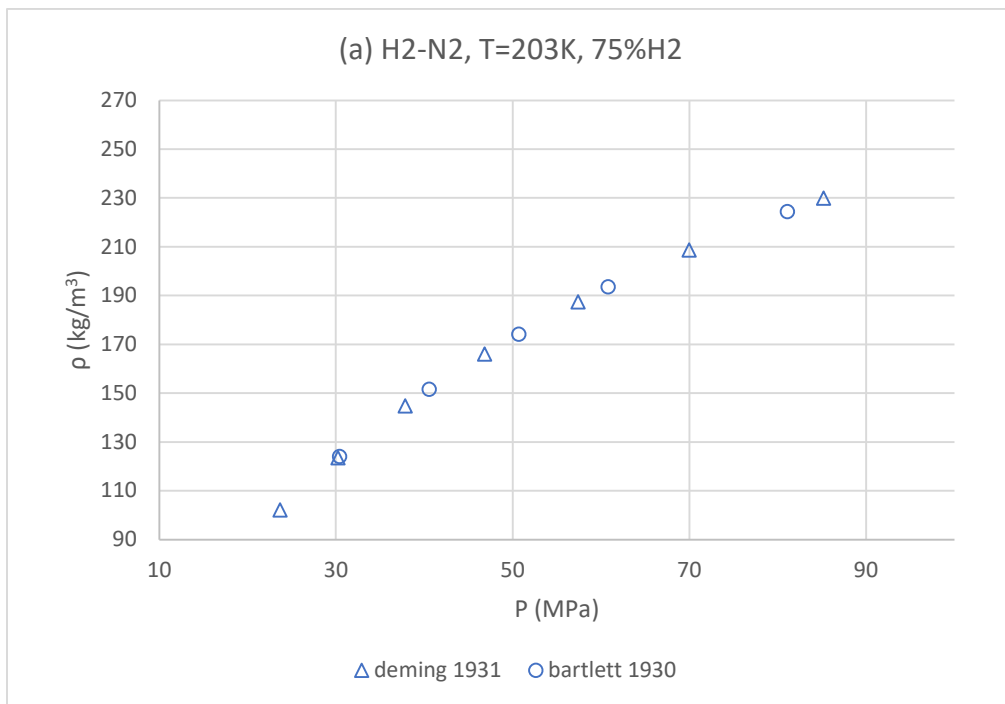


Figure 31: Comparison of Jaeschke and Humphreys 1991, Hernández-Gómez et al. 2017 and Bartlett, Cupples, and Tremearne 1927 at 325 K and a composition of hydrogen equal to (a) 0.25 and (b) 0.50

Comparing the data of Deming and Shupe 1931 to the ones of Bartlett et al. 1930 at temperature equal to 203 K and 295 K and with 75% hydrogen in the mixture a similar behavior is observed. What is also obvious in Figure 32 is that the mass density values increase while pressure increases on each one of the datasets, as expected.





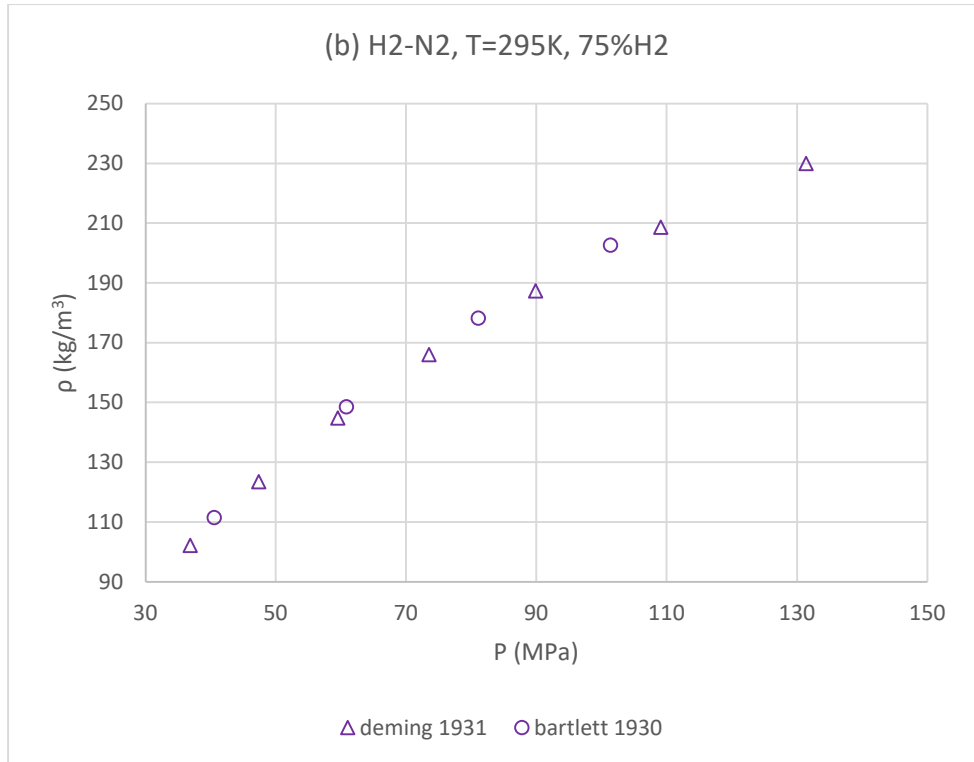


Figure 32: Comparison of Deming and Shupe 1931 and Bartlett et al. 1930 at a composition of hydrogen equal to 0.75 and (a) 203 K and (b) 295 K

Concluding the abovementioned statements, all of the available datasets for the binary mixture of H<sub>2</sub>-N<sub>2</sub> are reliable and should be included on the database.

On Table 45 below are stated the datasets that have been excluded from the database due to invalid behavior.

Table 45: Experimental data that have been considered as reliable for the binary mixture of H<sub>2</sub>-N<sub>2</sub> regarding thermophysical properties

Dataset	Included in the database
Jaeschke and Humphreys 1991	v
Hernández-Gómez et al. 2017	v
Deming and Shupe 1931	v
Bartlett et al. 1930	v
Bartlett, Cupples, and Tremearne 1927	v

#### 4.4 Model comparison on thermophysical properties data

After the evaluation of the available experimental data is completed, it is important to examine which thermodynamic models should be trusted for the calculation of thermophysical properties of these six binary mixtures. The thermodynamic models that are going to be evaluated are; GERG-2008, Peng-Robinson EoS, SRK EoS, PC-SAFT EoS and UMR-PRU on calculations relatable with energy properties such us molar enthalpy or Cp. The absolute relative average deviations of the model results compared to the experimental data

are presented on Table 46 for each binary mixture and each property. It is obvious that GERG-2008 results in better accuracy, which is expected because the model's parameters have been set after a fit to the available experimental data.

Table 46: The number of experimental points that have been used for the evaluation of the thermodynamic models regarding the thermophysical properties

Binary mixture	Total number of thermophysical-properties experimental data-points used
H <sub>2</sub> -CH <sub>4</sub>	1096 out of 1361
H <sub>2</sub> -C <sub>2</sub> H <sub>6</sub>	-
H <sub>2</sub> -C <sub>3</sub> H <sub>8</sub>	-
H <sub>2</sub> -CO	56 out of 114
H <sub>2</sub> -CO <sub>2</sub>	73 out of 119
H <sub>2</sub> -N <sub>2</sub>	1051 out of 1051

For the calculation of the errors occurred when comparing the GERG-2008 equation to experimental data there is presented the absolute average relative deviation (%ARD).

Table 47: Model accuracy regarding to the available thermophysical-properties experimental data

Binary mixture	Property	GERG 2008	PR EoS	SRK EoS	PC SAFT	UMR PRU
		%ARD				
H <sub>2</sub> -CH <sub>4</sub>	$\rho$	0.4	3.4	2.0	16.3	4.5
	JT	37.5	25.2	20.0	-	17.9
	w	0.04	0.9	1.2	-	0.7
H <sub>2</sub> -CO	$\rho$	2.8	6.5	3.5	3.3	-
	w	0.60	3.5	3.5	-	-
H <sub>2</sub> -CO <sub>2</sub>	$\rho$	1.1	3.4	5.1	13.4	3.4
H <sub>2</sub> -N <sub>2</sub>	$\rho$	0.1	7.1	1.0	1.0	16.1
	w	0.03	1.0	1.1	-	0.7
	C <sub>p,res</sub>	18.5	19.6	15.3	-	26.0

Joule-Thomson coefficient cannot be accurately predicted from the four thermodynamic models that have been used.

Last but not least, it is not possible to proceed to calculations for mixtures containing carbon monoxide using the model UMR-PRU because there are yet no available parameters for this component.

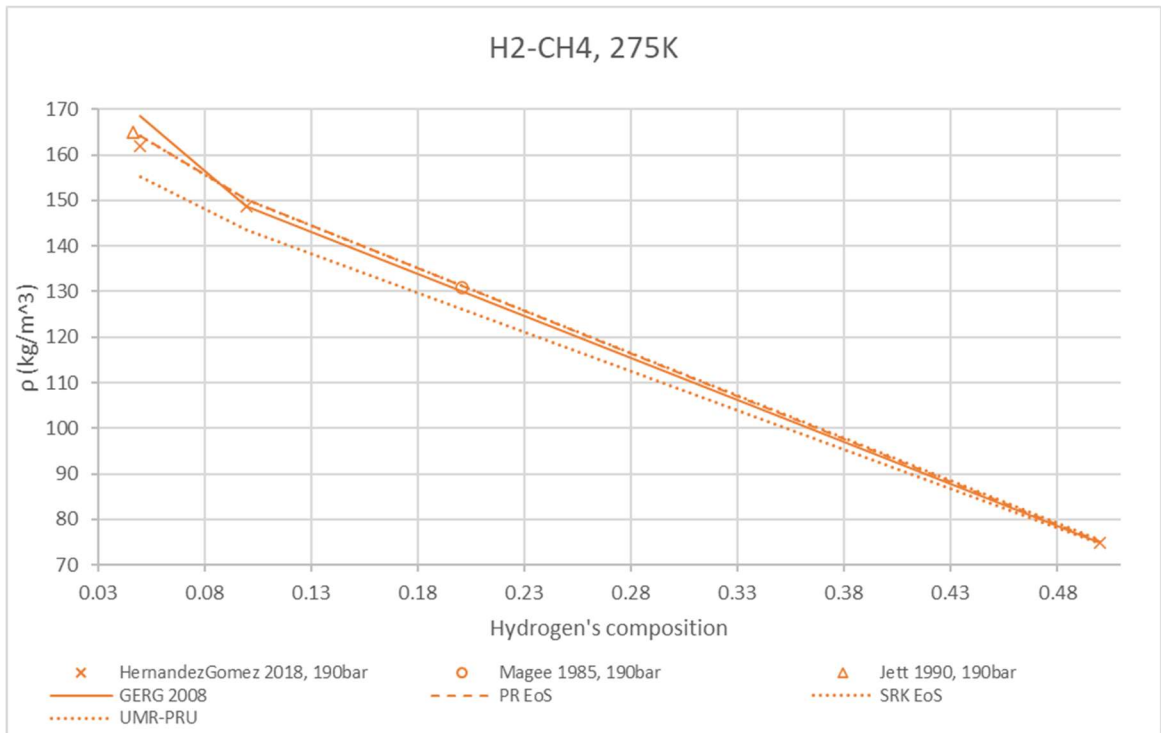
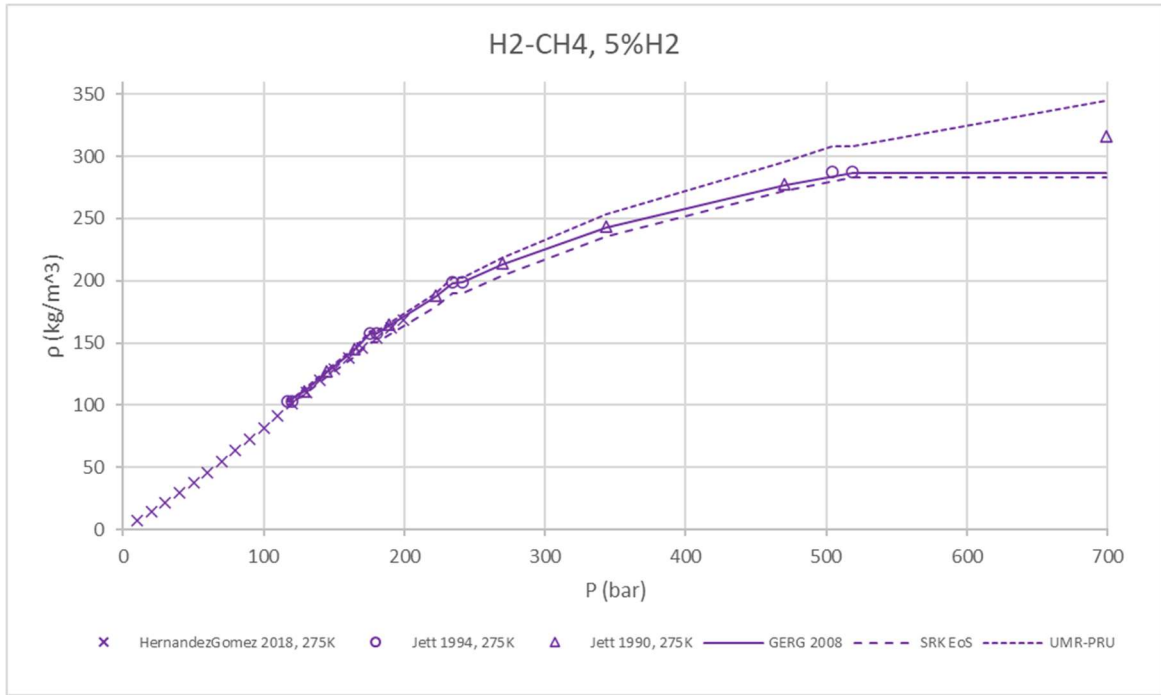


Figure 33: Model comparison with the available datasets in the binary mixture of H2-CH4

#### 4.5 Thermophysical properties data extension using GERG-2008

As it is thoroughly examined on sections 4.3 and 4.4, GERG-2008 EoS behaves very accurately regarding to single-phase density data, which is expected because the equations parameters have been fitted to valid available density data for these binary mixtures. GERG-2008 EoS, also, compares very accurately to speed of sound data for the binary mixtures of hydrogen mixed with methane, nitrogen and carbon monoxide. This model, though, fails significantly to predict JT coefficient and  $C_{p,res}$  for the mixtures that these kind of data are available.

Due to the very limited number of experimental data, especially in terms of high hydrogen compositions, it is important to extend the available database and evaluate the models' behavior. This is of major importance because the transition from natural gas streams to hydrogen streams can be achieved via achieving hydrogen injection to natural gases or similar gases so accurate prediction of the streams' behavior should be performed.

The extension of the available database will be performed using GERG-2008 EoS as the reference equation for density and sound velocity calculations. No one of the abovementioned thermodynamic models can be trusted for predicting the residual part of molar  $C_p$ , molar  $C_v$ , molar enthalpy and JT coefficient and so these properties will not be included in the extension.

The temperature range of properties' calculations is between 263.15 K and 323.15 K and the pressure range is between 1 bar and 300 bar which are relevant to natural gas pipeline transmission. Additionally, the mixtures that are to be examined contain hydrogen in the following compositions: [0.02, 0.05, 0.1, 0.2, 0.4, 0.6, 0.8, 0.9, 0.95, 0.98]. In the binaries of  $H_2-C_2H_6$ ,  $H_2-C_3H_8$  and  $CO_2$  the examined hydrogen composition will be over 0.8 in order to avoid the two-phase region.

Concluding that GERG-2008 equation is indeed the most accurate model that can be used for the calculation of thermophysical properties of different binary mixtures that can be found in natural gases, an evaluation of five other thermodynamic models is presented below. The models that are used are PR EoS, SRK EoS, PC SAFT EoS and UMR-PRU. The relative and absolute deviations between GERG-2008 and every other model will be presented in detail for the thermophysical properties of the examined six binary mixtures. The results for the binary of hydrogen mixed with carbon monoxide won't be presented with UMR-PRU due to lack of pure component parameters regarding to carbon monoxide.

For the calculation of the errors occurred when comparing the thermodynamic models to GERG-2008 there is presented the absolute average relative deviation (%ARD). In this case, the "experimental value" in equation 59 refers to the value given from GERG-2008 and the "calculated value" refers to the value given from the different thermodynamic models used for evaluation.

#### 4.5.1 Binary mixture of $H_2-CH_4$

As it is presented in Table 48 UMR-PRU and SRK EoS result into the most accurate predictions regarding to molar density predictions. All the evaluated thermodynamic models result in similar calculations as GERG-2008 while PC-SAFT EoS gives the largest deviation. Speed of sound can be predicted accurately from both PR EoS and SKR EoS with the best results given from SRK EoS. A general note for the thermophysical properties that are examined in this report is that the models fail to predict accurately their values for pressures below 50 bar and result in significantly smaller deviations as the pressure values reach up to 300 bar.

Table 48: Model results for the thermophysical properties of binary mixture of H<sub>2</sub>-CH<sub>4</sub> compared to GERG-2008 reference equation

Model	Single-phase molar density (mol/m <sup>3</sup> )	Speed of sound
	%ARD	%ARD
PR EoS	1.8	1.5
SRK EoS	1.0	0.8
PC SAFT	3.4	-
UMR - PRU	0.9	10.4

Indicatively, the density prediction behavior of the evaluated models is presented in Figure 34 below for different compositions

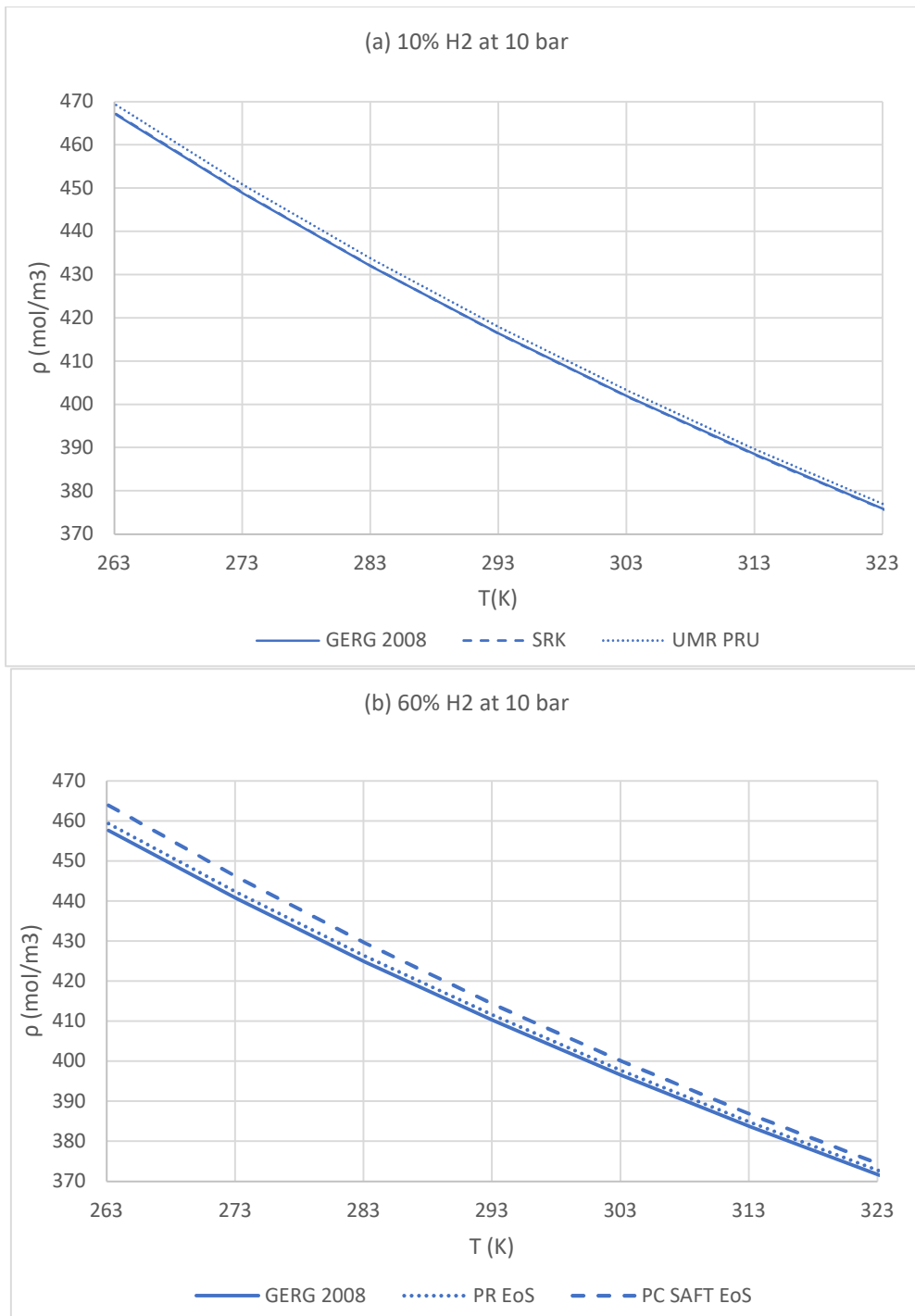


Figure 34: Comparison of the GERG-2008 equation with the equations of state in the binary mixture of H<sub>2</sub>-CH<sub>4</sub>

#### 4.5.2 Binary mixture of H<sub>2</sub>-C<sub>2</sub>H<sub>6</sub>

As it is presented in Table 49 SRK EoS results into the most accurate predictions regarding to molar density predictions. All the evaluated thermodynamic models result in similar calculations as GERG-2008 while PC-SAFT EoS gives the largest deviation. Speed of sound can be predicted accurately from both PR EoS and SKR EoS with the best results given from SRK EoS. A general note for the thermophysical properties that are examined in this report is that the models fail to predict accurately their values for pressures below 50 bar and result in significantly smaller deviations as the pressure values reach up to 300 bar.

Table 49: Model results for the thermophysical properties of binary mixture of H<sub>2</sub>-C<sub>2</sub>H<sub>6</sub> compared to GERG-2008 reference equation

Model	Single-phase molar density (mol/m <sup>3</sup> )	Speed of sound
	%ARD	%ARD
PR EoS	1.8	0.5
SRK EoS	0.3	0.1
PC SAFT	5.5	-
UMR - PRU	1.0	9.5

#### 4.5.3 Binary mixture of H<sub>2</sub>-C<sub>3</sub>H<sub>8</sub>

As it is presented in Table 50 UMR-PRU results into the most accurate predictions regarding to molar density predictions. All the evaluated thermodynamic models result in similar calculations as GERG-2008 while PC-SAFT EoS gives the largest deviation. Speed of sound can be predicted accurately from both PR EoS, SKR EoS and UMR-PRU with the best results given from SRK EoS. A general note for the thermophysical properties that are examined in this report is that the models fail to predict accurately their values for pressures below 50 bar and result in significantly smaller deviations as the pressure values reach up to 300 bar.

Table 50: Model results for the thermophysical properties of binary mixture of H<sub>2</sub>-C<sub>3</sub>H<sub>8</sub> compared to GERG-2008 reference equation

Model	Single-phase molar density (mol/m <sup>3</sup> )	Speed of sound
	%ARD	%ARD
PR EoS	1.7	0.4
SRK EoS	0.7	1.1
PC SAFT	4.2	-
UMR - PRU	0.6	0.5

#### 4.5.4 Binary mixture of H<sub>2</sub>-CO

The results for the binary of hydrogen mixed with carbon monoxide won't be presented with UMR-PRU due to lack of pure component parameters regarding to carbon monoxide.

As it is presented in Table 51 SRK EoS results into the most accurate predictions regarding to molar density predictions. All the evaluated thermodynamic models result in similar calculations as GERG-2008 while PC-SAFT EoS gives the largest deviation. Speed of sound can be predicted accurately from both PR EoS and SKR EoS with the best results given from SRK EoS. A general note for the thermophysical properties that are examined in this report is that the models fail to predict accurately their values for pressures below 50 bar and result in significantly smaller deviations as the pressure values reach up to 300 bar.

Table 51: Model results for the thermophysical properties of binary mixture of H<sub>2</sub>-CO compared to GERG-2008 reference equation

Model	Single-phase molar density (mol/m <sup>3</sup> )	Speed of sound
	%ARD	%ARD
PR EoS	1.8	1.4
SRK EoS	0.7	0.7
PC SAFT	2.7	-

#### 4.5.5 Binary mixture of H<sub>2</sub>-CO<sub>2</sub>

As it is presented in Table 52 SRK EoS results into the most accurate predictions regarding to molar density predictions. All the evaluated thermodynamic models result in similar calculations as GERG-2008 while PC-SAFT EoS gives the largest deviation. Speed of sound can be predicted accurately from both PR EoS and SKR EoS with the best results given from SRK EoS. A general note for the thermophysical properties that are examined in this report is that the models fail to predict accurately their values for pressures below 50 bar and result in significantly smaller deviations as the pressure values reach up to 300 bar.

Table 52: Model results for the thermophysical properties of binary mixture of H<sub>2</sub>-CO<sub>2</sub> compared to GERG-2008 reference equation

Model	Single-phase molar density (mol/m <sup>3</sup> )	Speed of sound
	%ARD	%ARD
PR EoS	2.7	0.9
SRK EoS	0.3	0.2
PC SAFT	4.4	-
UMR - PRU	1.0	1.3

#### 4.5.6 Binary mixture of H<sub>2</sub>-N<sub>2</sub>

As it is presented in Table 53 PC-SAFT EoS results into the most accurate predictions regarding to molar density predictions. All the evaluated thermodynamic models result in similar calculations as GERG-2008 while PC-SAFT EoS gives the largest deviation. Speed of sound can be predicted accurately from both PR EoS and SKR EoS with the best results given from SRK EoS. A general note for the thermophysical properties that are examined in this report is that the models fail to predict accurately their values for pressures below 50 bar and result in significantly smaller deviations as the pressure values reach up to 300 bar.



Table 53: Model results for the thermophysical properties of binary mixture of H<sub>2</sub>-N<sub>2</sub> compared to GERG-2008 reference equation

Model	Single-phase molar density (mol/m <sup>3</sup> )	Speed of sound
	%ARD	%ARD
PR EoS	2.0	3.5
SRK EoS	0.6	2.7
PC SAFT	0.5	-
UMR - PRU	9.1	6.0

#### 4.6 Discussion

The mix of hydrogen with natural gas streams can be a more sustainable solution for the fuel industry than the use of common natural gas. For this purpose, data related to the phase equilibrium of six binary mixtures containing hydrogen and natural common gases were collected and studied on this report. These mixtures are H<sub>2</sub>-CH<sub>4</sub>, H<sub>2</sub>-C<sub>2</sub>H<sub>6</sub>, H<sub>2</sub>-C<sub>3</sub>H<sub>8</sub>, H<sub>2</sub>-CO, H<sub>2</sub>-CO<sub>2</sub> and H<sub>2</sub>-N<sub>2</sub>, and the calculations that were performed were bubble point pressure and vapor phase composition calculations for various isotherms of these six different binary mixtures.

Moving to the evaluation of vapor-liquid equilibrium data that are available for the six binary mixtures, there were found various datasets covering a wide range of temperature and pressure conditions for each mixture. Street and Calado 1970 data cover a wide range of temperature and pressure values for the examined binary mixtures offering a lot of experimental data. Verschoyle 1931 is an unreliable source of data for the binary mixture of hydrogen mixed with carbon monoxide while its data are correct as it comes to hydrogen mixed with nitrogen. Akers and Eubanks 1960 and Augood 1957 are slightly inaccurate when compared to the rest of the datasets and especially when compared to Street and Calado data. Additionally, these two datasets contain a very limited variety of data points. As a general note, the datasets published before 1960 are the most unreliable ones. There is a need of extending the available database for the binary of hydrogen mixed with propane due to limited number of available experimental points. In terms of H<sub>2</sub>-CO binary mixture, it is also important to extend the available dataset in order to ensure the accuracy of the available data.

As it comes to the comparison of several thermodynamic models, the reference equation GERG-2008, the cubic equations PR and SRK EoS, PC-SAFT EoS and PR EoS coupled with an original UNIFAC-type G<sup>E</sup> model via the Universal Mixing Rules were evaluated regarding their accuracy on predicting the vapor-liquid equilibrium of the six abovementioned binary mixtures. The highest accuracy was stated by UMR-PRU, especially while calculating bubble point pressures. GERG-2008 does not result into the smallest deviations and it should not be used as a reference model for VLE calculations for binary mixtures that contain hydrogen. SRK EoS performed quite accurate results comparing to the available experimental data, especially for the vapor phase composition predictions for the binary mixtures of hydrogen mixed methane, ethane and nitrogen. PC-SAFT EoS cannot accurately predict the phase equilibrium behavior of binary mixtures that contain hydrogen.

The mix of hydrogen with natural gas streams can be a more sustainable solution for the fuel industry than the use of common natural gas. For this purpose, data related to the thermophysical properties of six binary mixtures containing hydrogen and natural common gases were collected and studied on this report. These mixtures are  $H_2-CH_4$ ,  $H_2-C_2H_6$ ,  $H_2-C_3H_8$ ,  $H_2-CO$ ,  $H_2-CO_2$  and  $H_2-N_2$ , and the properties of interest are single-phase molar density, residual molar isobaric ( $C_p$ ) and isochoric ( $C_v$ ) heat capacity, residual molar enthalpy, speed of sound and Joule-Thomson coefficient (JT). The temperature range of interest is between 263.15 K and 323.15 K and the pressure range is between 1 bar and 300 bar which are conditions relevant to natural gas pipeline transmission.

Several datasets for these six binary mixtures were evaluated and it was shown that some of them cannot be reliable, so they had to be excluded from the database. These datasets are the ones of Machado 1988, Cipollina et al. 2007. The available database is reach of data as it comes to single-phase density data for  $H_2$  mixed with  $CH_4$  or  $N_2$  but this is not the case for the rest of the examined thermophysical properties and binary mixtures. Especially for the binaries of  $H_2-C_2H_6$  and  $H_2-C_3H_8$  there are no correct data available.

What else is important to note is that the available datasets in online literature are in many cases old, focus on very low hydrogen molar composition in the mixtures and do not cover a wide range of temperatures and pressure conditions. The focus of the existent datasets is on molar composition that could be found in common natural gas mixtures which refers to very low hydrogen composition. So, in order to be confident about the thermodynamic models' behavior for mixtures that contain more than 10% hydrogen it is of major importance to enrich the existing database with new experimental data in order to create parameters for the thermodynamic models used in various simulation tools and achieve more accurate calculations.

The results of six different thermodynamic models were compared to the available experimental datasets. The models that were used are the reference equation for natural gases GERG-2008, Peng-Robinson EoS with a fitted acentric factor for hydrogen, SRK EoS, PC-SAFT EoS and UMR-PRU which is the PR EoS coupled with UNIFAC through the Universal Mixing Rule. The equations of state were compared with the reference equation GERG 2008 regarding to six different thermophysical properties of these binary mixtures, focusing on the residual parts of the examined properties. GERG-2008 is not the most accurate model for calculating thermophysical properties of binary mixtures of hydrogen with components that can be found in natural gases, while it can perform accurate calculations only regarding to single phase density and sound velocity data. It does not predict accurately the available Joule-Thomson coefficient and the residual part of heat capacity data. Thermophysical properties such as single-phase density and speed of sound were accurately predicted by all of the five models with GERG-2008 calculating the smallest deviations. The extension of the available database was performed using GERG-2008 EoS as the reference equation for density and sound velocity calculations. No one of the abovementioned thermodynamic models can be trusted for predicting the residual part of molar  $C_p$ , molar  $C_v$ , molar enthalpy and JT coefficient and so these properties will not be included in the extension.

The temperature range of properties' calculations is between 263.15 K and 323.15 K and the pressure range is between 1 bar and 300 bar which are relevant to natural gas pipeline transmission. Additionally, the mixtures that are to be examined contain hydrogen in the following compositions: [0.02, 0.05, 0.1, 0.2, 0.4, 0.6, 0.8, 0.9, 0.95, 0.98]. In the binaries of

H<sub>2</sub>-C<sub>2</sub>H<sub>6</sub>, H<sub>2</sub>-C<sub>3</sub>H<sub>8</sub> and CO<sub>2</sub> the examined hydrogen composition will be over 0.8 in order to avoid the two-phase region

In the binaries of hydrogen mixed with ethane and carbon dioxide there were no calculations for hydrogen molar composition prior to 80% due to the two-phase region and the same happens to the mixture of hydrogen with propane for hydrogen molar composition prior to 95%. All of the models used in this work (PR EoS, SRK EoS, PC SAFT EoS and UMR PRU) can predict the single-phase density and speed of sound, with SRK EoS resulting in the most successful calculations and PC-SAFT giving the worst results, always compared with the GERG 2008 reference equation.

It was interesting to conclude that the thermodynamic models that compared well to the experimental data of thermophysical properties failed to predict accurately the VLE data for the binary mixtures and vice versa. For example, PR EoS paired with the fitted acentric factor for hydrogen, as proposed by Aspen HYSYS, can predict relatively well the properties of binary mixtures containing hydrogen but failed to perform well in terms of the VLE calculations. It is important, though, to perform calculations with a thermodynamic model that can predict both the properties and the VLE with good accuracy.

To conclude the abovementioned statements GERG-2008 EoS is the equation that should be preferred for the calculations of single-phase density and sound velocity of the mixtures H<sub>2</sub>-CH<sub>4</sub>, H<sub>2</sub>-C<sub>2</sub>H<sub>6</sub>, H<sub>2</sub>-C<sub>3</sub>H<sub>8</sub>, H<sub>2</sub>-CO, H<sub>2</sub>-CO<sub>2</sub> and H<sub>2</sub>-N<sub>2</sub>,

Table 54: The most accurate EoS for each one of the examined properties for each one of the binary mixtures

Binary mixture	$\rho$	w	C <sub>p,res</sub>	JT	BPP	Y <sub>H2</sub>
H <sub>2</sub> -CH <sub>4</sub>	GERG-2008	GERG-2008	-	UMR-PRU	UMR-PRU	SRK EoS
H <sub>2</sub> -C <sub>2</sub> H <sub>6</sub>	GERG-2008	GERG-2008	-	-	UMR-PRU	PC-SAFT
H <sub>2</sub> -C <sub>3</sub> H <sub>8</sub>	GERG-2008	GERG-2008	-	-	UMR-PRU	UMR-PRU
H <sub>2</sub> -CO	GERG-2008	GERG-2008	-	-	PR EoS (experimental acentric factor)	GERG-2008
H <sub>2</sub> -CO <sub>2</sub>	GERG-2008	GERG-2008	-	-	UMR-PRU	SRK EoS
H <sub>2</sub> -N <sub>2</sub>	GERG-2008	GERG-2008	SRK EoS	-	UMR-PRU	PR EoS (fitted acentric factor)

## 5. Determination of the optimum interaction parameters on Peng - Robinson EoS

In section 4 of this text several thermodynamic models have been used to perform calculations regarding to VLE and thermophysical properties of hydrogen-containing binaries. More specifically, there has been a focus on binary mixtures that contain hydrogen and gases usually found in natural gas streams, such as methane, ethane, propane, carbon dioxide and nitrogen. After an evaluation of the available online experimental data a model comparison has been performed between GERG-2008, PR EoS, SRK EoS, PC SAFT EoS and UMR-PRU which is the PR EoS coupled with UNIFAC through the Universal Mixing Rule in order to evaluate the accuracy of the models.

It was expected from GERG-2008 which is used as a reference equation for natural gases to perform well for both VLE and thermophysical properties' calculations but it was found that this model cannot be trusted for the VLE calculations of the examined binary systems.

It was interesting to conclude that the thermodynamic models that compared well to the experimental data of thermophysical properties failed to predict accurately the VLE data for the binary mixtures and vice versa. For example, PR EoS paired with the fitted acentric factor for hydrogen, as proposed by Aspen HYSYS, can predict relatively well the properties of binary mixtures containing hydrogen but failed to perform well in terms of the VLE calculations. It is important, though, to perform calculations with a thermodynamic model that can predict both the properties and the VLE with good accuracy. For this purpose, it will be examined below if a regression of the binary interaction parameter ( $k_{ij}$ ) that is paired with PR EoS can improve the model's behavior. The initial calculations have been performed using the binary interaction parameters proposed by Aspen HYSYS for each binary mixture.

Table 55: Aspen HYSYS' proposed binary interaction parameters used for the calculations with PR equation of state

Binary mixture	PR EoS Kij parameters from Aspen HYSYS
H <sub>2</sub> -CH <sub>4</sub>	0.202
H <sub>2</sub> -C <sub>2</sub> H <sub>6</sub>	0.2231
H <sub>2</sub> -C <sub>3</sub> H <sub>8</sub>	0.2142
H <sub>2</sub> -CO	0.0253
H <sub>2</sub> -CO <sub>2</sub>	0.1202
H <sub>2</sub> -N <sub>2</sub>	-0.036

More specifically, a determination of the optimum  $k_{ij}$  of the six binary mixtures will be performed and it will be shown that the choice of different  $k_{ij}$  parameters can lead to better results. Special attention must be paid to the mixture of H<sub>2</sub> with CH<sub>4</sub> as it is the main component of natural gas streams.

Detailed knowledge of the vapor-liquid equilibrium and the thermophysical behavior of natural gas mixtures related to operation of natural gas pipelines is essential. It is important to understand the different behavior of the natural gas mixtures when they are mixed with hydrogen and the accuracy of the predictions of various thermodynamic models in these mixtures.

The average absolute relative deviations of the bubble point pressure and single-phase density calculations and the average absolute relative deviations along with the average absolute deviations for hydrogen's vapor molar composition calculations compared to the experimental data are presented in sections 5.1.1 to 5.1.6 below for the six binary mixtures respectively.

### 5.1.1 $k_{ij}$ Regression for the binary mixture of $H_2-CH_4$

In terms of the  $H_2-CH_4$  mixture, the datasets that were extracted from online literature and were used for the  $k_{ij}$  parameter fit are presented in Table 56 below.

Table 56: Experimental data that have been considered as reliable for the binary mixture of  $H_2-CH_4$

Dataset	Included in the database
Augood 1957	x
Benham 1957	x
Freeth 1931	x
Hong and Kobayashi 1980	v
Hu, Lin, Gu and Li 2014	v
Sagara, Arai and Saito 1972	v
Tsang, Clancy, Calado and Street 1980	v
Yorizane, Yoshimura, Masuoko and Toyama 1967	v
Kirk and Ziegler 1967	v
Hernández-Gómez et al. 2018	v
Jett, Fleyfel, and Kobayashi 1994	v
Jett 1990	v
Machado 1988	x
Magee et al. 1985	v
Chuang, Chappellear and Kobayashi 1976	v

Six different values for the  $k_{ij}$  parameter have been evaluated for this mixture and the average errors are presented below.

Table 57: The %ARD and AAD for the examined  $k_{ij}$  parameters for the binary mixture of  $H_2-CH_4$

$k_{ij}$	%ARD P	%ARD y	AAD y	%ARD dens
-0.2	44.3	6.5	0.041	2.9
-0.1	10.9	3.6	0.022	2.7
-0.05	20.3	3.3	0.020	2.6
0.1	102.9	4.9	0.029	2.3
0.202 Proposed by Aspen HYSYS	236.4	7.1	0.044	2.1
0.3	494.4	10.5	0.062	2.0

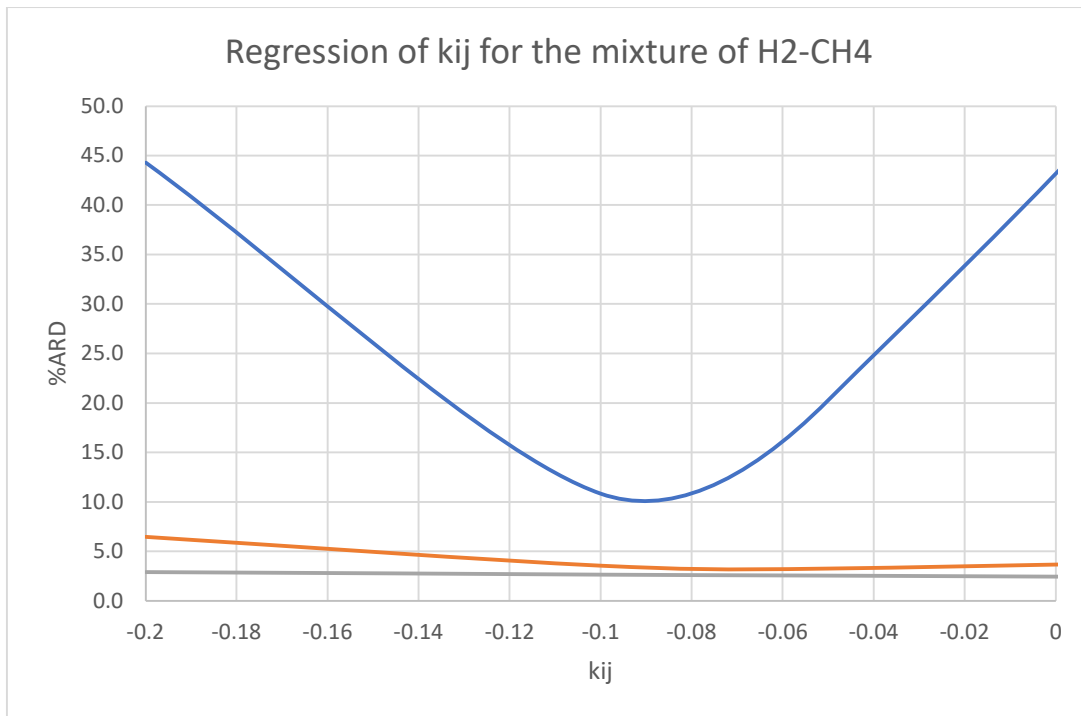


Figure 35: Regression of  $k_{ij}$  for the mixture of H<sub>2</sub>-CH<sub>4</sub> paired with PR EoS

It is obvious that, based on the collected experimental data for both thermophysical properties and two-phase equilibrium for the binary of H<sub>2</sub>-CH<sub>4</sub>, the  $k_{ij}$  value equal to 0.202 that is used from the Aspen HYSYS software results into very large deviation regarding to VLE calculations but respectively smaller deviation regarding to single-phase density calculations. A negative value, such as -0.09, should be used instead in order to perform the calculations more accurately.

On Figure 36 it is shown how PR EoS with the regressed  $k_{ij}$  parameter (set to -0.09) is compared with the UMR-PRU model which is the one performing the best results for this system.

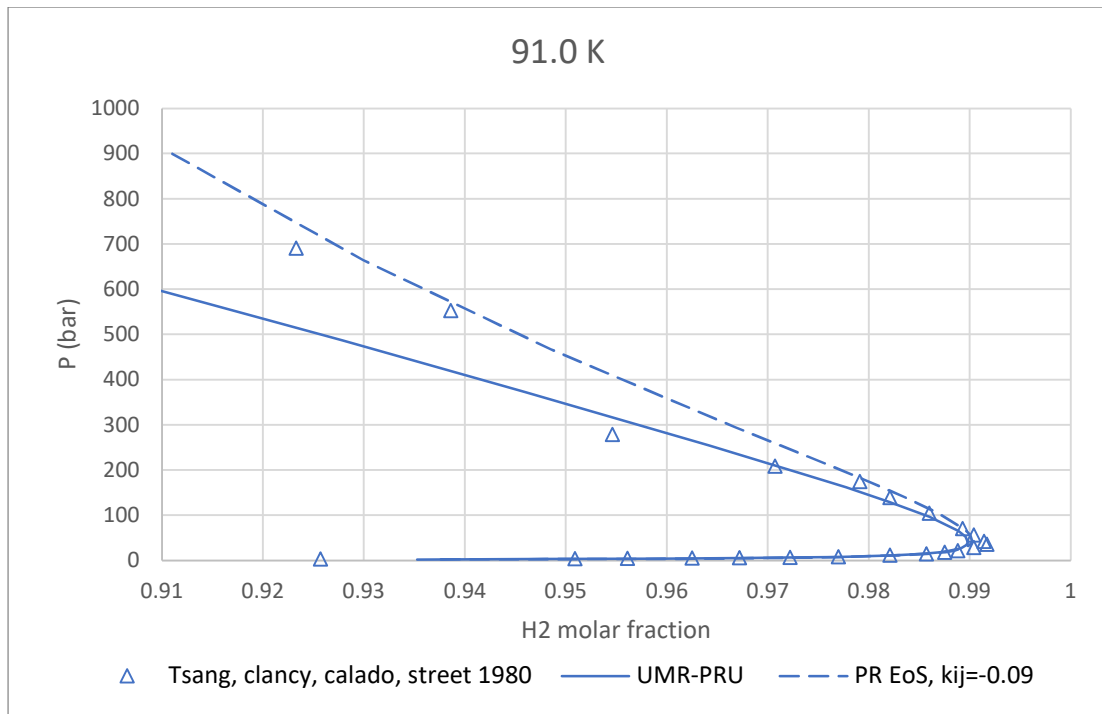


Figure 36: Comparison of UMR-PRU EoS and PR EoS with the regressed  $k_{ij}$  parameter for H<sub>2</sub>-Ch<sub>4</sub> mixture at 91.0 K

### 5.1.2 $k_{ij}$ Regression for the binary mixture of H<sub>2</sub>-C<sub>2</sub>H<sub>6</sub>

In terms of the H<sub>2</sub>-C<sub>2</sub>H<sub>6</sub> mixture, the datasets that were extracted from online literature and were used for the  $k_{ij}$  parameter fit are presented in Table 58 below.

Table 58: Experimental data that have been considered as reliable for the binary mixture of H<sub>2</sub>-C<sub>2</sub>H<sub>6</sub>

Dataset	Included in the database
Cohen and Hipnick 1967	v
Hiza, Heck and Kidney 1968	v
Sagara, arai and Saito 1972	v
Heintz and Street 1982	v

Eight different values for the  $k_{ij}$  parameter have been evaluated for this mixture and the average errors are presented below.

In Table 59 there is no available error between the calculated and experimental values of the mixture because there are no available data.

Table 59: The %ARD and AAD for the examined  $k_{ij}$  parameters for the binary mixture of H<sub>2</sub>-C<sub>2</sub>H<sub>6</sub>

$k_{ij}$	%ARD P	%ARD y	AAD y
-0.3	35.1	1.7	0.015
-0.22	32.3	1.4	0.012
-0.2	31.8	1.3	0.011
-0.18	31.6	1.3	0.011
-0.1	37.0	1.3	0.009
0	59.8	1.3	0.011
0.1	98.3	1.7	0.015
0.2231 Proposed by Aspen HYSYS	166.6	2.2	0.019

It is obvious that, based on the collected experimental data for both thermophysical properties and two-phase equilibrium for the binary of H<sub>2</sub>-C<sub>2</sub>H<sub>6</sub>, the  $k_{ij}$  value equal to 0.2231 that is used from the Aspen HYSYS software results into very large deviation regarding to VLE calculations. A negative value, such as -0.18, should be used instead in order to perform the calculations more accurately.

### 5.1.3 $k_{ij}$ Regression for the binary mixture of H<sub>2</sub>-C<sub>3</sub>H<sub>8</sub>

In terms of the H<sub>2</sub>-C<sub>3</sub>H<sub>8</sub> mixture, the datasets that were extracted from online literature and were used for the  $k_{ij}$  parameter fit are presented in Table 60 below.

Table 60: Experimental data that have been considered as reliable for the binary mixture of H<sub>2</sub>-C<sub>3</sub>H<sub>8</sub>

Dataset	Included in the database
Burris, Hsu, Reamer, Sage 1953	v
Trust, Kurata 1971	v

Six different values for the  $k_{ij}$  parameter have been evaluated for this mixture and the average errors are presented below.

Table 61: The %ARD and AAD for the examined  $k_{ij}$  parameters for the binary mixture of H<sub>2</sub>-C<sub>3</sub>H<sub>8</sub>

$k_{ij}$	%ARD P	%ARD y	AAD y
-0.3	28.3	3.5	0.025
-0.2	23.4	2.9	0.020
-0.18	23.7	2.9	0.022
0	28.3	2.7	0.018
0.1	45.2	3.4	0.023
0.2142 Proposed by Aspen HYSYS	70.5	5.2	0.030



It is obvious that, based on the collected experimental data for both thermophysical properties and two-phase equilibrium for the binary of H<sub>2</sub>-C<sub>3</sub>H<sub>8</sub>, the  $k_{ij}$  value equal to 0.2141 that is used from the Aspen HYSYS software results into very large deviation regarding to VLE calculations. A negative value, such as -0.2, should be used instead in order to perform the calculations more accurately.

#### 5.1.4 $k_{ij}$ Regression for the binary mixture of H<sub>2</sub>-CO

In terms of the H<sub>2</sub>-CO mixture, the datasets that were extracted from online literature and were used for the  $k_{ij}$  parameter fit are presented in Table 62 below.

Table 62: Experimental data that have been considered as reliable for the binary mixture of H<sub>2</sub>-CO

Dataset	Included in the database
Akers, Eubanks 1960	x
Augood 1957	x
Tsang, Clancy, Street and Calado 1980	v
Verschole 1931	x
Yorizane, Yoshimura, Masuoko, Toyama 1968	v
Scott and Bone 1929	v
Townend, Bhatt, and Bone 1931	v
Cipollina et al.2007	x

Five different values for the  $k_{ij}$  parameter have been evaluated for this mixture and the average errors are presented below.

Table 63: The %ARD and AAD for the examined  $k_{ij}$  parameters for the binary mixture of H<sub>2</sub>-CO

$k_{ij}$	%ARD P	%ARD y	AAD y	%ARD dens
-0.2	49.9	4.7	0.038	7.2
-0.12	32.0	3.3	0.024	7.0
-0.1	23.0	2.5	0.020	6.9
-0.08	19.3	2.1	0.015	6.8
0.0253 Proposed by Aspen HYSYS	54.4	2.1	0.015	6.5

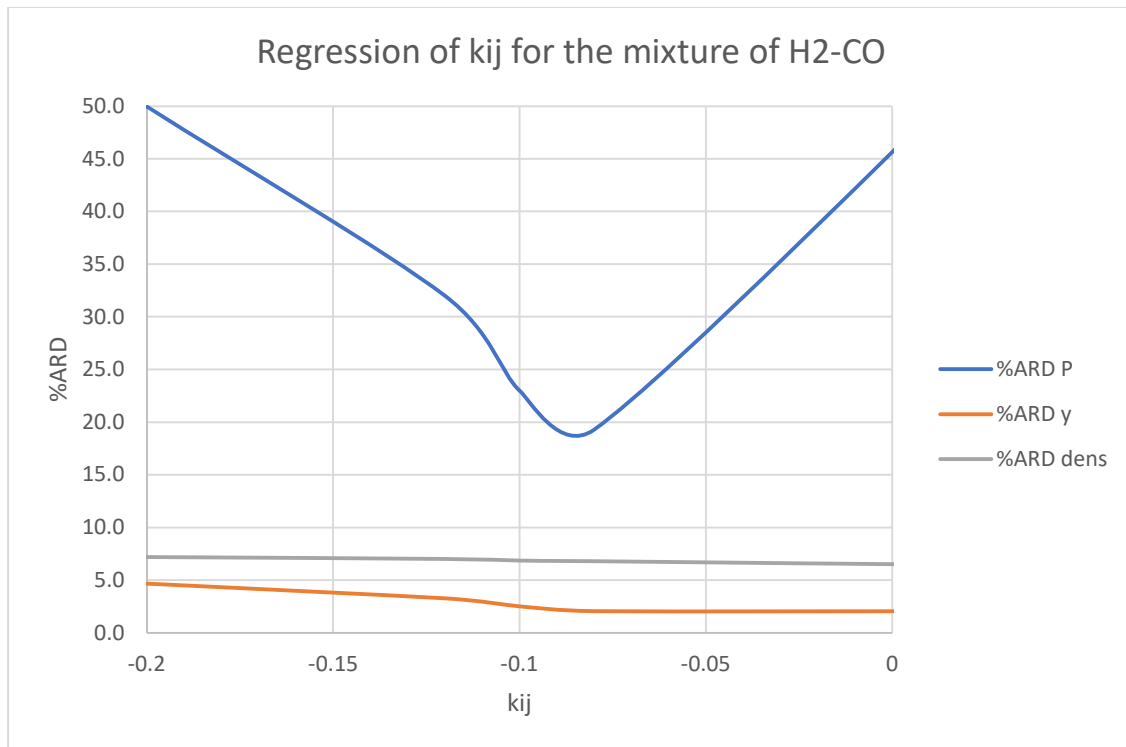


Figure 37: Regression of  $k_{ij}$  for the mixture of H<sub>2</sub>-CO paired with PR EoS

It is obvious that, based on the collected experimental data for both thermophysical properties and two-phase equilibrium for the binary of H<sub>2</sub>-CO, the  $k_{ij}$  value equal to 0.0253 that is used from the Aspen HYSYS software results into very large deviation regarding to VLE calculations but respectively smaller deviation regarding to single-phase density calculations. A negative value, such as -0.08, should be used instead in order to perform the calculations more accurately.

### 5.1.5 $k_{ij}$ Regression for the binary mixture of H<sub>2</sub>-CO<sub>2</sub>

In terms of the H<sub>2</sub>-CO<sub>2</sub> mixture, the datasets that were extracted from online literature and were used for the  $k_{ij}$  parameter fit are presented in Table 64 below.

Table 64: Experimental data that have been considered as reliable for the binary mixture of H<sub>2</sub>-CO<sub>2</sub>

Dataset	Included in the database
Zhang et al. 2002	v
Cipollina et al. 2007	x
Ababio and McElroy 1993	v
Souissi, Kleinrahm, Yang and Richter 2017	v
Bezanehtak et al. 2002	v
Augood 1957	x
Kaminishi, Toriumi 1966	v
Spano, Heck, Barrick 1968	v
Tsang, Street 1980	v
Yorizane, Yoshimura, Masuoka, Toyama 1968	x

Five different values for the  $k_{ij}$  parameter have been evaluated for this mixture and the average errors are presented below.

Table 65: The %ARD and AAD for the examined  $k_{ij}$  parameters for the binary mixture of H<sub>2</sub>-CO<sub>2</sub>

$k_{ij}$	%ARD P	%ARD y	AAD y	%ARD dens
-0.2	44.3	21.1	0.090	3.7
-0.1	20.4	19.8	0.082	3.5
-0.05	24.4	20.5	0.087	3.5
0.1202 Proposed by Aspen HYSYS	63.4	23.2	0.093	3.4
0.2	92.1	23.9	0.107	3.3

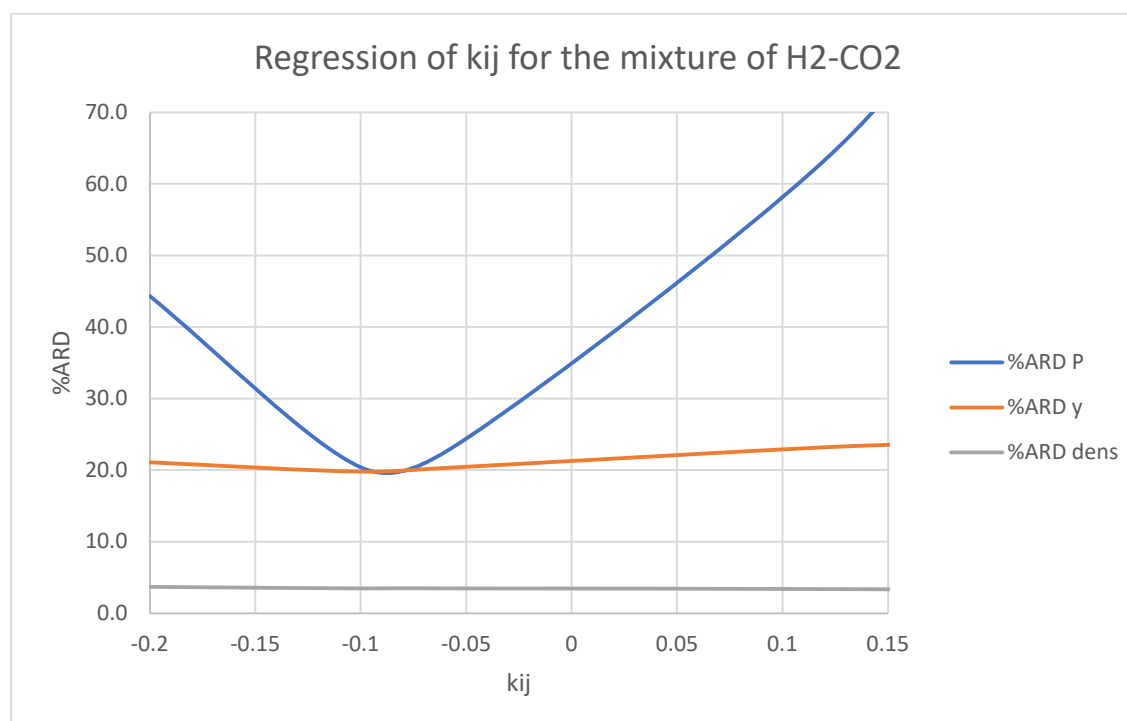


Figure 38: Regression of  $k_{ij}$  for the mixture of H<sub>2</sub>-CO<sub>2</sub> paired with PR EoS

It is obvious that, based on the collected experimental data for both thermophysical properties and two-phase equilibrium for the binary of H<sub>2</sub>-CO<sub>2</sub>, the  $k_{ij}$  value equal to 0.202 that is used from the Aspen HYSYS software results into very large deviation regarding to VLE calculations but respectively smaller deviation regarding to single-phase density calculations. A negative value, such as -0.1, should be used instead in order to perform the calculations more accurately.

### 5.1.6 $k_{ij}$ Regression for the binary mixture of H<sub>2</sub>-N<sub>2</sub>

In terms of the H<sub>2</sub>-N<sub>2</sub> mixture, the datasets that were extracted from online literature and were used for the  $k_{ij}$  parameter fit are presented in Table 65 below.

Table 66: Experimental data that have been considered as reliable for the binary mixture of H<sub>2</sub>-N<sub>2</sub>

Dataset	Included in the database
Akers, Eubanks 1960	x
Augood 1957	x
Gonikberg, Fastowski, Gurwitsch 1939	x
Maimoni 1961	v
Street, Calado 1978	v
Verschoyle 1931	v
Yoshimura, Yorizane, Naka 1971	v
Jaeschke and Humphreys 1991	v
Hernández-Gómez et al. 2017	v
Deming and Shupe 1931	v
Bartlett et al. 1930	v
Bartlett, Cupples, and Tremearne 1927	v

Five different values for the  $k_{ij}$  parameter have been evaluated for this mixture and the average errors are presented below.

Table 67: The %ARD and AAD for the examined  $k_{ij}$  parameters for the binary mixture of H<sub>2</sub>-N<sub>2</sub>

$k_{ij}$	%ARD P	%ARD y	AAD y	%ARD dens
-0.1	32.9	4.4	0.031	7.8
-0.036 Proposed by Aspen HYSYS	20.5	2.5	0.017	7.6
-0.02	15.9	2.2	0.015	7.6
0	16.5	2.0	0.014	7.6
0.02	25.3	2.5	0.017	7.6
0.05	97.7	2.9	0.020	7.5
0.1	176.4	3.8	0.025	7.4

It is obvious that, based on the collected experimental data for both thermophysical properties and two-phase equilibrium for the binary of H<sub>2</sub>-N<sub>2</sub>, the  $k_{ij}$  value equal to -0.036 that is used from the Aspen HYSYS software results into very large deviation regarding to VLE calculations but respectively smaller deviation regarding to single-phase density calculations. A  $k_{ij}$  value equal to -0.02 should be used instead in order to perform the calculations more accurately.

## 5.2 Discussion

The mix of hydrogen with natural gas streams can be a more sustainable solution for the fuel industry than the use of common natural gas. For this purpose, data related to the phase

equilibrium and thermodynamic properties of six binary mixtures containing hydrogen and natural common gases were collected and studied on previous reports. Five thermodynamic models were used for these calculations but failed to accurately predict both two-phase equilibrium and single-phase density behavior of each binary mixture.

In this work focus is placed indicatively on the determination of the  $k_{ij}$  parameters that are used on PR EoS. Similar procedure can be performed to determine also the  $k_{ij}$  parameters used by SRK EoS and PC-SAFT EoS. It is important to note that the parameters used by UMR-PRU are originally fitted to VLE experimental data.

It has been found that the binary interaction parameters paired with equations of state strongly affect the model's behavior. With a focus on the cubic equation of state PR EoS and on the binary mixtures, it was examined whether a fit of the  $k_{ij}$  parameters can significantly affect the final results.

Table 68: Proposed and regressed binary interaction parameters for the six binary mixtures

kij	H <sub>2</sub> -CH <sub>4</sub>	H <sub>2</sub> -C <sub>2</sub> H <sub>6</sub>	H <sub>2</sub> -C <sub>3</sub> H <sub>8</sub>	H <sub>2</sub> -CO	H <sub>2</sub> -CO <sub>2</sub>	H <sub>2</sub> -N <sub>2</sub>
Proposed by Aspen HYSYS	0.202	0.2231	0.2141	0.0253	0.1202	-0.036
Fitted parameter	-0.09	-0.18	-0.20	-0.08	-0.10	-0.02

The deviations occurred between model calculations and the experimental data for the thermophysical properties and two-phase equilibrium will be presented in Tables 69 and 70 for the mixtures.

Table 69: Model accuracy regarding to the thermophysical properties experimental data

Binary mixture	Property	GERG 2008	PR EoS $k_{ij}=0.202$	SRK EoS	PC SAFT	UMR PRU	PR EoS $k_{ij}=-0.09$
		%ARD					
H <sub>2</sub> -CH <sub>4</sub>	$\rho$	0.4	2.1	2.0	16.3	4.5	2.7
	JT	37.5	25.2	20.0	-	17.9	17.7
	w	0.04	0.9	1.2	-	0.7	1.1
Binary mixture	Property	GERG 2008	PR EoS $k_{ij}=0.0253$	SRK EoS	PC SAFT	UMR PRU	PR EoS $k_{ij}=-0.08$
		%ARD					
H <sub>2</sub> -CO	$\rho$	2.8	6.5	3.5	3.3	-	6.8
	w	0.60	3.5	3.5	-	-	3.5
Binary mixture	Property	GERG 2008	PR EoS $k_{ij}=0.1202$	SRK EoS	PC SAFT	UMR PRU	PR EoS $k_{ij}=-0.1$
		%ARD					
H <sub>2</sub> -CO <sub>2</sub>	$\rho$	1.1	3.4	5.1	13.4	3.4	3.5
Binary mixture	Property	GERG 2008	PR EoS $k_{ij}=-0.036$	SRK EoS	PC SAFT	UMR PRU	PR EoS $k_{ij}=-0.02$
		%ARD					
H <sub>2</sub> -N <sub>2</sub>	$\rho$	0.1	7.6	1.0	1.0	16.1	7.6
	w	0.03	1.0	1.1	-	0.7	0.9
	$C_{p,res}$	18.5	19.6	15.3	-	26.0	35.0

Table 70: Model accuracy regarding to the VLE experimental data

Binary mixture	Property	GERG 2008	PR EoS $k_{ij}=0.202$	SRK EoS	PC SAFT	UMR PRU	PR EoS $k_{ij}=-0.1$
%ARD							
H <sub>2</sub> -CH <sub>4</sub>	BPP	9.9	236.4	15.1	71.2	4.8	10.9
	y <sub>H2</sub>	6.0	7.1	3.3	12.7	3.8	3.6
Binary mixture	Property	GERG 2008	PR EoS $k_{ij}=0.2231$	SRK EoS	PC SAFT	UMR PRU	PR EoS $k_{ij}=-0.18$
%ARD							
H <sub>2</sub> -C <sub>2</sub> H <sub>6</sub>	BPP	15.1	166.2	16.0	47.7	11.2	31.6
	y <sub>H2</sub>	6.3	2.2	1.4	0.3	1.1	1.3
Binary mixture	Property	GERG 2008	PR EoS $k_{ij}=0.2141$	SRK EoS	PC SAFT	UMR PRU	PR EoS $k_{ij}=-0.2$
%ARD							
H <sub>2</sub> - C <sub>3</sub> H <sub>8</sub>	BPP	11.2	70.5	24.2	35.3	10.1	23.4
	y <sub>H2</sub>	3.8	5.2	6.4	3.9	1.5	2.9
Binary mixture	Property	GERG 2008	PR EoS $k_{ij}=0.0253$	SRK EoS	PC SAFT	UMR PRU	PR EoS $k_{ij}=-0.08$
%ARD							
H <sub>2</sub> -CO	BPP	22.1	54.4	32.4	146.7	-	19.3
	y <sub>H2</sub>	5.7	2.1	7.2	17.6	-	2.1
Binary mixture	Property	GERG 2008	PR EoS $k_{ij}=0.1202$	SRK EoS	PC SAFT	UMR PRU	PR EoS $k_{ij}=-0.1$
%ARD							
H <sub>2</sub> -CO <sub>2</sub>	BPP	19.4	63.4	20.4	119.9	15.0	20.5
	y <sub>H2</sub>	15.5	23.2	15.3	39.7	17.0	19.8
Binary mixture	Property	GERG 2008	PR EoS $k_{ij}=-0.036$	SRK EoS	PC SAFT	UMR PRU	PR EoS $k_{ij}=-0.02$
%ARD							
H <sub>2</sub> -N <sub>2</sub>	BPP	35.0	20.5	29.9	122.7	15.7	16.5
	y <sub>H2</sub>	5.2	2.5	3.3	10.0	3.6	2.0

It is obvious that a significant decrease is occurred in the error values referring to VLE calculations with PR EoS combined with the fitted  $k_{ij}$  parameters. The deviations for single-phase density results perform an increase which is though insignificant. So, as it is expected, a change in the  $k_{ij}$  parameter can widely affect bubble point pressure calculations and significantly affect the components' vapor phase calculations while at the same time single-phase density values are almost independent of this change. It is impossible to determine the optimum  $k_{ij}$  parameter of a binary mixture if the only available data are the single-phase density data. The regression of  $k_{ij}$  should be based on VLE data and mainly in bubble point pressure data for each mixture.

It can be concluded that the  $k_{ij}$  parameter adjustment leads to better accuracy in the VLE calculations regarding to all of the binary mixtures.

Focusing on the binary mixture of hydrogen mixed with methane GERG-2008 EoS gives the most accurate results for single-phase density calculations but UMR-PRU EoS is very accurate for VLE calculations. PR EoS with the adjusted  $k_{ij}$  parameter is not the most accurate model for these calculations but behaves better than UMR-PRU EoS in terms of single-phase density

calculations and better than GERG-2008 in terms of VLE calculations. Concluding the abovementioned statements, PR EoS can be used for calculations related to H<sub>2</sub>-CH<sub>4</sub> binary mixture since it gives quite satisfactory results. Additionally, the results were highly improved in terms of the JT calculations for which PR EoS with the regressed  $k_{ij}$  gave very similar results to UMR-PRU. The results were also slightly improved as it comes to speed of sound calculations. So PR EoS with a regressed  $k_{ij}$  parameter can be trusted for both VLE and thermophysical properties' calculations.

Focusing on the binary mixture of hydrogen mixed with ethane UMR-PRU EoS is very accurate for VLE calculations. PR EoS with the adjusted  $k_{ij}$  parameter is not the most accurate model for these calculations and gives high deviations regarding bubble point pressures. It can successfully, though, predict the vapor-phase component composition of the mixture. Concluding the abovementioned statements, PR EoS cannot be used for calculations related to H<sub>2</sub>-C<sub>2</sub>H<sub>6</sub> binary mixture and UMR-PRU should be used instead.

Focusing on the binary mixture of hydrogen mixed with propane UMR-PRU EoS is very accurate for VLE calculations. PR EoS with the adjusted  $k_{ij}$  parameter is not the most accurate model for these calculations and gives high deviations regarding bubble point pressures. It can successfully, though, predict the vapor-phase component composition of the mixture. Concluding the abovementioned statements, PR EoS cannot be used for calculations related to H<sub>2</sub>-C<sub>3</sub>H<sub>8</sub> binary mixture and UMR-PRU should be used instead.

Focusing on the binary mixture of hydrogen mixed with carbon monoxide GERG-2008 EoS gives the most accurate results for single-phase density calculations and for VLE calculations. PR EoS with the adjusted  $k_{ij}$  parameter is not the most accurate model for these calculations but behaves better than GERG-2008 in terms of VLE calculations regarding the phase component composition predictions. Concluding the abovementioned statements, PR EoS can be used for calculations related to H<sub>2</sub>-CO binary mixture since it gives quite satisfactory results. Additionally, there is no significant improvement on speed of sound calculations while using PR EoS with the fitted  $k_{ij}$  parameter.

Focusing on the binary mixture of hydrogen mixed with carbon dioxide GERG-2008 EoS gives the most accurate results for single-phase density calculations but UMR-PRU EoS and GERG-2008 behave similarly regarding VLE calculations. PR EoS with the adjusted  $k_{ij}$  parameter is not the most accurate model for these calculations but behaves similar to UMR-PRU EoS in terms of single-phase density calculations and better calculations. Concluding the abovementioned statements, PR EoS can be used for calculations related to H<sub>2</sub>-CO<sub>2</sub> binary mixture since it gives quite satisfactory results. For this binary mixture the examined models fail to give accurate results.

Focusing on the binary mixture of hydrogen mixed with nitrogen GERG-2008 EoS gives the most accurate results for single-phase density calculations but UMR-PRU EoS is very accurate for VLE calculations. PR EoS with the adjusted  $k_{ij}$  parameter is not the most accurate model for these calculations but behaves better than UMR-PRU EoS in terms of single-phase density calculations and better than GERG-2008 in terms of VLE calculations. Concluding the abovementioned statements, PR EoS can be used for calculations related to H<sub>2</sub>-N<sub>2</sub> binary mixture since it gives quite satisfactory results. Additionally, there is no significant improvement on speed of sound calculations while using PR EoS with the fitted  $k_{ij}$  parameter. As it comes to  $C_{p,res}$  calculations, the results occurred with the fitted  $k_{ij}$  parameter are significantly worse.

## 6. Conclusions and future work

Even though hydrogen is a very promising substitute of fossil fuels, the transition from natural gas to hydrogen cannot happen immediately. Usually, in natural gas mixtures the molar composition of hydrogen is found as trace or up to 0.05%. The transition to hydrogen energy could be achieved by producing hydrogen-containing mixtures of determined purity via steam reforming of natural gas or similar gases. For this purpose, detailed examination of the available thermodynamic models' accuracy on energy and transport related properties' calculations, relevant to pure hydrogen and mixtures of hydrogen with the main components of natural gas or similar gases, should be performed. In this work, focus is placed on the thermophysical behavior of pure hydrogen and on transport and energetic properties of binary mixtures containing hydrogen and components commonly found in NG or similar gases, such as methane, ethane, propane, nitrogen and carbon monoxide and dioxide. Attention should be paid also to the vapor-liquid equilibrium of the same binary mixtures as it is of major importance as it comes to storage conditions. Based on experimental data that can be found in online literature, the predictive accuracy of several thermodynamic models was evaluated and better knowledge about the models' behavior was stated. The under-evaluation thermodynamic models are; the cubic equations of state, Peng Robinson, Soave Redlich Kwong with hydrogen's experimental acentric factor combined with Soave's alpha function both combined with van der Waals mixing rules and UMR-PRU which is the PR EoS coupled with UNIFAC through the Universal Mixing Rule, also the soft equation PC-SAFT and last but not least, equation GERG-2008. Also, the examined properties are vapor pressure, molar density, residual molar  $C_p$ ,  $C_v$  and enthalpy, Speed velocity and JT coefficient in terms of pure hydrogen and VLE, single-phase density, residual molar  $C_p$ ,  $C_v$  and enthalpy, Speed velocity and JT coefficient in terms of binary mixtures.

After evaluating all the available datasets that were found in online literature both for pure hydrogen and the six binary mixtures, the invalid sets were excluded from the database. A plethora of data are available in terms of pure hydrogen but it was found that there is significant lack of experimental data especially as it comes to thermodynamic and physical properties of the examined mixtures.

It is clear that for calculating properties related to pure hydrogen the most trustworthy model that should be chosen is the reference EoS, GERG-2008. Even though it is the most accurate of the evaluated models, it cannot be used for the JT coefficient calculations and shouldn't be used for residual molar  $C_p$  and  $C_v$  either because it performs significantly high errors regarding the experimental data of these properties. The cubic EoS's are widely affected by the choice of acentric factor as well as the choice of the alpha function that is to me paired with them. In some cases, such as hydrogen referring to PR EoS, the fitting of the acentric factor and the pairing of the thermodynamic model with a multiparametric alpha function and a proper determination of each parameter, such as Mathias-Copeman equation, can lead to significantly improved results. The soft EoS, PC-SAFT, failed to calculate hydrogen's vapor pressures, which is a significant failure of the model and it should not be considered as reliable as it comes to hydrogen calculations.



Table 71: The most accurate EoS for each one of the examined properties for pure hydrogen

	d	C <sub>p,res</sub>	C <sub>v,res</sub>	H <sub>res</sub>	w	JT	p <sup>S</sup>
Thermodynamic Model	GERG-2008	SRK EoS 1	GERG-2008				
Software Tool	AGA8 code / NIST	ThermoCalc	AGA8 code / NIST				

The final choice of thermodynamic model regarding pure hydrogen calculations is stated below.

Table 72: The most accurate EoS for the calculations regarding pure hydrogen

	d	H <sub>res</sub>	w	p <sup>S</sup>
Thermodynamic Model	GERG-2008			
Software Tool	AGA8 code / NIST			

In the case of binary mixtures, the choice is not so clear. The number of experimental points and the components differ in every one of the six examined binary mixtures which leads to different results in each case. It is impossible to conclude in safe decisions as it comes to the properties of; residual molar C<sub>p</sub>, C<sub>v</sub>, enthalpy and JT coefficient due to lack of experimental data. The thermodynamic model choice for the properties of single-phase density and speed of sound for all of the six binary mixtures is common and is the reference equation, GERG-2008. As for the VLE calculations, the bubble point pressures are very well predicted by UMR-PRU and the model accuracy for vapor phase composition differs from mixture to mixture.

Table 73: The most accurate EoS for each one of the examined properties for each one of the binary mixtures

Binary mixture	ρ	w	C <sub>p,res</sub>	JT	BPP	Y <sub>H2</sub>
H <sub>2</sub> -CH <sub>4</sub>	GERG-2008	GERG-2008	-	UMR-PRU	UMR-PRU	SRK EoS
H <sub>2</sub> -C <sub>2</sub> H <sub>6</sub>	GERG-2008	GERG-2008	-	-	UMR-PRU	PC-SAFT
H <sub>2</sub> -C <sub>3</sub> H <sub>8</sub>	GERG-2008	GERG-2008	-	-	UMR-PRU	UMR-PRU
H <sub>2</sub> -CO	GERG-2008	GERG-2008	-	-	PR EoS (experimental acentric factor)	GERG-2008
H <sub>2</sub> -CO <sub>2</sub>	GERG-2008	GERG-2008	-	-	UMR-PRU	SRK EoS
H <sub>2</sub> -N <sub>2</sub>	GERG-2008	GERG-2008	SRK EoS	-	UMR-PRU	PR EoS (fitted acentric factor)

After the model comparison to the available experimental data regarding the thermophysical properties of the binary mixtures, an extension of the database was performed for the properties of single-phase density and speed of sound based on the best performing equation which was the reference EoS, GERG-2008. This extension was performed in order to examine how the evaluated models compare for higher hydrogen compositions than the ones described in the available data. It seems that the models have a similar behavior to GERG-2008 EoS as it comes to high-hydrogen composition in the mixtures, with SRK EoS which uses the experimental acentric factor for hydrogen giving the smallest deviations compared to GERG-2008 calculations. It is important to note that since GERG-2008's behavior for hydrogen molar composition over, in most cases, 10 % in these six binary mixtures is not based on

experimental data, the model's calculations could be incorrect for a composition range between 10 % and 100 %.

It was further evaluated whether a change of the  $k_{ij}$  parameters used for the binary mixtures on PR EoS indicatively could affect the model selection. A similar evaluation and adjustment can happen also to  $k_{ij}$  parameters of SRK and PC-SAFT EoS, but it wasn't examined in this work. UMR-PRU parameters were fitted to similar VLE data as the ones used in this thesis.

The final choice of thermodynamic model regarding each binary mixture that should be used for the calculations on both thermophysical-properties and VLE calculations is stated below.

*Table 74: Model selection for the calculations regarding each binary mixture*

Binary mixture	P	w	BPP	$Y_{H_2}$	Software tool
H <sub>2</sub> -CH <sub>4</sub>	PR EoS fitted acentric factor (set to -0.12) and fitted $k_{ij}$ (set to -0.09)				ThermoCalc
H <sub>2</sub> -C <sub>2</sub> H <sub>6</sub>	UMR-PRU				ThermoCalc
H <sub>2</sub> -C <sub>3</sub> H <sub>8</sub>	GERG-2008 EoS				Aspen HYSYS
H <sub>2</sub> -CO	GERG-2008 EoS				Aspen HYSYS
H <sub>2</sub> -CO <sub>2</sub>	UMR-PRU				ThermoCalc
H <sub>2</sub> -N <sub>2</sub>	PR EoS fitted acentric factor (set to -0.12) and fitted $k_{ij}$ (set to -0.02)				ThermoCalc

It is important to note that plenty of these datasets are rather old and focus on mixtures that contain very low compositions of hydrogen. In order to be able to predict correctly the behavior of hydrogen-containing streams it is important to renew the database with experimental data which have emerged from more modern and reliable measurements and cover a range for hydrogen's composition for 0.0 % to 100.0 %.

Additionally, it is important to extend the existing database with experimental data referring to hydrogen-containing ternary and multicomponent mixtures, which are absent from the available database in terms of thermophysical properties and very limited in terms of VLE. These datasets will help even more to evaluate the thermodynamic models' behavior and approach more realistic case studies.

It would, also, be interesting to evaluate the behavior of a thermodynamic model that can accurately predict hydrogen's quantum nature, such as the SAFT model with attractive potentials of Variable Range and Mie's monomer hard-core potential (SAFT-VR-Mie) which is meant to be successful for pure Hydrogen with its main success occurring in the cryogenic region[46], [47].

Further examination on the parameter fitting of the acentric factors of the pure components of the evaluated mixtures and of the binary coefficient parameters of the mixtures can be taken into consideration. With a focus on SRK EoS instead of PR EoS the final results could differ a lot and the measured deviations could be even more reduced.

## References

- [1] T. S. Ledley, E. Sundquist, D. K. Hall, S. E. Schwartz, J. D. Fellows, and T. L. Killeen, "Climate change and greenhouse gases," *Eos, Transactions American Geophysical Union*, vol. 80, no. 39, 2011, doi: <https://doi.org/10.1029/99EO00325>.
- [2] European Commission, "'The European Green Deal' COM/2019/640 final," 2019, Accessed: May 23, 2022. [Online]. Available: <https://eur-lex.europa.eu/legal-content/EN/TXT/?uri=CELEX:52019DC0640>
- [3] F. Dawood, M. Anda, and G. M. Shafiullah, "Hydrogen production for energy: An overview," *International Journal of Hydrogen Energy*, vol. 45, no. 7. Elsevier Ltd, pp. 3847–3869, Feb. 07, 2020. doi: 10.1016/j.ijhydene.2019.12.059.
- [4] M. Noussan, P. P. Raimondi, R. Scita, and M. Hafner, "The role of green and blue hydrogen in the energy transition—a technological and geopolitical perspective," *Sustainability (Switzerland)*, vol. 13, no. 1. MDPI AG, pp. 1–26, Jan. 01, 2021. doi: 10.3390/su13010298.
- [5] M. G. Sürer and H. T. Arat, "State of art of hydrogen usage as a fuel on aviation," *European Mechanical Science*, vol. 2, no. 1, pp. 20–30, Jan. 2018.
- [6] NIST, "NIST Chemistry WebBook," *NIST Standard Reference Database Number 69*.
- [7] R. D. McCarty, J. Hord, and H. M. Roder, *Selected Properties of Hydrogen (engineering design data)*, vol. 168. 1981. Accessed: Jun. 03, 2022. [Online]. Available: [https://books.google.no/books?id=HCuDRC6x\\_XgC&ots=SschXNmbNW&dq=selected%20properties%20of%20hydrogen&lr&hl=el&pg=PA13#v=onepage&q=selected%20properties%20of%20hydrogen&f=false](https://books.google.no/books?id=HCuDRC6x_XgC&ots=SschXNmbNW&dq=selected%20properties%20of%20hydrogen&lr&hl=el&pg=PA13#v=onepage&q=selected%20properties%20of%20hydrogen&f=false)
- [8] Y. Y. Milenko, R. M. Sibileva, and M. A. Strzhemechny, "Natural Ortho-Para Conversion Rate in Liquid and Gaseous Hydrogen," 1997.
- [9] S. Z. S. al Ghafri *et al.*, "Modelling of Liquid Hydrogen Boil-Off," *Energies (Basel)*, vol. 15, no. 3, p. 1149, 2022.
- [10] F. Dawood, M. Anda, and G. M. Shafiullah, "Hydrogen production for energy: An overview," *International Journal of Hydrogen Energy*, vol. 45, no. 7. Elsevier Ltd, pp. 3847–3869, Feb. 07, 2020. doi: 10.1016/j.ijhydene.2019.12.059.
- [11] Y. Peng and D. Robinson, "A New Two-Constant Equation of State," 1976. [Online]. Available: <https://pubs.acs.org/sharingguidelines>
- [12] O. Redlich and J. N. S Kwong, "ON THE THERMODYNAMICS OF SOLUTIONS. V An Equation of State. Fugacities of Gaseous Solutions1," UTC, 1948. [Online]. Available: <https://pubs.acs.org/sharingguidelines>
- [13] G. Soave, "Equilibrium constants from a modified Redkh-Kwong equation of state," Pergamon Press, 1972.
- [14] Leiden, "J.D. Van der Waals," 1873.
- [15] V. Louli *et al.*, "Measurement and prediction of dew point curves of natural gas mixtures," *Fluid Phase Equilibria*, vol. 334, pp. 1–9, Nov. 2012, doi: 10.1016/j.fluid.2012.07.028.

- [16] E. Voutsas, K. Magoulas, and D. Tassios, "Universal mixing rule for cubic equations of state applicable to symmetric and asymmetric systems: Results with the Peng-Robinson equation of state," *Industrial and Engineering Chemistry Research*, vol. 43, no. 19, pp. 6238–6246, 2004, doi: 10.1021/ie049580p.
- [17] J. Gross and G. Sadowski, "Perturbed-chain SAFT: An equation of state based on a perturbation theory for chain molecules," *Industrial and Engineering Chemistry Research*, vol. 40, no. 4, pp. 1244–1260, Feb. 2001, doi: 10.1021/ie0003887.
- [18] J. Gross and G. Sadowski, "Application of the perturbed-chain SAFT equation of state to associating systems," *Industrial and Engineering Chemistry Research*, vol. 41, no. 22, pp. 5510–5515, Oct. 2002, doi: 10.1021/ie010954d.
- [19] O. Kunz and W. Wagner, "The GERG-2008 wide-range equation of state for natural gases and other mixtures: An expansion of GERG-2004," *Journal of Chemical and Engineering Data*, vol. 57, no. 11, pp. 3032–3091, Nov. 2012, doi: 10.1021/je300655b.
- [20] G. W. Thomson, "THE ANTOINE EQUATION FOR VAPOR-PRESSURE. DATA." [Online]. Available: <https://pubs.acs.org/sharingguidelines>
- [21] DIPPR and AiChE, *Design Institute for Physical Properties*. 1996.
- [22] I. H. Bell, "AGA8," <https://github.com/usnistgov/AGA8>, Feb. 26, 2017.
- [23] V. Koulocheris, V. Louli, E. Panteli, S. Skouras, and E. Voutsas, "Modelling of hydrogen vapor-liquid equilibrium with oil & gas components," *Fluid Phase Equilibria*, vol. 494, pp. 125–134, Aug. 2019, doi: 10.1016/j.fluid.2019.04.010.
- [24] Ilke Senol, "Perturbed-Chain Statistical Association Fluid Theory (PC-SAFT) Parameters for Propane, Ethylene, and Hydrogen under Supercritical Conditions," *World Academy of Science, Engineering and Technology*, vol. 59, 2011.
- [25] Y. le Guennec, S. Lasala, R. Privat, and J. N. Jaubert, "A consistency test for  $\alpha$ -functions of cubic equations of state," *Fluid Phase Equilibria*, vol. 427, pp. 513–538, Nov. 2016, doi: 10.1016/j.fluid.2016.07.026.
- [26] C. L. Young, *Hydrogen and deuterium*. Pergamon Press, 1981.
- [27] J. Huey Hong and R. Kobayashi, "Vapor-Liquid Equilibrium Study of the H<sub>2</sub>-CH<sub>4</sub> System at Low Temperatures and Elevated Pressures," 1981. [Online]. Available: <https://pubs.acs.org/sharingguidelines>
- [28] M. Hu, W. Lin, A. Gu, and J. Li, "Isothermal vapor-liquid equilibrium in CH<sub>4</sub>/H<sub>2</sub>/N<sub>2</sub> system at a cryogenic temperature range from 100.0K to 125.0K," *Fluid Phase Equilibria*, vol. 366, pp. 16–23, Mar. 2014, doi: 10.1016/j.fluid.2014.01.002.
- [29] R. Beckmüller, M. Thol, I. H. Bell, E. W. Lemmon, and R. Span, "New Equations of State for Binary Hydrogen Mixtures Containing Methane, Nitrogen, Carbon Monoxide, and Carbon Dioxide," *Journal of Physical and Chemical Reference Data*, vol. 50, no. 1, Mar. 2021, doi: 10.1063/5.0040533.

- [30] A. Heintz and W. B. Street, "Phase Equilibria in the H<sub>2</sub>/C<sub>2</sub>H<sub>6</sub> System at Temperatures from 92.5 to 280.1 K and Pressures to 560 MPa," *Journal of Chemical and Engineering Data*, vol. 27, no. 4, pp. 465–469, 1982.
- [31] G. B. C. F. D. N. R. F. and D. L. T. K. Bezahehtak, "Vapor–Liquid Equilibrium for Binary Systems of Carbon Dioxide + Methanol, Hydrogen + Methanol, and Hydrogen + Carbon Dioxide at High Pressures," *Journal of Chemical & Engineering Data*, vol. 47, no. 2, pp. 161–168, 2002, Accessed: May 29, 2022. [Online]. Available: <https://pubs.acs.org/doi/full/10.1021/je010122m>
- [32] M. Yorizane, S. Yoshimura, H. Masuoka, and T. Naka, "Measurement and prediction of the vapor-liquid equilibrium relation at low temperature and high pressure for the hydrogen-nitrogen system," vol. 35, pp. 691–693, Accessed: May 29, 2022. [Online]. Available: [https://www.scopus.com/record/display.uri?eid=2-s2.0-84872714270&origin=inward&featureToggles=FEATURE\\_NEW\\_DOC\\_DETAILS\\_EXPORT:1](https://www.scopus.com/record/display.uri?eid=2-s2.0-84872714270&origin=inward&featureToggles=FEATURE_NEW_DOC_DETAILS_EXPORT:1)
- [33] J. R. S. , Machado, W. B. Streett, and U. Dieters, "PVT measurements of hydrogen/methane mixtures at high pressures," *Journal of Chemical & Engineering Data*, vol. 33, pp. 148–152, 1988.
- [34] R. , Hernández-Gómez, D. Tuma, E. Pérez, and C. R. Chamorro, "Accurate Experimental (p, ρ, and T) Data for the Introduction of Hydrogen into the Natural Gas Grid (II): Thermodynamic Characterization of the Methane–Hydrogen Binary System from 240 to 350 K and Pressures up to 20 MPa.," *J. Chem. Eng. Data*, vol. 63, pp. 1613–1630, 2018.
- [35] D. R. Augood, "The separation of HD and H<sub>2</sub> by absorptive fractionation," *Trans Inst Chem Eng*, vol. 35, pp. 394–408, 1957.
- [36] S.-Y. , Chuang, P. S. Chappellear, and R. Kobayashi, "iscosity of methane, hydrogen, and four mixtures of methane and hydrogen from -100. degree. C to 0. degree. C at high pressures," *J. Chem. Eng. Data*, vol. 21, pp. 403–411, 1976.
- [37] F. A. Freeth and T. T. H. Verschoyle, "Physical constants of the system methane-hydrogen," *Phys. Character*, vol. 130, pp. 453–463, 1931.
- [38] S. , Mihara, H. , Sagara, Y. Arai, and S. Saito, "The Compressibility Factors of Hydrogen Methane, Hydrogen Ethane and Hydrogen Propane Gaseous Mixtures," *Journal of Chemical & Engineering Data*, vol. 10, pp. 395–399, 1977.
- [39] D. Lozano-Martín, M. C. Martín, C. R. Chamorro, D. Tuma, and J. J. Segovia, "Speed of sound for three binary (CH<sub>4</sub> + H<sub>2</sub>) mixtures from p = (0.5 up to 20) MPa at T = (273.16 to 375) K," *International Journal of Hydrogen Energy*, vol. 45, no. 7, pp. 4765–4783, Feb. 2020, doi: 10.1016/j.ijhydene.2019.12.012.
- [40] R. E. Randelman and L. A. Wenzel, "Joule-Thomson Coefficients of Hydrogen and Methane Mixtures," 1988. [Online]. Available: <https://pubs.acs.org/sharingguidelines>
- [41] J. H. Hong and R. Kobayashi, "Phase equilibrium studies for methane/synthesis gas separation: the hydrogen-carbon monoxide-methane system," Apr. 1982.

- [42] A. Cipollina, R. Anselmo, O. Scialdone, G. Filardo, and A. Galia, "Experimental P-T- $\rho$  measurements of supercritical mixtures of carbon dioxide, carbon monoxide, and hydrogen and semiquantitative estimation of their solvent power using the solubility parameter concept," *Journal of Chemical and Engineering Data*, vol. 52, no. 6, pp. 2291–2297, Nov. 2007, doi: 10.1021/je700307r.
- [43] BATSANOV SS, *EXPERIMENTAL FOUNDATIONS OF STRUCTURAL CHEMISTRY*. 2008.
- [44] M. G. , Gonikberg, W. G. Fastowsky, and J. G. Gurwitch, "The solubility of gases in liquids at low temperatures and high pressures: the solubility of hydrogen in liquid nitrogen at temperatures of 79.0-109.0 [degree] K. and pressures up to 190 atm.," *National Research Council of Canada*, 1954.
- [45] H. , Knapp, K. Schmölling, and A. Neumann, "A. Measurement of the molal heat capacity of H<sub>2</sub>) N<sub>2</sub> mixtures. Cryogenics," *Guildf*, vol. 16, pp. 231–237, 1976.
- [46] M. Hammer and P.----- Flow, "Study of Hydrogen-PVT Accuracy of thermophysical models." [Online]. Available: [www.sintef.no](http://www.sintef.no)
- [47] M. Hammer, Ø. Wilhemsen, and A. Aase, "The SAFT-VR Mie equation of state," 2020. [Online]. Available: [www.sintef.no/energi](http://www.sintef.no/energi)

## Appendices

### Appendix A

The UNIFAC group interaction parameters used for UMR-PRU have been extracted from publications related to UMR-PRU[15], [23]. For the binary mixture of hydrogen and carbon monoxide the calculations will not be performed with UMR-PRU EoS because there are no published adjusted parameters yet.

m	n	$A_{mn}$ (K)	$B_{mn}$ (-)	$C_{mn}$ ( $K^{-1}$ )	$A_{nm}$ (K)	$B_{nm}$ (-)	$C_n$ ( $K^{-1}$ )
CH <sub>4</sub>	H <sub>2</sub>	387.15	1.291	8.35E-04	-82.98	-0.121	3.02E-03
C <sub>2</sub> H <sub>6</sub>	H <sub>2</sub>	517.10	4.375	1.59E-02	-185.68	-2.540	-3.16E-03
CH <sub>2</sub>	H <sub>2</sub>	-8.51	-0.934	2.38E-03	168.74	-0.711	-6.85E-04
ACH	H <sub>2</sub>	328.04	-3.016	2.13E-03	8.32	1.879	-1.08E-03
ACCH <sub>3</sub>	H <sub>2</sub>	83.44	-4.348	8.14E-04	233.79	10.954	-1.37E-02
CO <sub>2</sub>	H <sub>2</sub>	521.47	0.783	0	-53.53	-3.276	0
N <sub>2</sub>	H <sub>2</sub>	-86.71	-1.009	0	-19.32	-0.220	0

Table A 1: UNIFAC group interaction parameters estimated for the UMR-PRU model.

## Appendix B

For the calculation of the ideal parts of the thermophysical while using GERG-2008 EoS the parameters proposed are stated below.

Table B 1: GERG-2008 EoS parameters for the calculation of ideal properties

k	$n_{oi,k}^{\circ}$	$\theta_{oi,k}^{\circ}$
Methane		
1	19.59754	0
2	-83.9597	0
3	3.00088	0
4	0.76315	4.306474
5	0.0046	0.936221
6	8.74432	5.577234
7	-4.46921	5.722644
Nitrogen		
1	11.08344	0
2	-22.2021	0
3	2.50031	0
4	0.13732	5.251823
5	-0.1466	-5.39307
6	0.90066	13.78899
7	0	0
Carbon dioxide		
1	11.92518	0
2	-16.1188	0
3	2.50002	0
4	2.04452	3.022758
5	-1.06044	-2.84443
6	2.03366	1.589964
7	0.01393	1.121596
Ethane		
1	24.67547	0
2	-77.4253	0
3	3.00263	0
4	4.33939	1.831882
5	1.23722	0.731307
6	13.1974	3.378007
7	-6.01989	3.508722
Propane		
1	31.60293	0
2	-84.4633	0
3	3.02939	0
4	6.60569	1.297522
5	3.197	0.543211
6	19.1921	2.583146
7	-8.37267	2.777773



Hydrogen		
1	13.79647	0
2	-175.864	0
3	1.47906	0
4	0.95806	6.891654
5	0.45444	9.847635
6	1.56039	49.76529
7	-1.3756	50.36728
Carbon monoxide		
1	10.8145	0
2	-19.8437	0
3	2.50055	0
4	1.02865	11.67508
5	0.00493	5.305158
6	0	0
7	0	0

The binary interaction parameters of the mixtures using GERG-2008 are presented below

*Table B 2: GERG-2008 EoS binary interaction parameters for the six binary mixtures*

Mixture ij	$\beta_{v,ij}$	$\gamma_{v,ij}$	$\beta_{T,ij}$	$\gamma_{T,ij}$
CH <sub>4</sub> -H <sub>2</sub>	1	1.018703	1	1.352643
N <sub>2</sub> -H <sub>2</sub>	0.972532	0.970115	0.946134	1.175697
CO <sub>2</sub> -H <sub>2</sub>	0.904142	1.152793	0.94232	1.782925
C <sub>2</sub> H <sub>6</sub> -H <sub>2</sub>	0.925367	1.106072	0.93297	1.902008
C <sub>3</sub> H <sub>8</sub> -H <sub>2</sub>	1	1.074006	1	2.308215
CO-H <sub>2</sub>	1	1.121416	1	1.377505

## Appendix C

Indicative figures that display the results of model comparison regarding pure hydrogen.

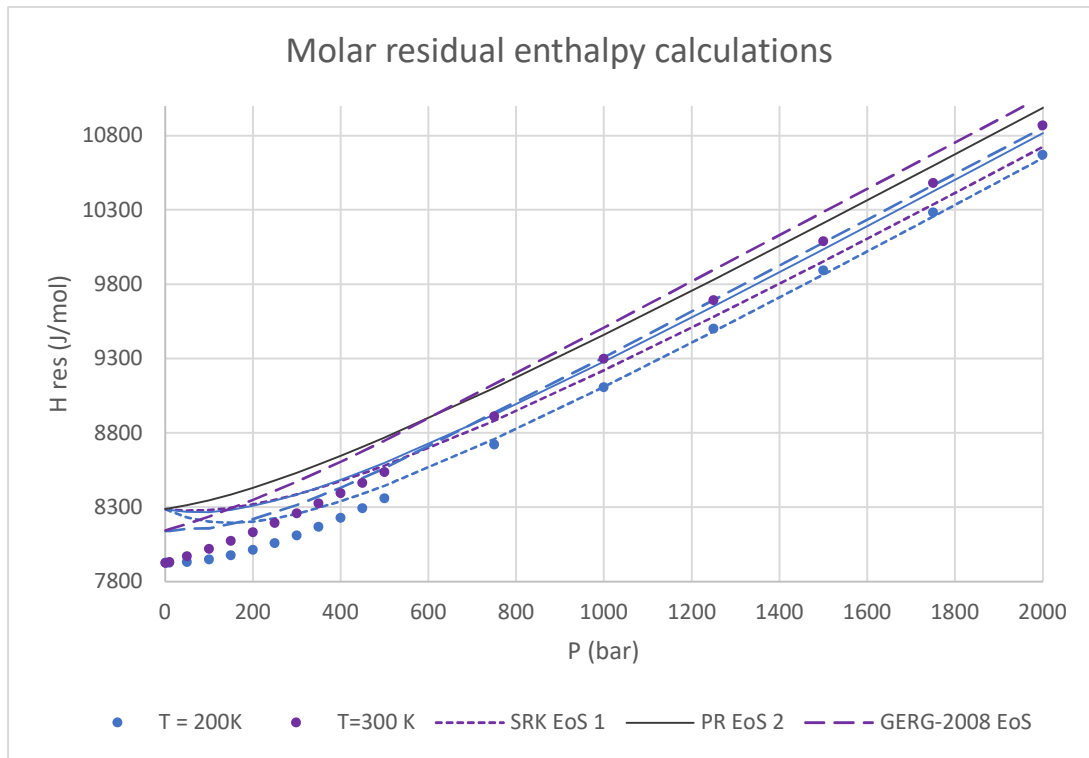


Figure C 1: Comparison of GERG-2008 EoS, PR EoS 2 and SRK EoS 1 regarding molar residual enthalpy of pure  $H_2$

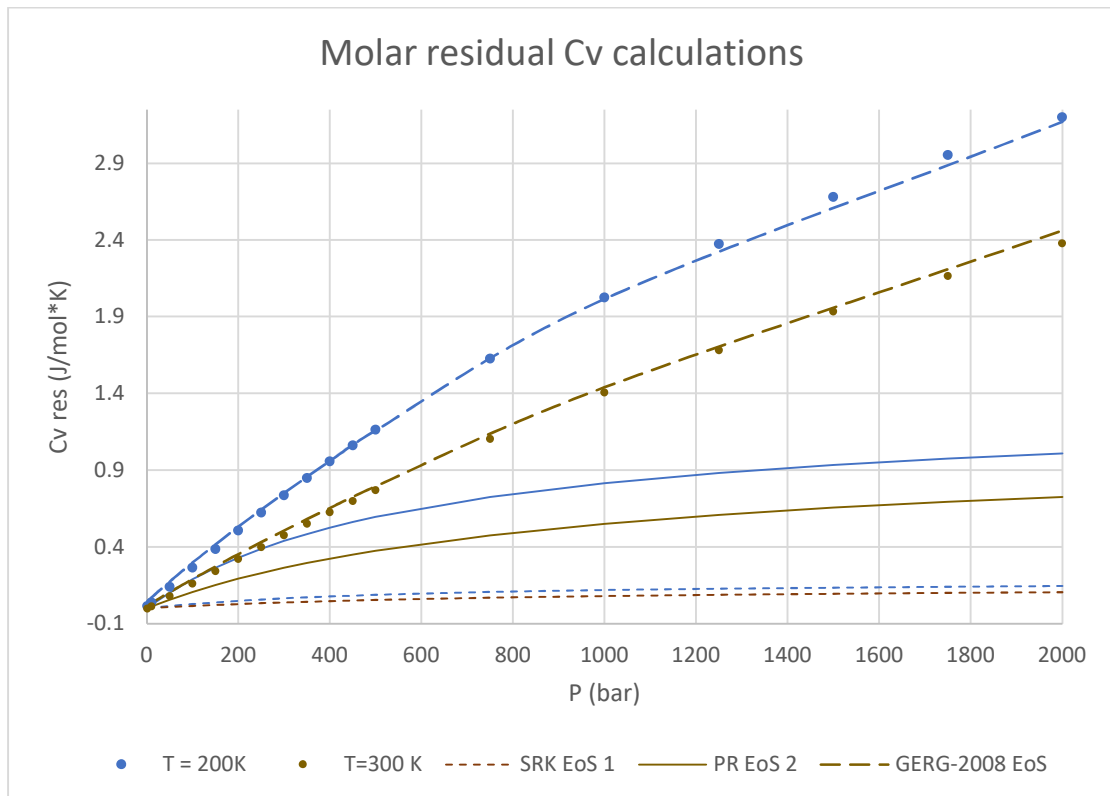


Figure C 2: Comparison of GERG-2008 EoS, PR EoS 2 and SRK EoS 1 regarding molar residual  $C_v$  of pure  $H_2$

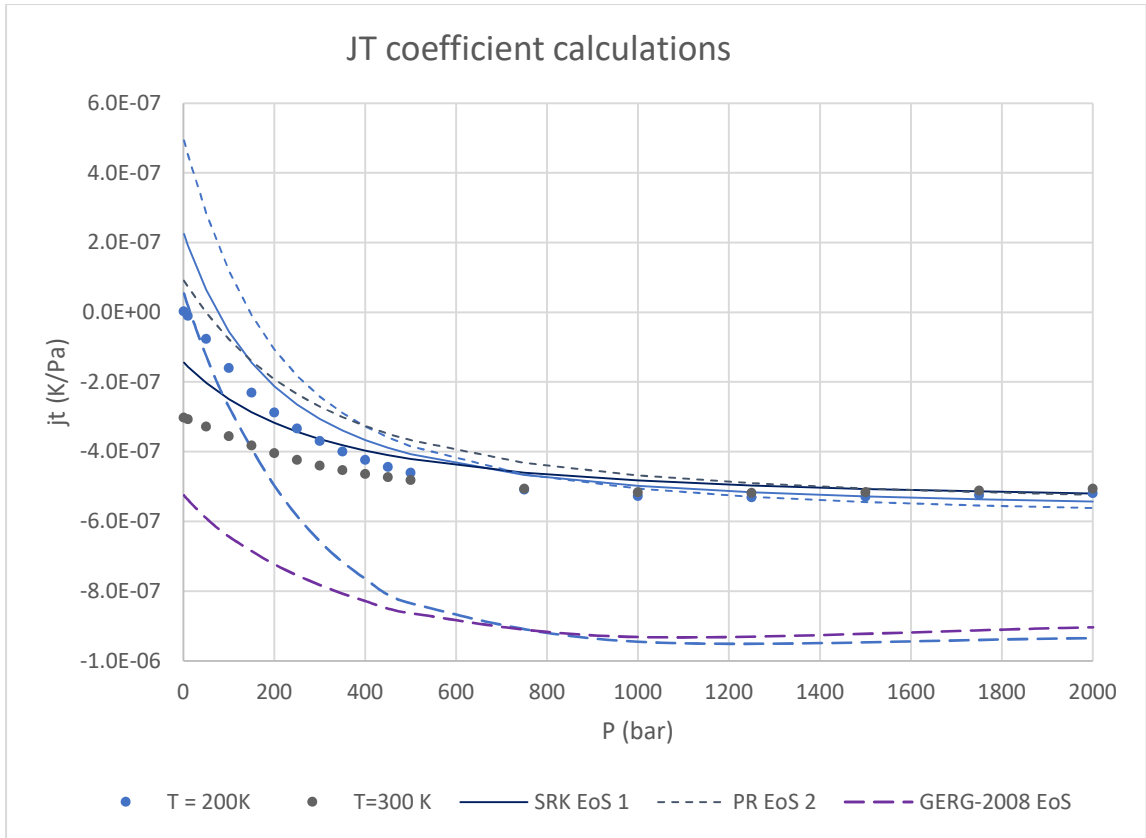


Figure C 3: Comparison of GERG-2008 EoS, PR EoS 2 and SRK EoS 1 regarding JT coefficient of pure H2

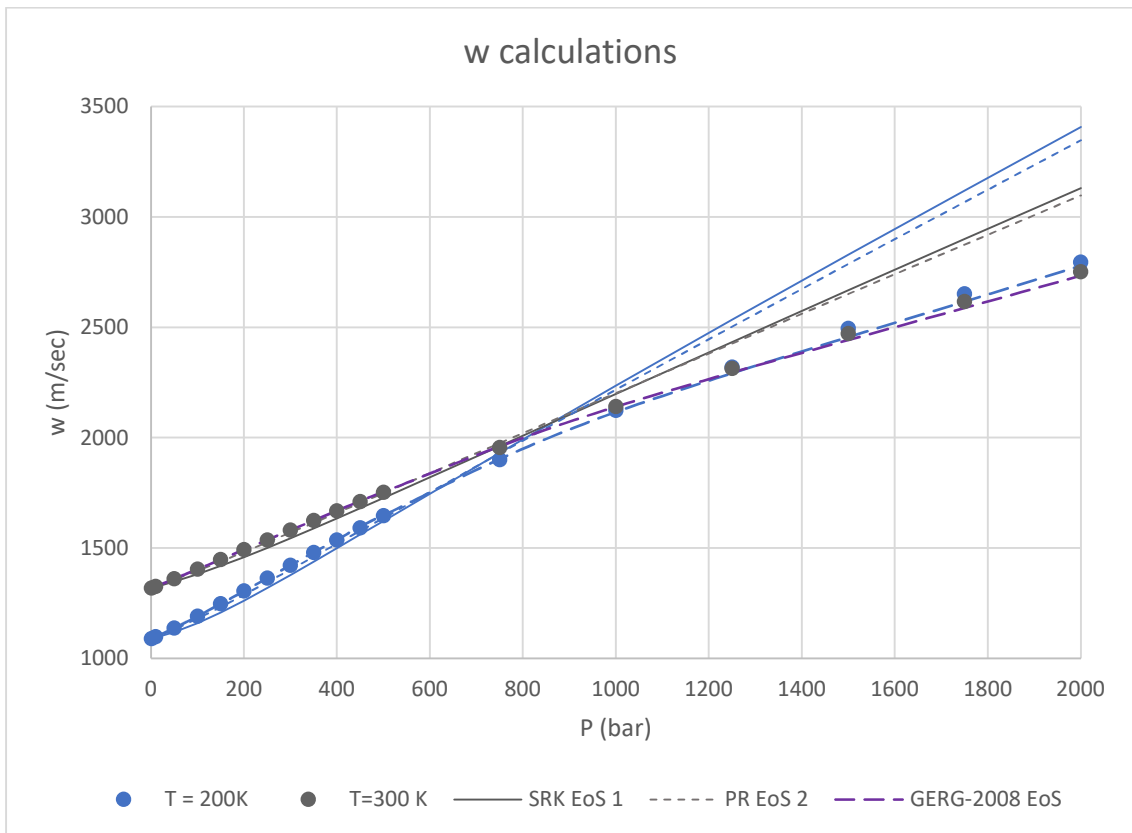


Figure C 4: Comparison of GERG-2008 EoS, PR EoS 2 and SRK EoS 1 regarding sound velocity of pure H2

## Appendix D

Indicative figures that display the results of model comparison regarding thermophysical property calculations of hydrogen containing binary mixtures.

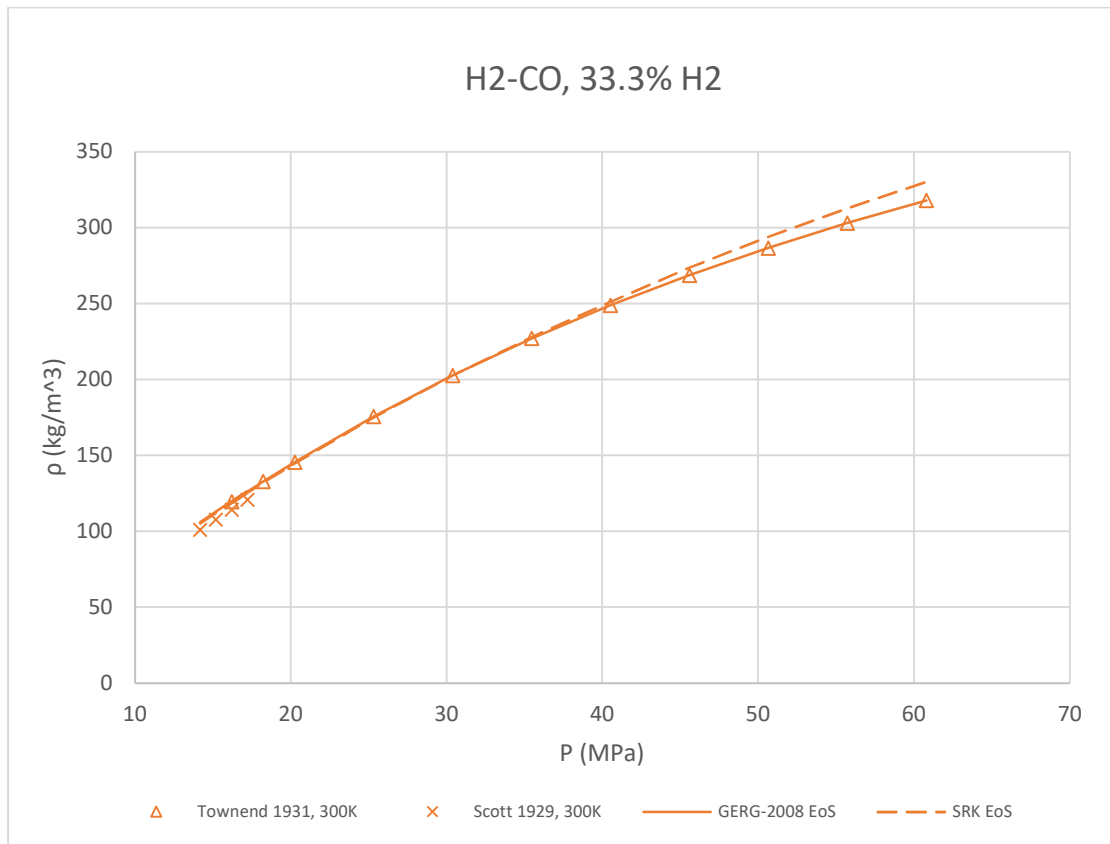


Figure D 1: Model comparison regarding single-phase density data of H2-CO

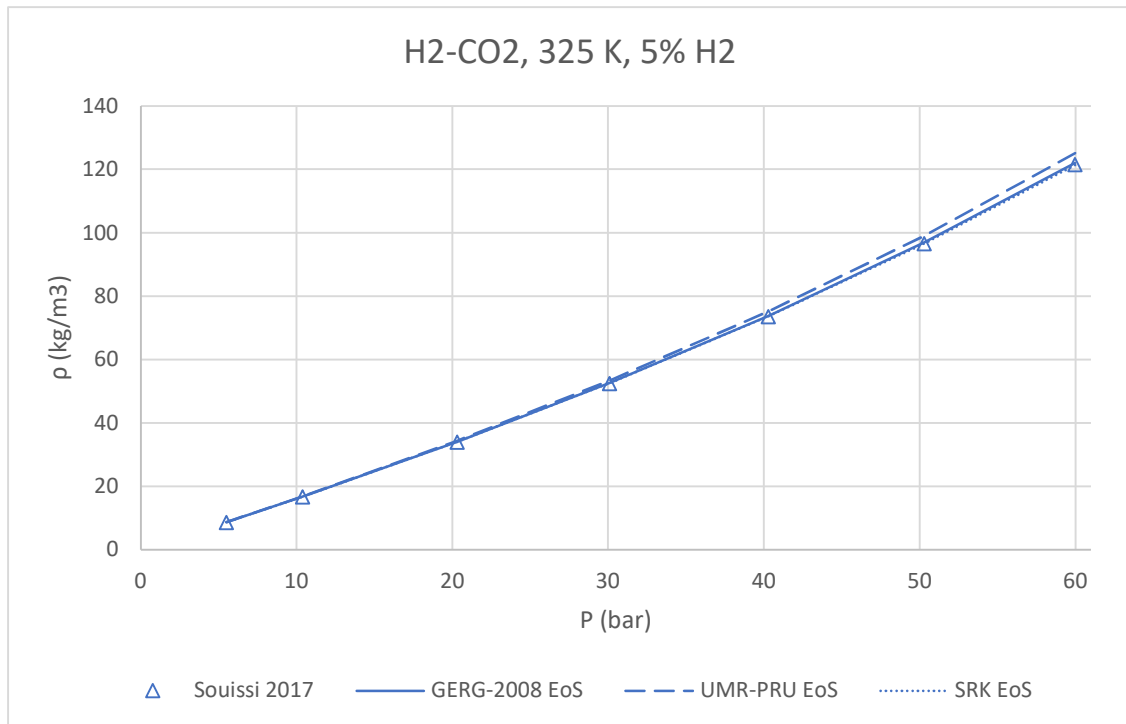


Figure D 2: Model comparison regarding single-phase density data of H2-CO<sub>2</sub>

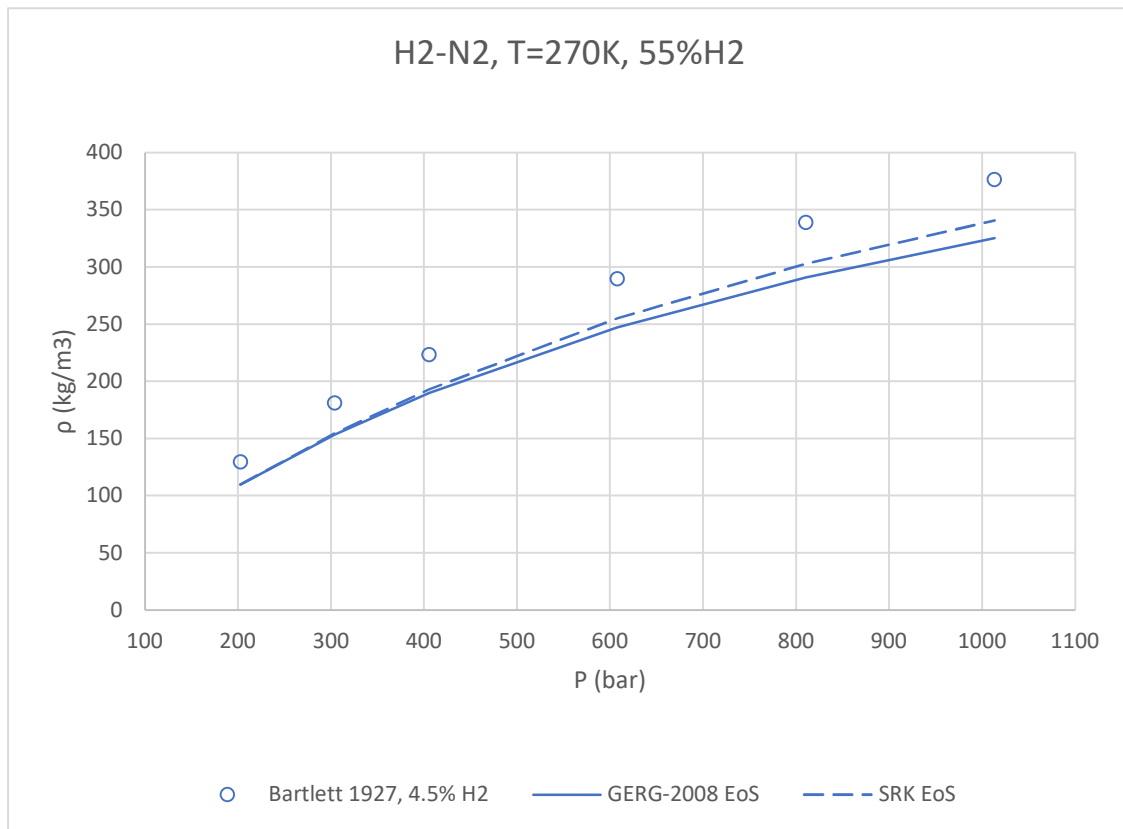


Figure D 3: Model comparison regarding single-phase density data of H2-N2

## Appendix E

Indicative figures that display the results of model comparison regarding VLE calculations of hydrogen containing binary mixtures.

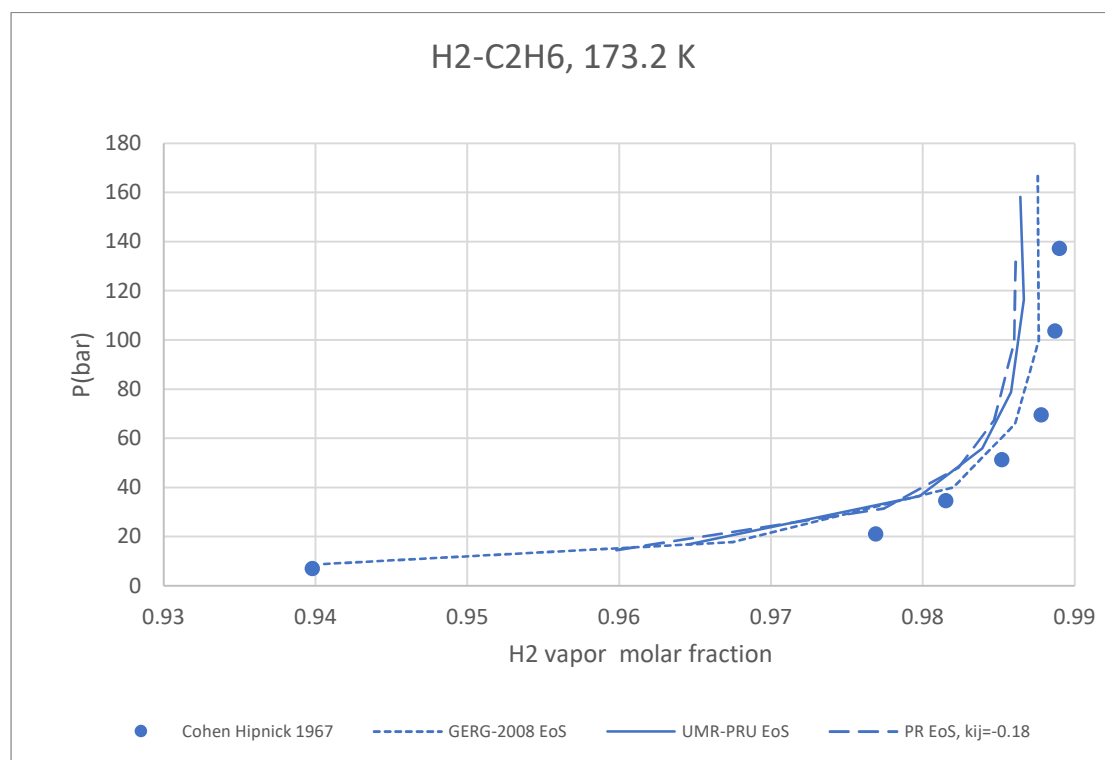


Figure E 1: Model comparison regarding VLE data of H2-C2H6

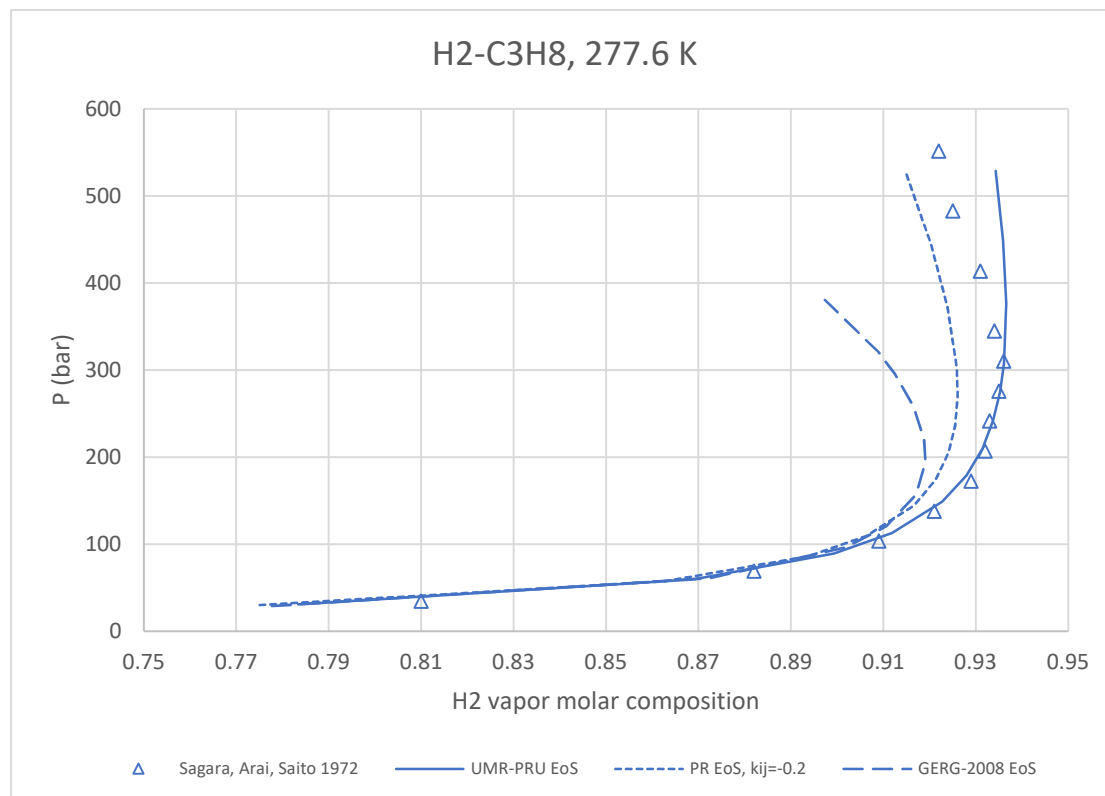


Figure E 2: Model comparison regarding VLE data of H2-C3H8

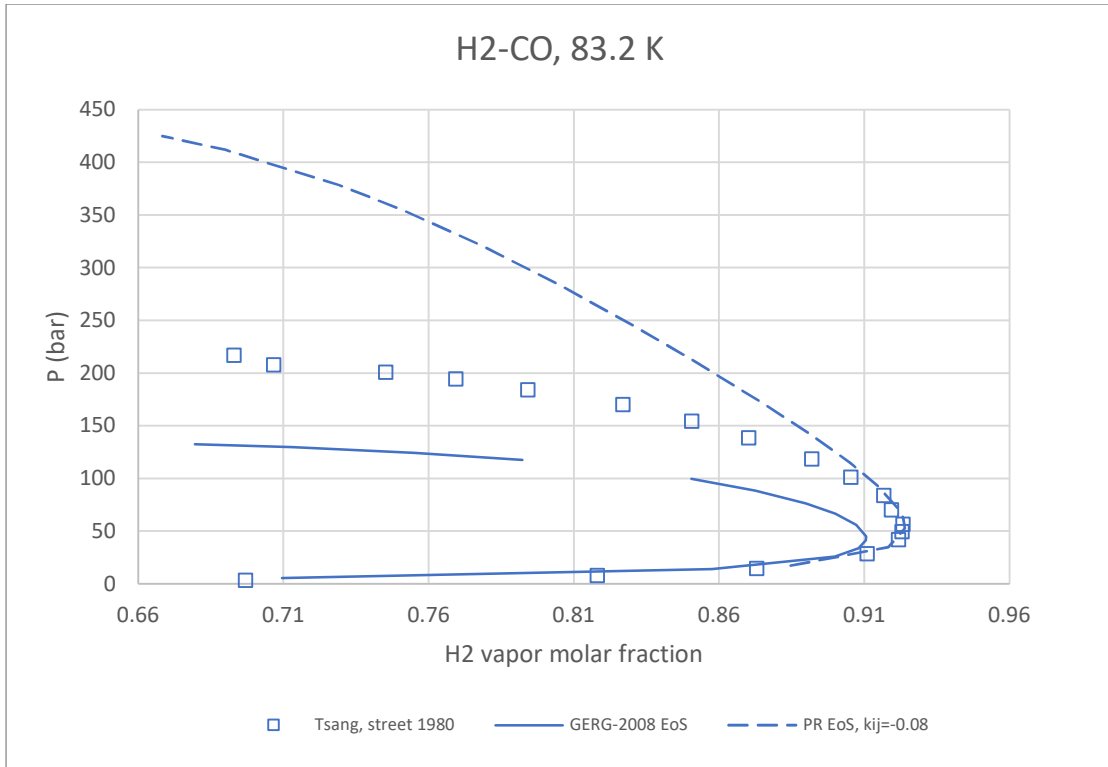


Figure E 3: Model comparison regarding VLE data of H2-CO

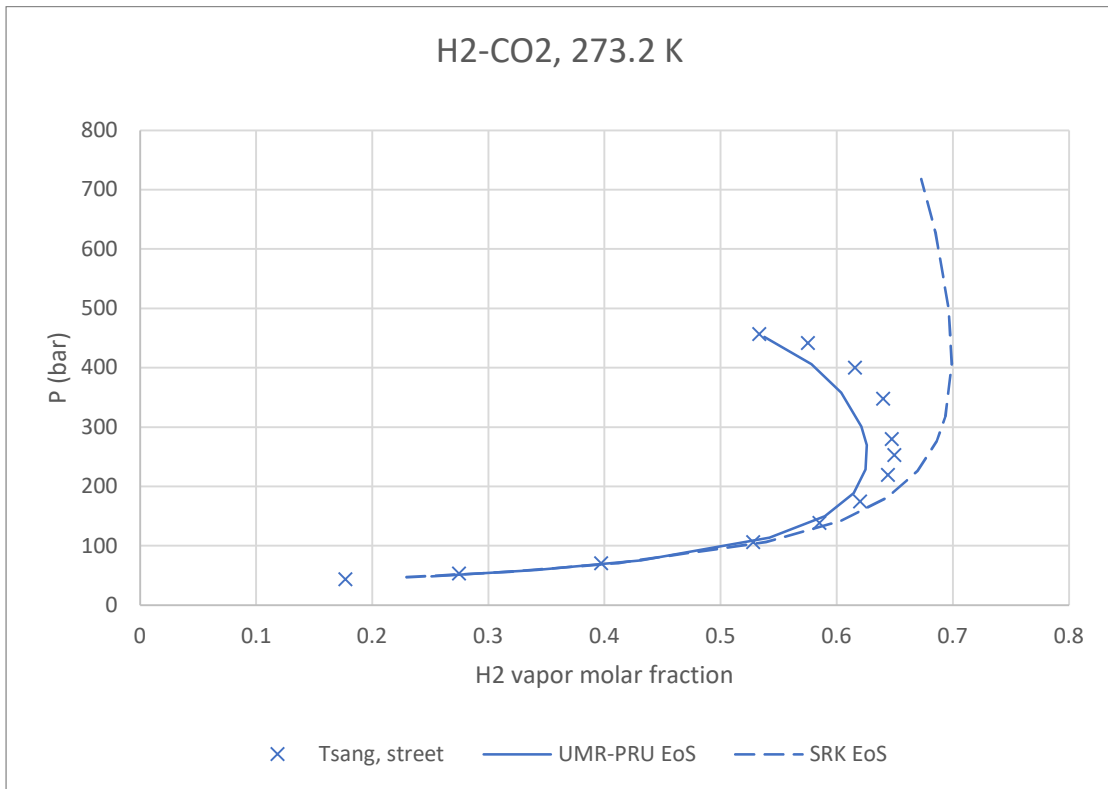


Figure E 4: Model comparison regarding VLE data of H2-CO2

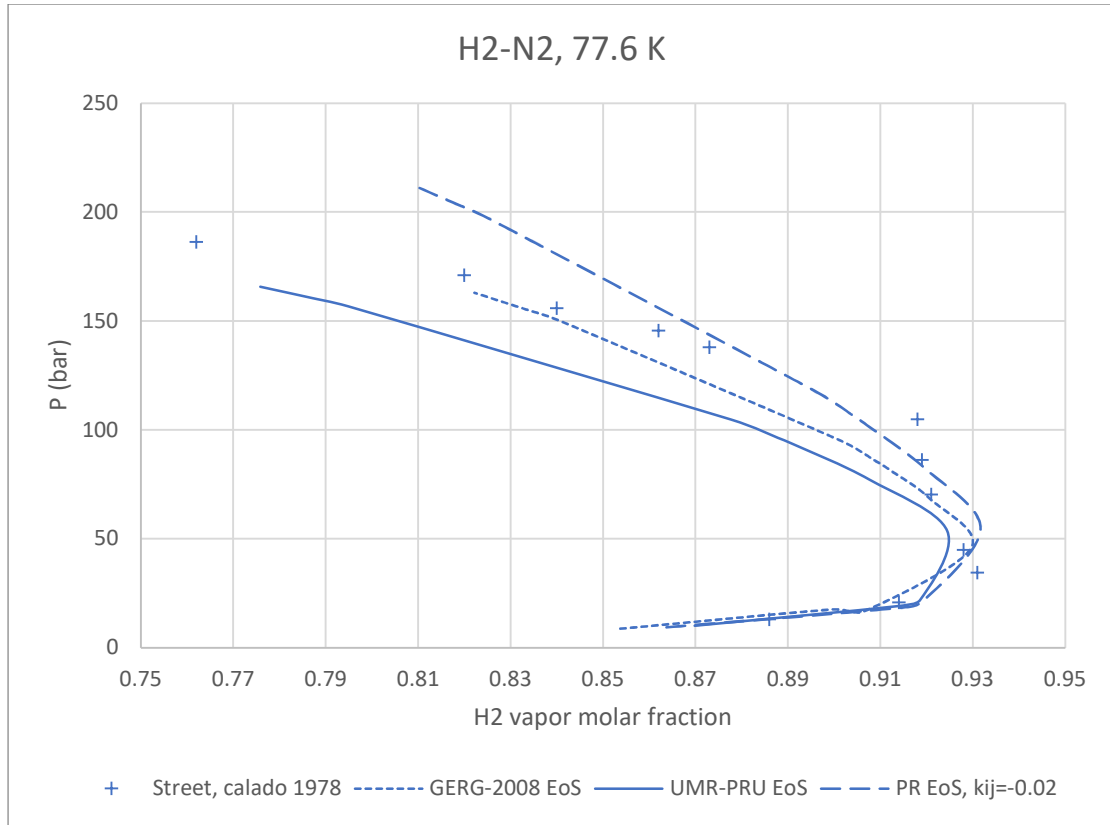


Figure E 5: Model comparison regarding VLE data of H2-N2



## Appendix F

The  $k_{ij}$  parameter fitting for the rest three systems, for hydrogen mixed with ethane, propane and nitrogen, are presented below.

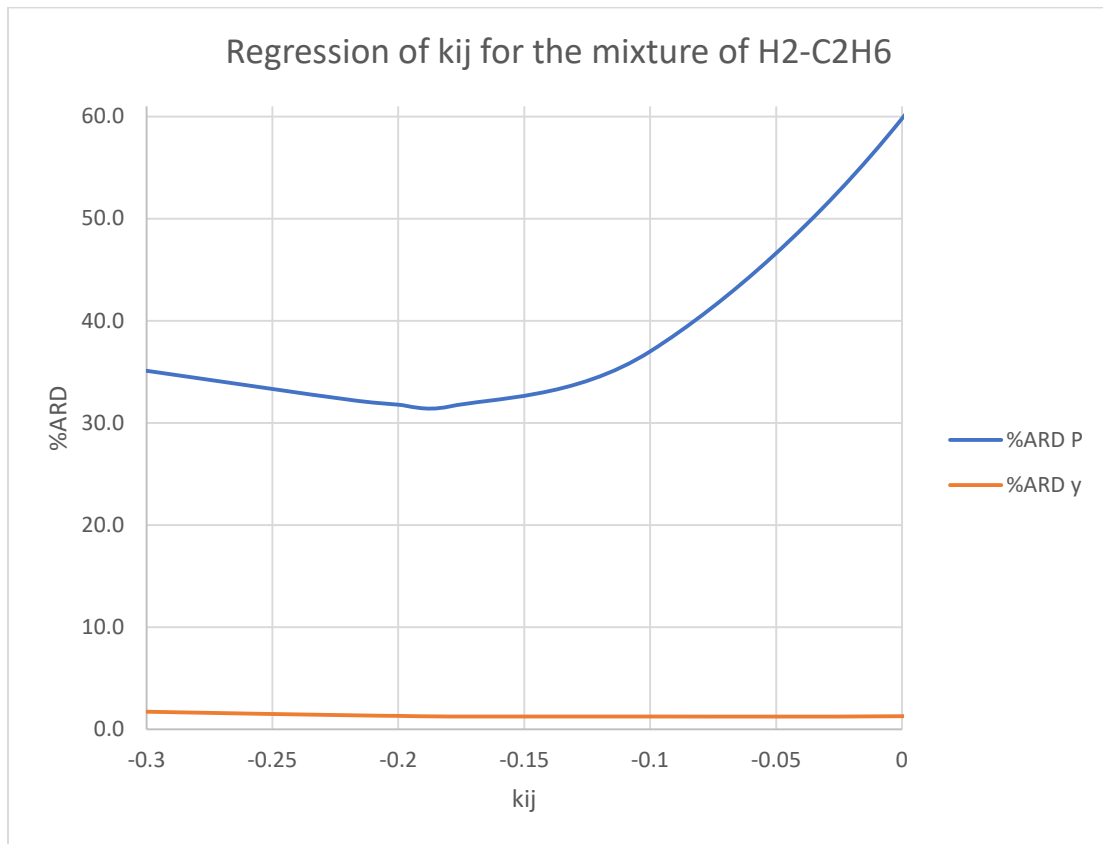


Figure F 1: Determination of  $k_{ij}$  parameter for PR EoS based on BPP data for the mixture of H<sub>2</sub>-C<sub>2</sub>H<sub>6</sub>

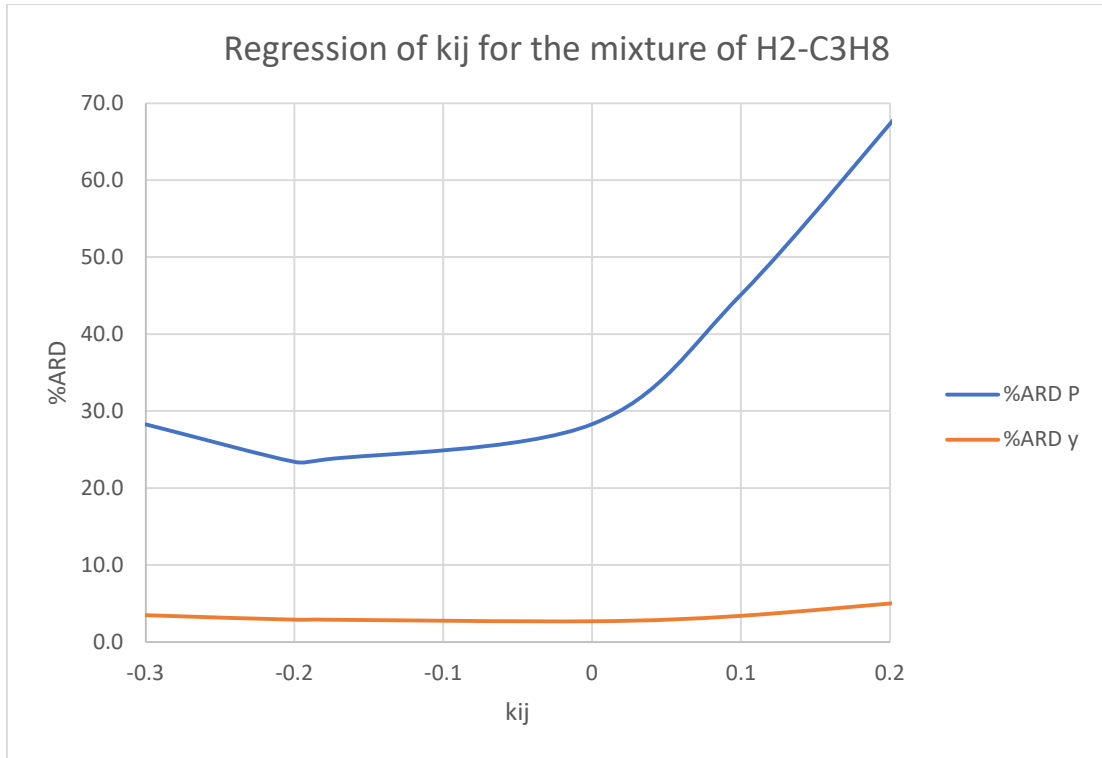


Figure F 2: Determination of  $k_{ij}$  parameter for PR EoS based on BPP data for the mixture of H<sub>2</sub>-C<sub>3</sub>H<sub>8</sub>

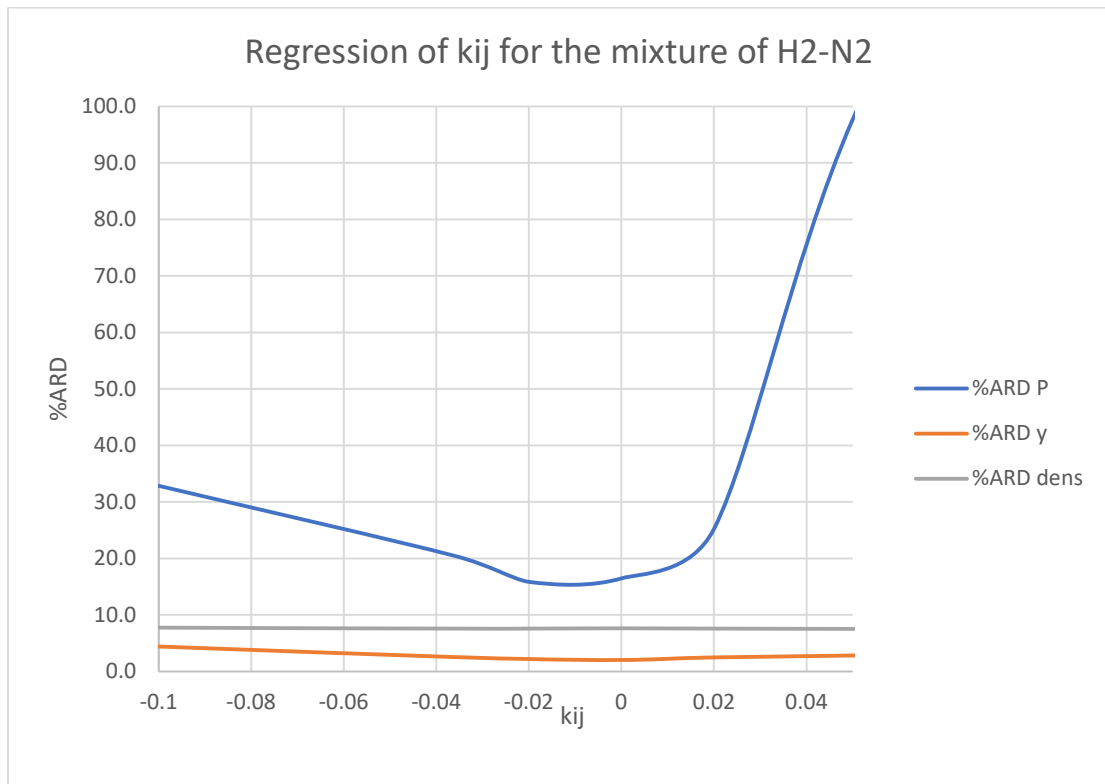


Figure F 3: Determination of  $k_{ij}$  parameter for PR EoS based on BPP data for the mixture of H<sub>2</sub>-N<sub>2</sub>

